OAK RIDGE NATIONAL LABORATORY
MANAGED BY UT-BATTELLE FOR THE DEPARTMENT OF ENERGY

ORNL/LTR-2011/79

Reactor and Nuclear Systems Division

Application Areas of Potential Challenge to Nuclear Criticality Safety Margins for Future High Temperature Gas Reactor Fuel Cycle Activities

D. A. Reed

March 18, 2011

Prepared for
Office of Nuclear Regulatory Research
Nuclear Regulatory Commission
under contract JCN N6773

Prepared by
OAK RIDGE NATIONAL LABORATORY
P.O. Box 2008
Oak Ridge, Tennessee 37831-6285
managed by
UT-BATTELLE, LLC
for the
U.S. DEPARTMENT OF ENERGY
under contract DE-AC05-00OR22725

ABSTRACT

Fuel cycle activities for future high temperature gas reactors (HTGRs) will involve uranium enrichments and fissile material configurations that differ significantly from those of current light water reactor (LWR) fuel cycle activities. LWR fuel cycle activities are supported by a wealth of applicable critical experiment benchmarks that allow margins of subcriticality to be well-defined. In contrast, few critical experiments are clearly applicable to several portions of the HTGR fuel cycle. This work identifies HTGR fuel cycle activities presenting potential concern for reliable demonstration of an adequate margin of subcriticality. Recommendations are developed to address these areas of concern.

TABLE OF CONTENTS

Page

TABLE OF CONTENTS (continued)

TABLE OF CONTENTS (continued)

Page

TABLE OF CONTENTS (continued)

LIST OF FIGURES

LIST OF FIGURES (continued)

LIST OF FIGURES (continued)

LIST OF TABLES

LIST OF TABLES (continued)

1. INTRODUCTION

This paper presents work performed under Tasks 1 and 2 of the Nuclear Regulatory Commission (NRC) project JCN N6773, titled "Neutronics for Fuel Greater than 5 Weight % Enrichment."

The objectives of Task 1 are to investigate and identify potential nuclear criticality safety (NCS) issues associated with future high temperature gas reactor (HTGR) fuel cycles and to recommend how these issues may be addressed.

The objectives of Task 2 are to assess currently available critical experiment benchmark data for applicability to future HTGR fuel cycles, to identify fuel cycle activities where inadequate coverage by benchmarks exists, and to recommend critical experiments to fill gaps in benchmark coverage.

For these objectives, the latest sensitivity and uncertainty (S/U) analysis techniques for NCS, as provided in the ORNL SCALE (Standardized Computer Analyses for Licensing Evaluation)[1] code system, are applied to identify gaps in benchmark coverage.

1.1 BACKGROUND

Several variations of high-temperature gas-cooled reactors (HTGRs) are under consideration in the United States and internationally for future nuclear power plants. The various designs focus on either of two fuel assembly types: pebble fuel or prismatic fuel. Both fuel forms employ carbon as a moderator. Prototypic test reactors employing both types of fuel have been or are being operated.

Basics of fuel fabrication techniques have been demonstrated at laboratory and pilot scales. However, fuel fabrication techniques continue to be developed, and many processing conditions and equipment design aspects of industrial-scale fuel production remain to be determined.

HTGR core neutronics and thermal properties necessitate consideration of fuel forms not based on simple low-enrichment uranium (LEU, defined here as unirradiated uranium enriched to 20 wt % or less in the ^{235}U isotope) and use of fuel reprocessing and recycling technologies. It is assumed that the initial generation of HTGRs in the United States will involve use of LEU as the fuel form in a "once-through" fuel cycle, with some or all of the fresh fuel being at enrichment levels above 5 wt % ^{235}U.

As "Generation I" and then "Generation II" LWRs were developed, operated, and improved, the LWR fuel cycle development and deployment was actively supported by performance of critical experiments. Consistent with the technology needs at the time, these experiments focused on unirradiated LEU having ^{235}U enrichments not exceeding 5 wt %. The experiments generally focused on well-moderated (by water) conditions that were judged to present the greatest accident risk. The experiments addressed both homogeneous fuel-moderator mixtures (e.g., solutions) and heterogeneous fuel-moderator mixtures. However, the heterogeneous experiments were typically limited to LWR fuel rod or fuel assembly forms, and usually did not address extremely overmoderated or unmoderated rod spacing.

In comparison, few critical experiments have been performed that support industrial-scale deployment of once-through LEU HTGR fuel cycles. Some portions of the current critical experiment database are applicable to some HTGR fuel cycle activities, but there are some future HTGR fuel cycle activities for which the current critical experiment database is inadequate.

In recent years, the NRC has sponsored development of advanced S/U methods for NCS. These methods serve multiple purposes, such as

- assessing similarity of postulated normal or abnormal fuel material configurations ("application models") and critical experiment benchmarks ("similarity" refers to the extent to which computational biases for benchmark experiments and computational biases in application models are shared),
- determination of upper subcritical limits (k_{USL}'s) based on similarity coefficients of applications and experiments (k_{USL} refers to a maximum value of computed k_{eff} for an application that indicates a reliably subcritical condition),
- determination of bias "penalties" to account for gaps in validation coverage and/or uncertainties in neutron cross section data, and
- efficient design of critical experiments so as to obtain the maximum benefit from such measurements.

The overall objective of NRC Project N6773 is to apply technical expertise in nuclear fuel cycle technology and the latest developments in NCS S/U methods, so as to identify and help address criticality safety data issues that may be associated with deployment of a future HTGR fuel cycle in the United States.

1.2 SCOPE

The scope of this work is limited as follows:

- A once-through HTGR fuel cycle (no fuel reprocessing) with LEU feed is considered. The maximum enrichment considered for the LEU feed is 20 wt % ^{235}U.
- The initial process step considered is the uranium enrichment process.
- The final process step considered is long-term spent fuel storage at the reactor facility.

As prototypic bases for fuel design and associated fuel cycle activities, the Chinese High Temperature Reactor (HTR) and the Japanese High Temperature Test Reactor (HTTR) are primarily employed. As needed, additional information pertaining to potential HTGR fuel cycle activities are drawn from the United States Next Generation Nuclear Plant (NGNP) Project, the South African Pebble-Bed Modular Reactor (PBMR) Project, and other United States and international HTGR-related design efforts.

2. OVERVIEW OF THE FUEL CYCLE FOR HTGRS

Figure 2.1 provides an overview of major processing steps of the HTGR fuel cycle, presuming use of unirradiated enriched uranium as fuel and no fuel recycle. The initial fuel cycle steps leading to preparation of natural-enrichment UF_6 are shown for completeness; there are no associated criticality issues prior to UF_6 enrichment. Since the ultimate disposition of the spent fuel is unknown, the final step shown is long term storage at reactor facilities. Figure 2.1 includes neither other major storage steps within the fuel cycle nor transport steps (within and between facilities).

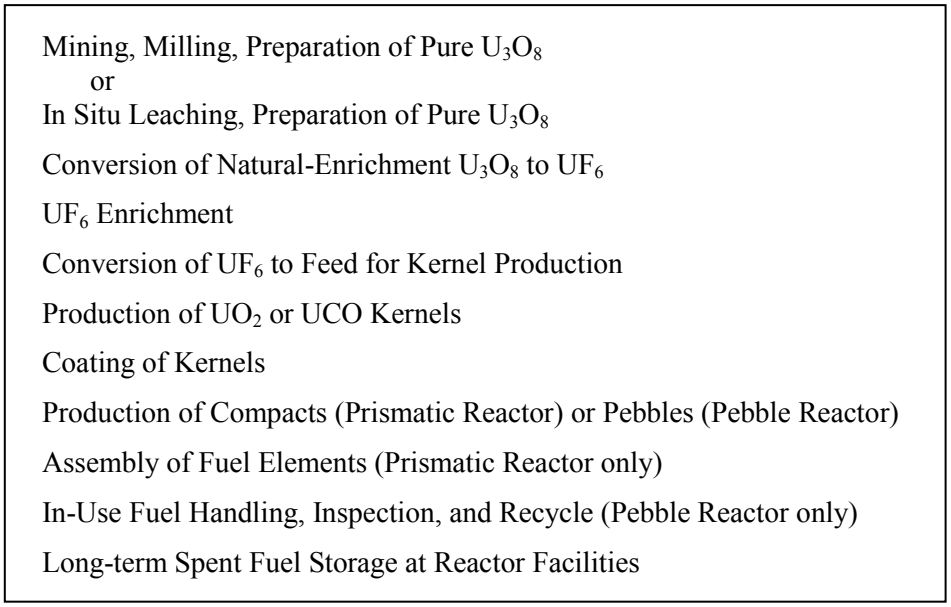

Figure 2.1. Major processing steps of HTGR fuel cycles.

It is anticipated that the next U.S. HTGR plant will result from the DOE Next Generation Nuclear Plant (NGNP) Project. Although participants in this project may include NRC licensees and foreign countries/companies, research and development, preparation, and transport of the NGNP reactor fuel to the reactor site are expected to be under DOE control. Front-end fuel cycle activities for the NGNP are not the focus of this paper. Instead, the focus is on industrial-scale fuel cycle activities that will be required if deployment of commercial U.S. HTGRs follows the NGNP demonstration.

The first two steps of the HTGR fuel cycle (preparation of natural-enrichment U_3O_8 and UF_6) are identical to the current United States once-through LWR fuel cycle. As noted, these fuel cycle steps have no associated nuclear criticality safety concerns and will not be discussed further.

The enrichment step of the HTGR fuel cycle has an important difference compared to the U.S. LWR fuel cycle: HTGR fuel will employ higher ^{235}U enrichment. Initial pebble reactors will likely utilize fuel of enrichment between 5% and 10%. Initial prismatic reactors will likely utilize fuel of above 10% (possibly up to ~20%) enrichment. Within the next few years, evolution of more advanced (higher burnup) LWR fuel designs will likely utilize fuel enrichments only slightly above 5%. Thus, deployment of an HTGR fuel cycle will require resolution of criticality safety issues in uranium enrichment facilities and for enriched UF_6 transport that are specifically related to the HTGR fuel cycle.

At an HTGR fuel fabrication facility, the first process will be to convert UF_6 into some other chemical form that is suitable feed for HTGR fuel kernel manufacture. There are generally two routes to

accomplish this. Existing LWR fuel manufacture could be maintained, where UF_6 is directly converted to uranium oxide using a "dry" process involving steam reaction with prompt removal of the HF vapor. The oxide could then be dissolved in nitric acid (and further steps performed) to yield a feed material for HTGR fuel kernel manufacture. Alternatively, the UF_6 could be reacted in a "wet" process with water to yield uranyl fluoride solution. Chemical complexion (to remove the HF reactant in the solution) and further purification/processing of the solution would then be performed to yield feed solution for fuel kernel manufacture.

The next major step in HTGR fuel fabrication is to convert the uranium feed solution into UO_2 or UCO fuel "kernels." [Uranium oxycarbide (UCO) is actually a mixture of UO_2 and uranium carbide (UC_2), typically with a stoichiometric ratio approximating $UC_{0.5}O_{1.5}$.] There are a wide variety of laboratory-tested process routes to achieve kernel production, but all involve initial processes with liquid forms of uranium and final processes that involve high temperature sintering of final, uncoated fuel particles. Further technology development in kernel production is likely.

Coating of the kernels is performed by continuous vapor deposition (CVD) techniques, using fluidized-bed chemical reactor technology to apply multiple coating layers to the kernels. The objective is to provide a robust, particle-level barrier to retain fission products even under high levels of burnup and temperature exposure. Such coated fuels particles are referred to as "CFPs" or "TRISO particles" (tri-layered isotropic-coated particles). Quality goals include achieving near-zero defects in particle coating. It appears this quality objective is doable even though a kilogram of uranium may consist of about one million CFPs, and a reactor's inventory may range well into the billions of CFPs. The success of particle coating is strongly related to aspects of kernel manufacture. Continued evolution of particle coating technology is also expected.

Production of HTGR fuel compacts or pebbles involves mixing of the CFPs with graphite powder and resin binders, pressing the mixture into desired shapes, and application of heat treatments. Pebble pressings are coated with a dense layer of graphite, machined, and further heat treated to form finished fuel pebbles. These processes must be performed in a manner to both avoid damage to the CFPs and to yield compacts or pebbles with required thermal conduction and mechanical integrity.

Fuel compacts must be loaded into prism-shaped, machined blocks of graphite to form prismatic fuel assemblies. This may involve sealing compacts into thin-wall graphite tubes which are then installed into the graphite blocks. Pebble manufacture will proceed to completion at the fuel fabrication facilities, but final assembly of compacts, graphite tubes, and graphite blocks may occur either at the fuel fabrication facility or the HTGR reactor facility.

Since the two types of HTGR fuel (pebbles and prismatic assemblies) are markedly different, storage, use, and handling at the reactor sites have significant differences.

At some point following initial start-up of a pebble reactor, addition of fresh pebbles to the upper portion of the reactor would commence. Pebbles would be routinely withdrawn from the lower portion of the reactor and either returned to the reactor or dispositioned to storage tanks. Thus pebble fuel is routinely transferred through a piping network that involves the reactor and multiple tanks (e.g., fresh pebble tanks, spent pebble tanks, interim storage tanks, damaged pebble tanks, dummy or carbon-only pebble tanks). This piping and tank network represents a major complication for operation of a pebble fuel reactor. Unless all tanks are designed for fresh pebbles (not likely), then criticality safety controls will have to be applied to the pebble management systems. These controls could involve limits on pebble inventory (e.g., how much partially burned fuel is allowed in an interim storage tank) or fuel burnup (e.g., radiation measurements to confirm some prescribed minimum burnup before transfer of pebbles to spent fuel

tanks). If burnup credit is employed, then data will be needed to accurately correlate radiation measurements to fuel composition and to validate criticality safety computational methods.

At prismatic HTGRs, management of fresh and spent prismatic fuel will be under more direct operator control. Again, depending on the design of spent fuel storage at HTGR facilities, burnup credit may or may not be a criticality safety issue.

For either pebble or prismatic fuel, whether fresh or spent, there will be economic and design factors that provide incentive for efficient storage of the fuel (i.e., without utilization of excessive facility structures and support systems). However, storage of pebble fuel will likely present greater criticality safety design issues, because compact placement of many pebbles into individually large tanks will be a favored storage approach. Prismatic fuel assembly storage can readily be designed to ensure some limited but controlled spacing between individual fuel assemblies. This can assist in storage designs that can accommodate large numbers of fuel prisms while assuring criticality safety by design, and perhaps with minimal or no reliance on fuel burnup.

Transport of enriched UF_6 from enrichment facilities to fuel fabrication facilities will present a licensing challenge due to criticality safety considerations. Although this paper addresses a limited portion of the criticality safety issue with transporting UF_6 enrichments of up to 20% in bulk containers, the overall risks will require a more comprehensive assessment to support licensing changes that will be desired.

Transport of fuel forms to the HTGR reactor sites would be performed in yet-to-be-designed shipping containers. Some currently licensed containers may exist for these types of fuel, but are not practical to support full-scale HTGR deployment.

This paper does not address transport of spent HTGR fuel from reactor sites to other locations, or the ultimate disposition of spent HTGR fuel.

3. CRITICALITY SAFETY CONSIDERATIONS AND DATA NEEDS FOR THE HTGR FUEL CYCLE

Section 3 discusses criticality safety aspects of individual activity areas for the HTGR fuel cycle. To support this objective, the information provided includes operational and design details of existing and proposed reactors, descriptions of technologies and methods for reactor fuel fabrication, and regulatory considerations. Much of Section 3 information is drawn from a number of open-literature, nonproprietary sources itemized in the reference list as References 2–64. Reference citations are not necessarily provided in Section 3, particularly where information discussed may be contained in multiple references.

3.1 NCS CONSIDERATIONS COMMON TO PRISMATIC AND PEBBLE REACTOR FUEL CYCLES

3.1.1 UF6 Enrichment

For the HTGR fuel cycle considered here (once-through use of enriched uranium fuel), the enrichment will be in the range of 5% to 20%. This will require that existing or future enrichment facilities be capable and licensed to perform uranium enrichments to higher levels than associated with current LWR fuel cycles.

Within enrichment processes, the primary margin of subcriticality is due to exclusion of significant amounts of neutron moderator materials from within the enrichment equipment. Neutron moderators are precluded by a combination of administrative controls over how the equipment is operated and equipment design features that prevent moderator entry.

For gaseous diffusion–based enrichment processes, large process equipment is required to house the diffusion membranes. To maintain the required pressure differentials and flow of UF_6 through these membranes, many large capacity pumps are required. The low efficiency of isotopic separation by diffusion, the large gas flow rates, and the need for various large-geometry auxiliary equipment components preclude design of diffusion plants in a manner that ensures subcriticality through limited geometry.

In contrast, more contemporary enrichment processes require fewer and smaller pumps, have smaller in-process uranium inventories, and may utilize connecting pipes and other components that can be designed with a geometry ensuring subcriticality. Thus, more modern enrichment processes can support production of higher enrichments of uranium, with margins of subcriticality independently supported by exclusion of moderators and (for a majority of the process) by geometric design.

Gaseous-based (UF_6) uranium enrichment processes are operated at less-than-atmospheric pressure to control worker exposure to HF vapor, a reaction by-product released by the chemical reaction of UF_6 with moisture in the air. However, this mode of operations results in some level of continual air in-leakage through locations in the system such as valves, seals, or other locations. A consequence of air in-leakage is that admitted atmospheric moisture reacts with UF_6 gas, resulting in potential deposits of various hydrated uranyl oxyfluoride compounds ($UO_xF_y{\cdot}zH_2O$).

Fissile deposits resulting from long-term accumulation caused by air in-leakage have been a criticality safety concern in historical gaseous diffusion plant operations, as exemplified by discovery in the 1990s of several deposits at the K-25 Gaseous Diffusion Plant in Oak Ridge, Tennessee.[2] The largest of these deposits was estimated to contain about 500 kg U at 3.3% enrichment. For such deposits resulting from air in-leakage, it appears that the moderation ratio [defined as the hydrogen to uranium atom ratio (H:U

ratio)] of the deposits may be inherently limited. In the K-25 example, the H:U ratio of the largest deposit was only about 3.5. Although this deposit did present a significant criticality safety concern, the as-found deposit was subcritical due to the low enrichment of the uranium, the low moderation ratio, and the distribution of the deposit.

Such a deposit as that found at the K-25 plant is less likely with modern UF_6-based enrichment technologies and would likely present significantly lesser criticality safety concern. For example, for the centrifuge process at the National Enrichment Facility (New Mexico), the maximum size of the UF_6 product pipe work is 5.9 in. in diameter.[3] Such a limited diameter remains subcritical for uranyl oxyfluoride deposits regardless of uranium mass or H:U ratio, for uranium enrichments up to 20%.

Most currently licensed or planned domestic sources for uranium enrichment are limited to maximum enrichments of ~5%. These facilities would require criticality safety reassessment to address the higher enrichments and to support licensing revisions related to the HTGR fuel cycles.

Some equipment- or process-specific criticality safety issues are likely to be determined by such new analysis. For example, the National Enrichment Facility utilizes some process equipment (such as cold traps and chemical traps) that range up to an 8 in. diameter, with a maximum analyzed enrichment value of 6%. All current and planned domestic enrichment facilities use 30-in.-diameter (or larger) cylinders for UF_6 storage and transport; this practice would necessitate reassessments and licensing revisions to address HTGR-level enrichments.

3.1.2 UF_6 Transport

To support the HTGR fuel cycle, bulk transport of solid UF_6 from enrichment facilities to fuel fabrication facilities, at enrichments above 5%, will be required. Per unit of generated electricity, the amount of enriched UF_6 to be transported will be less for the HTGR fuel cycle than for the current LWR fuel cycle, due to (a) the higher ^{235}U enrichment of the UF_6, (b) the higher burnup achievable in HTGRs, and (c) the higher thermal efficiency of HTGRs. However, the number of UF_6 packages to be transported (for a given amount of electricity production) could be greater than or less than for the current LWR fuel cycle, depending on the particular enrichment(s) used for the HTGR fuel cycle and future regulatory decisions for enriched UF_6 packaging. Current regulatory requirements for transport are discussed below.

For enriched UF_6 transport in "specification packages," requirements of 49 CFR[4] §173.417 (b)(3) must be met. As part of those requirements,

- the UF_6 cylinder must be designed and maintained according to ANSI N14.1,[5] *American National Standards Institute: Nuclear Materials—Uranium Hexafluoride—Packaging for Transport;*
- the cylinder must be enclosed within a protective overpack meeting design and construction requirements of 49 CFR §178.356 (for 5-, 8-, and 12-in.-diameter cylinders) or 49 CFR §178.358 (for 30 in. cylinders); and
- cylinder loadings must not exceed limits of Table 3.1.

Table 3.1. Current regulatory limits for UF_6 transport cylinders as "Specification Packages" [*Source*: 49 CFR §173.417 (b)(3)]

Cylinder diameter (in.)	Maximum weight of UF_6 contents (kg)	Maximum ^{235}U enrichment (wt % ^{235}U)
5	25	100.0
8	116	12.5
12	209	5.0
30	2250 or 2282[a]	5.0

[a]The lower value is for "30A" cylinders, the upper value is for "30B" cylinders. For the 30 in. cylinders, the maximum allowed H:U atom ratio is 0.088.

Not shown on Table 3.1 are 48-in.-diameter UF_6 transport cylinders. The model 48X cylinder (9540 kg UF_6 capacity) with an overpack is licensed as a performance package for shipment of UF_6 at 4.5% enrichment.[6]

The designs of the first three cylinders of Table 3.1 (diameters of 5, 8, or 12 in.) ensure subcriticality regardless of the level of hydrogen moderation present, for the stated enrichment limits. However, the 30- and 48-in.-diameter cylinders are of sufficient geometry that a criticality accident is physically possible within a single cylinder, either due to misloading (e.g., admission of sufficient neutron moderators prior to or during cylinder loading), or due to neutron moderator intrusion (e.g., breach of a cylinder during a transport accident coupled with entry of water due to fire-fighting, precipitation, or immersion).

Because individual 30 and 48 in. UF_6 cylinders are not intrinsically safe by design for ~5% enrichment UF_6 under water entry conditions, these large cylinders are designated as "moderation controlled." Title 49 CFR §173.417 (b)(3) and Ref. 6 restrict UF_6 shipments in the 30 and 48 in. cylinders to a maximum moderation ratio (H:U atom ratio) of 0.088. In practice, shippers assure this moderation ratio is not exceeded by verifying (by sampling) that the purity of the loaded UF_6 is greater than 99.5%.

As an alternative to "specification package" shipments of fissile materials, 49 CFR §173.417 (b)(1) allows for shipment of fissile materials in "performance packages." (Performance packages must meet design and approval requirements of 10 CFR[7] Part 71; requirements for performance packages are discussed in more detail below.) Since there are no currently approved performance packages for shipment of UF_6 at greater than 5% enrichment, the only currently authorized options for such shipments are the 5 and 8 in. UF_6 cylinders listed on Table 3.1 as specification packages.

For the current LWR fuel cycle, virtually all enriched UF_6 shipments are performed in 30-in.-diameter cylinders (as specification packages) and 48-in.-diameter cylinders (as performance packages). To move to a fuel cycle primarily based on use of the 5- or 8-in.-diameter UF_6 cylinders, significant nuclear industry cost would be incurred for capital expenditures, such as procurement of the cylinders and shipping overpacks, and modifications of enrichment and fuel fabrication facilities to accommodate loading, unloading, and handling of the smaller cylinder and package designs. Operating costs may increase due to a larger number of cylinder operations (more cylinder loading/unloading cycles and associated cylinder handling), and possibly greater transport costs would be incurred due to less efficient utilization of cargo space per individual transport vehicle.

As part of the HTGR fuel cycle development, a strong industry desire to obtain approval for shipments of greater than 5% enrichment UF_6 in 30 in. or larger UF_6 cylinders will occur. To obtain such approval, only two options exist:

- obtain regulatory approval for use of 30 in. or larger cylinders/overpacks as performance packages in accordance with 49 CFR §173.417 (b)(1) and 10 CFR Part 71, or
- obtain revision of the Code of Federal Regulations [49 CFR §173.417 (b)(3)] to increase the specification package enrichment limit for 30 in. cylinders/overpacks or to add the 48 in. cylinder with overpack, with an allowed enrichment above 5%.

Potential challenges exist for either option.

Title 10 CFR §71.55 and §71.59 provide a variety of technical requirements for each performance package design. Performance of the design under both regulatory-specified "normal" conditions of transport and "hypothetical accident conditions" of transport must be demonstrated by testing or analysis, or by a combination of testing and analysis. Subcriticality of the design, both for individual packages and for package arrays, must be demonstrated by criticality safety analysis. The primary design, testing, and analysis requirements of 10 CFR §71.55 and §71.59 are addressed below.

Title 10 CFR Part 71 requirements of particular interest for licensing of performance packages for enriched UF_6 transport are identified in §71.55(b), (c), and (g):

> 10 CFR §71.55(b)
> Except as provided in paragraph (c) or (g) of this section, a package used for the shipment of fissile material must be so designed and constructed and its contents so limited that it would be subcritical if water were to leak into the containment system, or liquid contents were to leak out of the containment system so that, under the following conditions, maximum reactivity of the fissile material would be attained:
>
> (1) The most reactive credible configuration consistent with the chemical and physical form of the material;
> (2) Moderation by water to the most reactive credible extent; and
> (3) Close full reflection of the containment system by water on all sides, or such greater reflection of the containment system as may additionally be provided by the surrounding material of the packaging.
>
> 10 CFR §71.55(c)
> The [NRC] Commission may approve exceptions to the requirements of paragraph (b) of this section if the package incorporates special design features that ensure that no single packaging error would permit leakage, and if appropriate measures are taken before each shipment to ensure that the containment system does not leak.
>
> 10 CFR §71.55(g)
> Packages containing uranium hexafluoride only are exempt from the requirements of paragraph (b) of this section provided that:
>
> (1) Following the tests specified in §71.73 ("Hypothetical accident conditions"), there is no physical contact between the valve body and any other component of the packaging, other than at its original point of attachment, and the valve remains leak tight;
> (2) There is an adequate quality control in the manufacture, maintenance, and repair of packaging;

(3) Each package is tested to demonstrate closure before each shipment; and
(4) The uranium is enriched to not more than 5 weight percent ^{235}U.

The subcriticality requirement of 10 CFR §71.55(b) is not met by the designs of the 30 or 48 in. UF_6 cylinders, and the exemption of 10 CFR §71.55(g) is not applicable for enrichments greater than 5%. Thus the only means to obtain approval, under current regulations, for shipment of 30 in. or larger UF_6 cylinders with enrichments of greater than 5% is 10 CFR §71.55(c): NRC Commission approval for exception to the subcriticality requirement of 10 CFR §71.55(b).

All package designs must be demonstrated as subcritical following damage that may result from regulatory-specified "hypothetical accident" condition tests. Current 30 and 48 in. UF_6 package designs (cylinders equipped with protective valve covers, cylinders contained within approved overpacks) can be shown to preclude water in-leakage following the regulatory puncture test:

> 10 CFR §71.73(c)(3)
> Puncture. A free drop of the specimen through a distance of 1 m (40 in.) in a position for which maximum damage is expected, onto the upper end of a solid, vertical, cylindrical, mild steel bar mounted on an essentially unyielding, horizontal surface. The bar must be 15 cm (6 in.) in diameter, with the top horizontal and its edge rounded to a radius of not more than 6 mm (0.25 in.), and of a length as to cause maximum damage to the package, but not less than 20 cm (8 in.) long. The long axis of the bar must be vertical.

A license applicant seeking approval for use of existing 30 or 48 in. UF_6 cylinder packages (at greater than 5% enrichment as a performance package) would likely use results of the regulatory-specified puncture test (40 in. drop onto a 6-in.-diameter post) as a basis for requesting exception to the subcriticality requirement of 10 CFR §71.55(b).

Federal Register Vol. 65, No. 137[8] states "NRC practice has been to certify fissile UF_6 packages (including the cylinder which is the containment vessel and a protective overpack) that are shown to be leak tight when subject to the hypothetical accident tests ...".

However, it is possible that future NCS licensing decisions for shipment of greater than 5% enrichment in the 30 or 48 in. cylinders will include consideration of the increased likelihood for a criticality accident, should water enter such a package due to a transport accident. The criticality accident risk (presuming water entry associated with a transport accident) may be far greater than the risk associated with water entry to cylinders currently limited to 5% enrichment material.

A second issue that may be encountered during licensing actions regards demonstration that a single cylinder of unmoderated UF_6 remains subcritical under the fully reflected condition requirement of 10 CFR §71.55(b)(3). As shown in Section 4, it is likely that for some enrichment less than 20%, the 48 in. cylinder design is not subcritical under this reflector condition.

A third issue is more general. There are few critical experiments that are applicable to unmoderated UF_6 calculations in the low enrichment (<20%) range, and uncertainties in nuclear data that affect computed k_{eff} values for such systems are large. To justify a license application (or regulatory revision) for enrichment increases, computations are necessary to demonstrate subcriticality of individual packages and arrays of packages under regulatory-specified conditions. As enrichment increases of ~7 % and higher are addressed, the validity of such computations will likely become a licensing concern.

These three technical issues, all related to use of 30 and 48 in. cylinders for UF_6 enriched to HTGR levels, are evaluated in subsequent sections of this paper.

3.1.3 UF_6 Storage

At both the enrichment facilities and at the fuel fabrication facilities, storage of UF_6 cylinders will be required in order to accommodate scheduling of production and transport activities.

For the larger UF_6 cylinders (48 and 30 in. diameters), storage of the cylinders in simple planar arrays, with no stacking, would be expected. At enrichment facilities, overpacks would not be typically employed during general cylinder storage. Instead, overpacking of cylinders would only occur as part of preparation for off-site shipment. At fuel fabrication facilities, cylinder storage may occur with or without overpacking. At fabrication facilities, there would be little incentive to store cylinders without overpacks, since the overpacks would likely be returned to the enrichment facility along with the emptied UF_6 cylinders.

Whether storage occurs with or without overpacks, the larger UF_6 cylinders should have an adequate margin of subcriticality for placement into a planar array configuration, provided there is no stacking of the containers, the containers remain undamaged, and the containers are subject to some evaluated enrichment limit.

Additional considerations for large cylinder storage involve where to permit container storage (i.e., outdoors or restricted to dedicated locations within facilities) and the means of container handling (e.g., typical forklifts, specially designed lifting machines, and overhead cranes).

Outdoor storage of cylinders without overpacks exposes the (painted) mild steel cylinders to weathering conditions and precipitation. Outdoor storage also may increase the probability of damage due to severe weather phenomena (e.g., projectiles driven by high winds/tornados). This is of particular relevance to storage of enriched uranium in the 30 and 48 in. cylinders if plausible mechanisms exist for breach of the cylinder wall followed by water entry.

Events involving undetected breach of large UF_6 cylinders in outdoor storage are known. In 1990, at the Portsmouth Gaseous Diffusion Plant, two 48 in. UF_6 cylinders (stored at separate locations) containing depleted UF_6 were found to have through-wall breaches.[9] The cause was determined to be operator error during forklift handling of the cylinders. The breach in each cylinder occurred at locations below the UF_6 fill line. Reaction of the UF_6 with atmospheric moisture and/or rain caused self-plugging of the ruptures but made subsequent detection less likely since the color of the reaction products was similar to the color of the paint on the mild steel walls. If similar damage were to occur to a cylinder of enriched UF_6, with the breach located above the UF_6 fill line, opportunity may exist for subsequent rainwater entry and collection, resulting in potential for a criticality accident.

3.1.4 UF_6 Conversion

The first chemical process step at HTGR fuel fabrication facilities will be conversion of enriched UF_6 to some form suitable as feed to the fuel kernel manufacture process. The choice of UF_6 conversion technique will likely be influenced by the process selected for manufacture of fuel kernels.

For HTGR fuel kernel manufacture, the most likely (and presently best proven) techniques for reliable manufacture of UO_2 or UCO fuel particles (kernels) involve uranium in an aqueous form (typically as uranyl nitrate solution), for the input feed to the initial kernel formation step. The chemical form and other specifications for the feed material for the kernel process will likely dictate what the most economic process is for UF_6 conversion.

The first operation for UF_6 conversion is known—phase change of the UF_6 and transfer into a reaction system. UF_6 transport cylinders will be removed from overpacks and placed into autoclaves to heat the solid UF_6 to either a liquid or gas phase for transfer. The means of autoclave heating is relevant to criticality safety of this operation step, because the autoclaves will be of sufficient geometry to support a criticality accident and there is some possibility of minor or major UF_6 leaks (i.e., valve or connection-line failure, cylinder rupture). If the autoclaves employ steam as the heat source (typical of some past UF_6 autoclave operations in the United States), then the combination of moderator provision, adequate fissile mass, and the large geometry of the autoclave may support credible criticality accident scenarios.

For the chemical reaction/conversion of the UF_6, there are two basic options: "dry process" and "wet process" routes.

The dry process route involves reaction of UF_6 vapor with steam and hydrogen in a cylindrical reactor. This route is currently the preferred and most economical route used for current U.S. manufacture of LWR fuel. The HF vapor by-product is routed to off-gas processing equipment for recovery of HF acid for other industrial uses. The UO_2 particulate is removed from the reactor for subsequent manufacturing steps.

The wet process routes involve reaction of UF_6 vapor (or possibly UF_6 liquid) with water. The wet process route, with UF_6 in the vapor phase, is the formerly preferred technique for U.S. LWR fuel manufacture. Alternatively, UF_6 vapor can be mixed with CO_2 and NH_3 gases and then reacted with water (this is the current manufacturing technique in Brazil). In the first option, the resulting UO_2F_2-HF solution is moved to other solution systems where ammonium is added to convert the uranium to ammonium diuranate (ADU) particulate, which is subsequently filtered as a "wet cake." In the second option, ammonium uranyl carbonate particulate is formed and then filtered. The ADU wet cake is transferred to furnaces for reaction with hydrogen to form UO_2. The ammonium uranyl carbonate wet cake is reacted with hydrogen and steam in furnaces to form UO_2. Since the furnace product is typically in the form of fused, hard "clumps," grinding of furnace product is required to obtain a uniform particulate for subsequent process steps.

The result of either the "dry" or "wet" processes summarized above is UO_2 particulate. For HTGR fuel manufacture, the most likely next step would be to dissolve the UO_2 in nitric acid, resulting in a pure uranyl nitrate solution.

Although the specific initial UF_6 chemical conversion means and subsequent chemical processing to prepare feed to HTGR fuel kernel manufacturing processes are not currently known, it is noted that the various operations described above are well-proven at an industrial scale, for uranium enrichments up to 5%. For all of the chemical conversion processes and equipment noted, criticality safety would need to be incorporated by design. This would primarily be done by use of limited equipment dimensions, based on the maximum uranium enrichment to be processed. To obtain desired production rates using limited geometry equipment (and thus limited throughput), use of parallel lines of chemical processing equipment will likely be needed.

The chemical conversion techniques will also involve several auxiliary feed and waste handling systems, such as reagent liquids or gases, waste liquids and solids, and multiple types of off-gas filtration and treatment. The systems used to convert UF_6 to forms suitable to HTGR fuel kernel manufacture will likely be complex, requiring detailed systems analysis to assure that criticality accident mechanisms are identified and suitably eliminated or controlled.

3.1.5 Kernel Fabrication

Kernel fabrication generally consists of two phases of operations: "wet" processing involving aqueous and possibly organic liquids, where the fissile material is either in solution or is present as a solids-liquids mixture, and "dry" processing, where minimal or no neutron moderator is present. There are a variety of solid, liquid, and gaseous reagents that may be used, depending on which kernel manufacturing technique is employed.

All kernel processing methods may be characterized as follows:

Feed (sometimes called "broth") preparatory steps

In the best-proven methods for HTGR fuel kernels, the fissile input is usually in the form of uranyl nitrate solution. To create the solution, a minimal amount of nitric acid is used, resulting in an "acid deficient" solution (essentially composed only of uranyl nitrate and water). There are kernel manufacturing methods in which the uranium oxide is not dissolved but is instead mixed with water in a suspension.

Depending on the kernel manufacturing method, a variety of reagents may be mixed with the uranyl nitrate solution or oxide suspension. Examples include

- few or no additives (for "external" gelation methods),
- hexamethylenetetramine (HMTA) and urea (for "internal" gelation methods), and
- sodium or ammonium salts of alginate plus certain additional metallic compounds that
- have bivalent or trivalent ion forms such as Ca^{2+} or Al^{3+} (for "suspension" methods).

Additionally, for formation of UCO fuel, some form of carbon-containing material (e.g., carbon black, Tamol) in fine particulate or liquid form will be a broth component.

Droplet formation steps

The broth is pumped through small, usually vertically oriented nozzles. The nozzles are subject to cyclic movement. The nozzle size, shape, orifice diameter, and mechanical movement (distance and speed), in conjunction with the feed material properties (e.g., viscosity), are carefully controlled to result in precise droplet size. Once emitted from the nozzles, the droplets immediately assume a spherical shape due to surface tension. This step of the process determines the fissile inventory in individual kernels.

Kernel formation steps

The droplets are created above the liquid level in a vertical column containing an aqueous liquid (e.g., ammonium hydroxide solution for "external" gelation processes, water for "suspension" processes) or an organic liquid (e.g., silicone oil, trichloroethylene). Most external gelation processes introduce the droplets into a flowing stream of ammonia gas, to solidify the outer shell of the droplets prior to the droplets entering the liquid media. Once in the liquid, the droplets further solidify due to reaction with ammonium hydroxide solution (for external gelation processes) or due to heat application (for internal gelation processes). The wet kernels are allowed to reside in the liquid of the column for some period of time to allow solidification to complete. This step is referred to as "aging" and usually involves some form of gentle mixing such as by introduction of a sparge gas.

Kernel washing steps

The kernels are "washed" with water, a water-miscible alcohol (e.g., isopropanol), or some other liquid. The washing step may be either in the initial column where the droplets and kernels were formed, or one or more separate columns to which the wet kernels are transferred. In general, the kernels are porous and/or permeable: washing steps remove unwanted liquids and soluble materials from inside the kernels.

Kernel drying steps

The wet or damp kernels are typically removed from the washing columns for drying at low temperatures (e.g., 100–180°C), usually under an air atmosphere. The drying step is intended to perform simple evaporation of water, alcohol, or other washing fluids.

Kernel furnace treatments

After drying, the kernels are moved from the drying apparatus for processing in one or more furnaces, usually in two stages of treatment (medium temperatures, e.g., 500 to 600°C, and high or sintering temperatures, e.g., 1500 to 1800°C). The medium-heat treatment decomposes and removes certain constituents that are either reaction by-products or are materials used as binders for droplet formation. Both the medium- and high-temperature treatments serve to reduce higher oxides (e.g., UO_3 or U_3O_8) to UO_2. Additionally, the high temperature treatment serves to cause reaction of some uranium to form UC_2 (for UCO fuels) and to fuse, or sinter, the uranium compounds to cause crystalline grain growth. The result of the grain growth is that porous void spaces in the kernels are removed and the average density of the kernels approaches to within 96% or more of theoretical density. For the medium- and high-temperature treatments, various gas flows may be maintained through the furnaces, such as hydrogen (for reduction of higher oxides), carbon monoxide (for UCO fuel manufacture), and carrier gases (such as argon).

For successful manufacture of HTGR fuel, it is vital that all specified parameters for the uncoated kernels be achieved: particle size, particle purity, near-spherical geometry, desired density, etc. Throughout the kernel manufacturing processes, quality control monitoring and sampling will be expected. There may be intermediate or final "sizing" steps, such as processing of dried kernels or final microspheres to remove oversize, undersize, or out-of-round kernels or microspheres. Chemical sampling, density measurements, and other inspections of the uncoated microspheres will be necessary.

Any out-of-specification kernel or microsphere batches, as well as materials subjected to destructive chemical or mechanical analysis processes, become salvage materials. The salvage materials are valuable and, if possible, must be reprocessed for reintroduction to the kernel manufacturing process. Reprocessing (often referred to as "recovery" or "recycle") may involve chemical operations such as dissolution, concentration, and purification. The recycle feed stream may represent several percent of the total fissile material flow through the kernel manufacturing process. Recycle equipment could include acid dissolvers, solution evaporators, and solvent extraction systems (such as pulse columns, mixer-settlers, or ion exchange columns). For both the kernel manufacturing and recycle operations, there will be solid, liquid, and gaseous waste streams potentially containing fissile material.

Criticality safety considerations will likely be the limiting design factor for many equipment components in the kernel manufacture and recycle systems. For most equipment items, incorporation of criticality safety via limited equipment dimensions would be the primary means of criticality prevention. To achieve desired manufacturing rates, some individual processing steps (e.g., the kernel formation step) will require multiple identical equipment items operated in parallel.

In general, the radius of the initial droplets and the wet and dried kernels is on the order of ~1000 to 3000 μm. The radius of the final uncoated microspheres is ~500 to 2000 μm. In certain "wet" portions of the kernel manufacturing process, the fissile material and liquids will not be a homogeneous (solution-like) mixture. Also, for possible off-normal conditions involving water intrusion into dry processes, the resulting fissile mixtures will not be homogeneous. Depending on the extent of heterogeneity and the uranium enrichment levels, moderated low-enrichment uranium configurations may have a higher neutron multiplication factor (i.e., a higher value of k_{eff}) than for comparable homogeneous fissile solutions. The criticality safety evaluations for the kernel manufacturing process will need to include this consideration.

Another criticality safety consideration for kernel formation and purification processes for recycle material is that some organic liquids have a hydrogen density greater than that of water. Thus, the specific organic liquids that may be used in the kernel manufacture or the recycle processes need to be addressed in the criticality safety evaluations.

Even though the final uncoated microspheres and upstream materials may contain carbon (in the case of UCO fuel manufacture), the expected proportions of carbon and uranium are sufficiently low that for most kernel manufacturing steps, the limiting moderator conditions for criticality analyses will be associated with various hydrogenous liquids.

3.1.6 Kernel Coating

One of the most important safety aspects of HTGR fuel is that the individual fuel particles, or kernels, are coated so as to reliably retain fission products under high burnup and temperature conditions.

Coated kernels are frequently referred to as coated fuel particles (CFPs) or "TRISO" (tri-structural isotropic) fuel particles. Most contemporary HTGR fuel particle coatings consist of a porous inner pyrolytic carbon (PyC) layer in contact with the fuel particle, a second denser PyC layer, a layer of silicon carbide (SiC), and a final dense layer of PyC. In some HTGR technology reports, the two inner PyC layers are identified as "IPyC" and the outer layer is identified as "OPyC."

The PyC layers are generated using various combinations of acetylene (C_2H_2) and argon (Ar), or propylene (C_3H_3) and argon. The SiC layer is generated using a mixture of hydrogen (H_2) and methyltrichlorosilane (CH_3SiCl_3, or MTS). As an alternative to the SiC layer, a zirconium carbide (ZrC) layer may be applied. If so, gases used to form the ZrC layer would include zirconium bromide ($ZrBr_4$), methane (CH_4), and hydrogen.

To achieve the TRISO coatings, fluidized-bed reactor systems (also called "coaters") are used. Industrial-scale fluidized reactors for HTGR particle coating will likely be operated in a batch-mode fashion, with charge loadings of at least a few kilograms of uncoated kernels. Reactant and carrier gases are admitted to the bottom of the coater through diffuser inlets, so as to "fluidize" the particle batch. The admitted gases are sequenced in stages to form the individual TRISO layers. Alternatively, a series of fluidized-bed reactors could be used, with each reactor applying only one particle layer.

As the particles are coated, it is vital that uniform-thickness particle layers be generated. The particles, fluidized by the up flowing gases, are in continual mechanical impact with each other and with the internal surfaces of the reactor vessel. This mechanical action poses a risk of damaging the developing particle layers. As the reactor charge increases, the gas flow rates needed to fluidize the particles and the mechanical loadings on the particles increase. As the diameter of the fluid bed increases, diffuser design to achieve uniform agitation becomes more difficult, and required gas flow rates increase (resulting in

increased mechanical loading on the particles). Thus, there are inherent limitations on the fluidized reactor design based on process and quality control issues.

As part of the fluidized reactor system, the reactor itself will be surrounded by a heating system (e.g., a graphite electrical-resistance heater). A cooling system (possibly employing water as the coolant) may be provided where gas lines connect to the reactor. A scrubber (using aqueous recirculating liquid) would be expected for treatment of emissions in the reactor exhaust line.

Systems will be needed to transfer uncoated kernel charges into the reactor and to withdraw coated-particle product. Such systems would include reactor feed and product vessels, and interconnected piping and valve controls. Feed and product transfers may be performed by use of vacuum or pressurized gas sweep (or both) as motive forces. Auxiliary equipment for the transfer systems (such as vacuum systems and off-gas filtration) would be included.

The particle coating process will require quality control monitoring and product sampling. As for kernel manufacture, sample materials and out-of-specification product batches will need to be reprocessed before return as feed to the kernel manufacturing process. However, coated particle reprocessing will be more difficult due to presence of SiC or ZrC particle coatings. Coated-particle salvage will need to be crushed to a particle diameter smaller than the SiC or ZrC coating diameter (to effectively break this coating for all particles). Crusher product can then be burned in a furnace to effectively remove all carbon of the PyC layers (and to convert the UC_2 of UCO fuel to uranium oxide). Nitric acid may be used to dissolve the uranium oxide, with SiC or ZrC materials being removed from the dissolver slurry by filtration. Complete dissolution may be more difficult than typical; the sintering treatment performed on the kernels may result in a crystalline structure for the oxide that resists ready dissolution in nitric acid. The dissolver product may require purification to remove excess nitric acid and contaminants, in order to meet feed specifications for the kernel manufacturing process.

Since the intended particle-coating operations all involve fissile material in a "dry" form, considerable criticality safety margin is expected for all normal-condition coating operations. The primary focus of the criticality analysis will be associated with postulated off-normal conditions that involve mixture of neutron-moderating liquids with the fuel particles. Example off-normal conditions that may require consideration are intrusion of water or scrubber fluid into a fluidized-bed reactor or feed/product handling vessels, or migration of fissile materials to the scrubber.

As noted for kernel manufacture, heterogeneity of postulated mixtures of fissile materials and moderator liquids must be considered in the criticality analyses for the particle coating process. The radius of the coated particles (with all layers applied) is expected to be in the range of ~800 to 2000 μm. Direct application of criticality data for homogeneous fissile mixtures to coated, uncoated, or partially coated fuel materials may not be conservative.

3.2 NCS CONSIDERATIONS SPECIFIC TO THE PRISMATIC REACTOR FUEL CYCLE

3.2.1 Pressing and Treatment of Compacts

Fuel compacts for HTGR prismatic reactors are expected to be in the shape of annular or solid cylinders. As example dimensions for an annular fuel compact, Japan's HTTR uses dimensions of 2.6 cm outer diameter, 1.0 cm inner diameter, and 3.9 cm height. The French ANTARES project proposes a solid cylindrical compact, with dimensions of 1.25 cm diameter and 5.0 cm height.

HTGR fuel compacts are anticipated to consist of coated fuel particles embedded in a carbon-based matrix. An example manufacturing sequence involves

- preparation of a mixture of graphite powder and a phenolic resin,
- blending of the coated fuel particles with the graphite-resin mixture,
- pressing of "green" compacts,
- a low-temperature furnace cycle (~200^{o}C) to polymerize the resin,
- a medium-temperature furnace cycle (~800^{o}C under N_2 flow) to drive off volatile organics, and
- a high-temperature furnace cycle (~1800^{o}C under vacuum) to harden the matrix and yield finished compacts.

The above process is only an example; considerable variations from the process outline given above may be found in HTGR technology reports.

Large numbers of compacts will be required for refueling of HTGRs, and thus this portion of HTGR fuel manufacture process will be automated to the extent practical. However, there is considerable industrial-scale experience with automation of similar operations for LWR fuel pellet manufacture. A primary technical challenge for HTGR compact manufacture is to avoid damage to the coated particles during the pressing operation.

There is little criticality safety concern associated specifically with the action of pressing compacts. The compacting operation will likely utilize one or more rotary tables, with the fissile material configurations and inventories of the tables not presenting a criticality safety concern.

Instead, the primary criticality safety foci associated with compact manufacture will likely be

- storage configurations (e.g., portable containers, storage racks) for coated particle feed awaiting input to the compact manufacturing process,
- the vessel(s) used to blend the coated particles with the graphite and binder materials,
- furnace loading configurations, and
- storage configurations for finished compacts (e.g., portable containers, storage racks).

In contemporary LWR pellet manufacturing operations, the vessel size and fissile inventories used for the blending of organic binder and UO_2 may be capable of supporting a criticality accident, due to either inadvertent water ingress, or due to excess charging of binder material. For HTGR fuel manufacture, the design of the graphite-resin-fuel blending vessel is identified as a focus area for future HTGR fuel cycle criticality safety analyses.

There may be a desire to maximize the fuel loading of a furnace, while also minimizing the internal volume and footprint of the furnace. The final furnace treatment requires very high temperatures and vacuum conditions. For this case, furnace designers may wish to have multiple vertical layers of trays of compacts within a furnace, with minimal free void space between trays laterally or vertically, and minimal free space elsewhere in the furnace interior. This type of configuration may present a challenge for future criticality safety analysis, if inadvertent water ingress to the furnace is possible during loading or unloading operations (or during furnace cool-down).

3.2.2 Assembly and Storage of Fuel Rods and Prismatic Elements

For prismatic HTGR reactors, the fuel compacts will likely be sealed within thin-wall graphite sleeves prior to loading into the hexagonal prism fuel blocks.

In the case of the HTTR, the fuel compacts were loaded into the graphite sleeves at the fuel fabrication facility and then transported to the reactor for installation in the graphite fuel blocks. Loading and sealing of compacts into the graphite sleeves, and loading of the graphite fuel rods into the graphite fuel block, are mechanical operations. For large-scale HTGR fuel fabrication operations, it is possible that one or both of these operations could be partially automated. Loading and sealing of the sleeves may be performed under a low-pressure helium atmosphere.

Exposure of the fuel rods and/or the completed fuel assemblies to temperatures typical of reactor operating temperatures may be performed as part of final fuel testing, to verify that the components remain undamaged due to thermal expansion expected at reactor operating temperatures. Such testing would be done within furnaces, possibly under an inert atmosphere.

There should be few criticality safety issues associated with handling and assembly of individual fuel rods or fuel assemblies due to the rather limited ^{235}U inventory of a single fuel assembly. More likely, the areas of focus for criticality safety of fuel rod and fuel assembly operations would be for

- storage configurations of fuel rods (e.g., portable containers, storage racks),
- storage configurations involving significant numbers of completed fuel assemblies, and
- material inventories and configurations within furnaces.

Using the HTTR fuel as an example, an individual fuel rod contains ~190 g U. Assuming a maximum enrichment of 20 wt % for some future, similar HTGR fuel rod design, a single fuel rod would likely contain no more than 40 g ^{235}U. However, the expected HTGR fuel rod dimensions are such that significant fissile inventories could be present in storage or as an individual furnace treatment operation. Thus, storage areas containing multikilogram ^{235}U inventories in fuel rod form will require criticality safety controls in the form of spacing and/or neutron absorbers to ensure subcriticality. Furnaces used to heat test fuel rods may employ similar controls and/or fissile mass limits.

Once HTGR fuel is in assembly form, significant numbers of assemblies, in rather compact arrangements, are necessary to achieve a criticality risk. This remains true even if burnable neutron absorbers are not present (or are not credited in the criticality safety analyses). However, there likely will be some forms of spacing and/or neutron absorber controls for loaded fuel assemblies, if significant inventories of these assemblies are present at the fuel fabrication or reactor sites.

At HTGR reactor sites, storage of fresh fuel will likely be in a configuration conducive to access by the reactor refueling/defueling machine. As an example of such an application, Japan's HTTR has a fresh fuel storage vault that is accessible from the floor level of the reactor high bay. The vault is located below the high bay floor level and consists of a number of individual steel storage tubes. Each tube contains a single column of fuel assemblies, stacked five levels high. Each tube is sealed by a top plate, which is removed for access of the fuel by the refueling/defueling machine. The storage tubes are arranged in a rectangular lattice, with adequate spacing between tubes to maintain subcriticality of the fresh fuel array under fully loaded conditions (an inventory equal to about 1.5 times the reactor capacity).

For fuel compacts, carbon is present as a neutron moderator. The overall ratio of carbon to ^{235}U remains below levels representing "optimum" neutron moderation. As a result, inadvertent introduction of water to furnace operations or storage configurations for compacts will likely represent the limiting (worst-case) upset condition for criticality safety analysis.

The fissile content of HTGR prismatic fuel is mixed with moderator at two differing scales of heterogeneity:

- the fissile particles are intermixed with carbon on a very small scale, as coatings on the kernels and the intervening carbon matrix within the compacts; and
- the fuel rods are moderated by graphite on a much larger scale, characterized by the rod diameter and spacing within the graphite fuel blocks.

For criticality safety calculations involving multigroup cross sections, problem-dependent cross section library adjustment techniques must be available to properly account for double-heterogeneity effects.

3.2.3 Transport of Fresh Prismatic Fuel Assemblies

To support future HTGR fuel transport, it is assumed that new shipping containers (specific to the fuel assembly dimensions) will be designed, licensed, and procured.

The new shipping containers could be designed to hold more than one fuel assembly per shipping container. If so, the number of assemblies per container would be small. More likely, the new shipping container design would accommodate one fuel assembly per container, to aid in package handling and to afford protection to individual assemblies during package handling and loading/unloading.

To license the package for transport, the normal-transport-condition criticality safety analyses required by 10 CFR 71 would require criticality data specific to the fuel assembly design (i.e., at the appropriate enrichment, with fuel rods configured in a graphite matrix in a fashion simulating the neutronics of the assembly design).

The hypothetical accident condition analyses would require additional criticality safety data appropriate to fuel assembly design, neutronically simulating conditions where water has intruded into void spaces of the fuel assemblies and packages, and between packages.

For both the normal-condition and hypothetical accident condition analyses, criticality data may be needed to address neutron-moderating and/or neutron-absorbing properties of the packaging materials. This need is dependent on the extent to which packaging materials affect determination of the package criticality safety index.

3.2.4 At-Reactor-Site Storage of Spent Prismatic Fuel

Future storage of spent prismatic fuel at future HTGR reactor sites is assumed to be only in the form of intact fuel assemblies. For purposes of this review, "spent" fuel is regarded to include any prismatic fuel assemblies removed from the reactor, regardless of the extent of fuel burnup. Also, handling of spent fuel assemblies (movement to or from storage) is regarded as part of storage operations.

The precise storage configuration or configurations for spent fuel at future U.S. HTGRs cannot be stated at this time. Some details are available to characterize facilities at Japan's HTTR for storage of prismatic fuel; the HTTR spent fuel storage facilities are used as an example to identify potential criticality safety issues and data needs.

For defueling, the containment dome in the reactor high bay is removed, and connection hardware is attached to one of several riser plugs in the top head of the reactor vessel. Using a high bay crane, the 150 ton fuel handling machine is placed over the riser. The fuel handling machine is shielded and may be used to retrieve and contain at least five fuel assemblies at a time. (One HTTR bibliographic reference

states the machine has a capacity for ten fuel assemblies.) Since each fuel column within the reactor contains five stacked fuel assemblies, a fuel handling machine capacity of at least five assemblies is desired to support relocation of partially burned fuel within the core.

A spent fuel storage pool is provided within the reactor building, accessible from the high bay. The water pool has concrete construction for the floor, walls, and ceiling, plus a stainless steel liner. The upper surface of the concrete ceiling is at the floor level of the high bay. Spent fuel is stored in vertical tubes, with fuel elements resting on each other in a vertical stack. A shielding plug is installed in the top of each storage tube, and the top surface of the shield plugs is flush with the high bay floor level. The portions of the storage tubes that hold fuel assemblies are below the pool's water level. Auxiliary systems are provided for cooling, recirculation, and filtration of the pool water. With this design, the spent fuel is stored dry, under a controlled atmosphere.

The spent fuel pool storage tubes are configured in a rectangular array (9 × 7 pattern); each tube can hold five stacked fuel assemblies. Thus the spent fuel pool capacity is 315 fuel assemblies, approximately twice the 150-assembly inventory of the reactor. Spent fuel is allowed to reside in the pool for approximately two years prior to being moved to a separate storage facility located at the HTTR site. Specific details of this long-term storage facility are not identified in the bibliographic references, but it appears this second storage facility does not involve use of water for heat removal.

For movement of spent fuel to the spent fuel storage pool, a storage tube shielding plug is removed, the fuel handling machine is moved from the reactor riser location and installed on top of the open storage tube, and up to five fuel assemblies are installed in the storage tube. The fuel handling machine is relocated and the shield plug is reinstalled.

For spent fuel storage, the criticality analysis would need to demonstrate subcriticality of the intended conditions for storage of spent fuel, with the spent fuel storage arrays completely loaded with the most reactive fuel assemblies allowed for storage. Additionally, the criticality analysis would need to determine credible off-normal storage conditions and demonstrate subcriticality for postulated credible off-normal conditions.

Examples of off-normal conditions that should be addressed in the criticality analysis include

- equipment failures, such as in-leakage of pool water to one or more storage tubes, in-leakage of water from some high bay source into one or more storage tubes, and loss of pool water;
- operational mistakes, such as placement of incorrect fuel assemblies into storage (assemblies with less burnup than required, if such operational limits are specified for criticality safety purposes), drop of a fuel assembly, and placement of a fuel assembly into a tube that already contains its limit of five assemblies; and
- natural phenomena effects, such as change of spacing between the storage tubes due to a seismic or dropped load event.

NCS computations addressing fuel storage must conservatively model the fuel composition, with adequate allowance to cover uncertainties for the fuel (and burnable absorber) makeup. Also, the computational method must be validated for the fuel compositions that are modeled.

Fuel for future HTGRs will likely incorporate burnable neutron absorbers. If the reactivity of future HTGR fuel increases with initial reactor exposure/burnup, two significant issues may exist for criticality analysis of HTGR spent fuel storage:

(1) how to predict and demonstrate conservatism for the fuel (and burnable absorber) compositions used in the criticality models, for maximum-reactivity partially burned fuel assemblies; and

(2) how to determine or account for potential bias (nonconservatism) in NCS code k_{eff} predictions, given little or no applicable benchmark data for partially burned HTGR fuels.

While similar issues exist for contemporary storage of BWR spent fuel, the extent of the material composition uncertainties and the absence of applicable benchmark data may be more significant for storage of HTGR spent prismatic fuel.

Existing core neutronics codes for BWRs (and pressurized water reactors, PWRs) are well-proven through hundreds of reactor-years of LWR operation. Codes that predict isotopic and compositional changes in LWR fuel (and burnable absorbers) have reasonable analytic (chemical and isotopic) measurement bases for comparison/checking of code predictions. In contrast, operation of the initial generation of HTGRs will be done with newly developed neutronics codes and little or no measurement data for spent fuel compositions (which vary as a function of fuel design, fuel burnup, and reactor operating conditions such as temperature and power levels).

As one design approach for storage of HTGR spent fuel, the storage facilities could be designed utilizing a fresh-fuel model (based on assemblies having the highest ^{235}U enrichment and loading), but with the burnable neutron absorber omitted from the NCS models. This approach would result in a conservative NCS model, with very small uncertainties in the modeled fuel composition. For this approach, NCS code validation could be more easily demonstrated, since initial reactor start-up configurations could be utilized as part of the validation effort. However, this approach may increase costs associated with the spent fuel storage designs.

The NCS data needs to support spent fuel storage strongly depend on the margin of subcriticality built into the spent fuel storage configurations, and the approach used by the NCS analysis to conservatively model the spent fuel.

3.3 NCS CONSIDERATIONS SPECIFIC TO THE PEBBLE REACTOR FUEL CYCLE

3.3.1 Pressing, Treatment, and Machining of Pebbles

Fuel elements for HTGR pebble reactors are expected to be in the shape of spheres, approximately 6 cm in diameter. This diameter is used for China's HTR-10 and is the same diameter planned for pebble fuel for use in South Africa's PBMR.

Each HTGR pebble fuel will consist of a central sphere (approximately 5 cm in diameter) of coated fuel particles embedded in a carbon-based matrix. A layer of annealed graphite approximately 0.5 cm thick surrounds the fuel region to provide structural rigidity and neutron moderation.

An example manufacturing sequence involves

- preparation of a mixture of graphite powder and a phenolic resin;
- blending of the coated fuel particles with the graphite-resin mixture;
- pressing of the fuel region of the pebbles, followed by pressing of the outer graphite layer about the fuel region;
- a low-temperature furnace cycle (~800^{o}C, under argon) to carbonize the resin;
- a high-temperature furnace cycle (~2000^{o}C under vacuum) to complete volatilization and obtain high mechanical strength; and
- machining of the final pebbles to obtain the desired surface finish and shape.

As an individual HTGR will require large numbers of fuel pebbles, the pebble manufacture process will be automated as practical. A primary challenge for HTGR pebble manufacture is to obtain the desired mechanical strength for the fuel pebbles so that the pebbles can withstand impacts and weight loadings associated with in-reactor recycle operations.

There is little criticality safety concern associated specifically with the action of pressing or machining spheres, since each sphere will likely contain only 5 to 10 grams of heavy element. The primary criticality safety considerations for pebble manufacture are similar to those for HTGR compact manufacture:

- storage configurations (e.g., portable containers, storage racks) for coated particle feed awaiting input to the pebble manufacturing process,
- the vessel(s) used to blend the coated particles with the graphite and binder materials,
- furnace loading configurations, and
- storage configurations for finished pebbles (e.g., portable containers, storage racks).

3.3.2 Storage of Fresh Pebble Fuel

For HTGR fuel in finished pebble form, a significant inventory of fresh pebbles would be needed to achieve critical conditions provided there is no neutron moderator material other than that incorporated into the fuel form.

At the fuel fabrication facility, pebble storage will likely be in portable containers, to facilitate inventory management, handling, and preparation of the materials for transport. Such containers would likely be of metal outer construction, with the containers being securely closed during on-site movement and storage.

For fuel pebbles at the storage facility, NCS controls would be expected for containers used for pebble handling and storage and for storage arrays where such containers are accumulated.

At HTGR reactor sites, storage of fresh pebbles will differ significantly from storage techniques at the fabrication facility. Reactor site storage of fresh pebble fuel is addressed in Section 3.3.4.

3.3.3 Transport of Fresh Pebble Fuel

There are likely currently licensed shipping containers for which pebble fuel is a permitted fuel form. However, the large numbers of pebbles needed to support reactor fueling operations warrant development of a more practical shipping container design, specific to the new fuel form.

Even though very large, bulk transport containers for fresh fuel could be designed, it is more likely that the new shipping containers will be based on standard industry drums or boxes, using economical packaging/cushioning materials (e.g., foamglas) to protect the contents. Due to the large inventory of pebbles required to achieve critical conditions, division of a bulk shipment into multiple individual packages (with some spacing between payloads afforded by container and packaging materials) should result in a container design warranting few or no additional specific design attributes for criticality safety.

3.3.4 At-Reactor-Site Fuel Handling and Storage Systems

New or recycled fuel pebbles are continuously fed into the top of the core region of HTGR pebble-bed reactors. At a similar rate, pebbles are withdrawn from the bottom of the reactor core. The additions or withdrawals are performed by pneumatic (helium as the motive gas) and gravity actions through piping

networks. Pebble transfers are performed at intervals ranging from one every few minutes, to one every few tens of seconds.

Within the HTGR core, the fuel loading is gradually moving downward. The fuel inventory/fuel level within the reactor can be adjusted, and additional non-fuel ("dummy") pebbles can be included in the core loading to adjust moderation levels within the core and/or to compensate for the fissile content of the fuel pebbles (e.g., as may be needed for initial reactor start-up). Individual fuel pebbles would reside in the reactor for a total of a few years, during which time each pebble would be routed through the recycle system several times.

Because of this on-line refueling and fuel mixing capability, it is unlikely that pebble-type HTGRs will incorporate burnable neutron absorbers into the fuel pebble design, or that fresh reactor fuel will consist of pebbles with varying ^{235}U enrichment levels.

Primary storage of spent fuel pebbles will be within tanks provided as part of the reactor fuel handling and storage systems. This may represent the only on-site storage method for spent fuel. Alternatively, on-site storage may employ some combination of storage in shielded casks (potentially similar to current on-site storage of LWR spent fuel in dry form) and storage in the tanks of the reactor fuel handling systems.

To further describe HTGR fuel pebble storage and handling, the conceptual design for the South African PBMR fuel handling and storage system (FHSS) design is used as an example.

Initial core designs for the PBMR included provision of a free-form central moderator-reflector consisting of graphite (dummy) pebbles. Later design proposals involved provision of a fixed column of graphite. Even if a fixed central column of graphite is employed, graphite pebbles will likely be distributed throughout the fuel pebbles during routine reactor operation.

The PBMR FHSS design included 12 tanks to hold spent fuel pebbles or "used" pebbles. "Used" pebbles refer to partially burned pebbles that are intended for return to the reactor. Used pebbles would not normally be stored in the tanks, except for reactor shutdowns for maintenance wherein partial or complete reactor defueling is required. Also, the FHSS design included two additional tanks, one for fresh fuel pebbles and one for graphite pebbles. These tanks were of design similar to the tanks for spent fuel, with potentially different dimensions and capacity and differing design features. (Heat removal and radiation shielding would not be factors in the fresh fuel tank design.) Several smaller tanks were included for collection and storage of damaged fuel pebbles.

As part of the PBMR FHSS design, each tank and the reactor would have pebble removal devices. Systems would be provided to detect damaged pebbles, to discriminate between fuel and graphite pebbles, and to measure the burnup of pebbles, as individual pebbles are routed from the core to various locations in the system. Since virtually all tanks need multiple interconnections, a rather complicated piping network for pebble transfer is needed. Throughout the piping network, there would be diverter valves to control routing of individual pebbles, and additional valves to apply pneumatic forces at various locations. Systems are needed for conditioning of air used to provide heat removal from the spent fuel pebble tanks, to remove dust generated within the piping system, and to allow remote maintenance. Essentially all of the FHSS tanks and transfer equipment would require shielding and confinement, with placement within the reactor building.

The FHSS design also allowed for transfer of spent fuel pebbles from the storage tanks to shielded casks, and to remove individual pebbles for analysis (e.g., for transfer to other facilities for destructive analyses).

The FHSS design for each spent fuel storage tank is a carbon-steel, vertical cylindrical tank, with the capacity for ~500,000 fuel pebbles, about 40% greater than the inventory of fuel pebbles in the reactor core. As described by bibliographic references, the criticality analysis for the PBMR spent fuel storage tanks takes credit that the pebble contents have a burnup level that is about 80% of the average burnup of pebbles in the reactor core. The spent fuel tank analysis demonstrated subcriticality for the case of optimum water moderation between fuel spheres, and for the case where pebbles are at the highest packing factor that can exist "in a finite volume" of spheres. Details of the PBMR FHSS criticality analyses are not available, so it is not clear whether all three conditions (burnup, moderation, packing fraction) were simultaneously considered, whether more than one tank was evaluated for presence of water moderator, or whether water reflection about a tank (or tanks) was considered as part of the water intrusion case.

Some bibliographic figures indicate the PBMR fresh pebble storage tank is of comparable dimensions to the design of spent fuel tanks, but the fresh pebble tank would not be expected to have air-cooling as the spent fuel tanks do. Conceptually, the FHSS could inadvertently route fuel pebbles to the graphite pebble storage tank.

For at-reactor pebble fuel handling systems, examples of off-normal conditions that should be addressed in the criticality analysis (and demonstrated to be subcritical for conditions determined to be credible) include

- equipment failures, such as introduction of water to fuel storage tanks due to broken water lines or fire sprinkler system releases;
- operational mistakes, such as routing of fuel of excess reactivity to fuel storage tanks having burnup-exposure requirements for storage of fuel, and routing of fuel to graphite storage tanks; and
- natural phenomena effects, such as change of spacing of storage tanks or massive water entry to the shielded areas for fuel tanks due to a seismic event.

Although misrouting of fuel is listed as an example of an operational mistake, such may also be the result of equipment failures, or a combination of human and equipment failures, due to the automation of the pebble fuel handling and storage systems.

4. PROCESS APPLICATION MODELS AND COMPUTED DATA

4.1 INTRODUCTION

This section provides computed data illustrating the relationship of critical conditions or values (e.g., k_{eff}, critical mass, critical dimension) as a function of physical parameters (e.g., enrichment, neutron moderation, and material configuration) for the HTGR fuel cycle. Although computed k_{eff} biases or uncertainties are not assessed in this section, the results help identify fuel cycle activities where focus should be placed on assurance of adequate margins of subcriticality.

Hypothetical fissile material configurations are identified for use by Section 6 as HTGR fuel cycle "application models." In Section 6, the similarities of the application models to available critical experiment benchmarks are assessed. "Comparison models" are also identified for Section 6 use. The primary difference of the comparison and application models is that the comparison models have ^{235}U enrichments that are outside the HTGR fuel cycle enrichment range. The comparison models assist in determining the utility of critical experiment benchmarks that are outside the HTGR enrichment range.

Although many application models have very simple configurations (e.g., sphere or cylinder geometry), the criticality physics of those models should be reasonably representative of the physics of many HTGR normal- or upset-condition fissile material configurations.

Some configurations are presented for computed k_{eff} values of 0.95 (or 0.90). The sole purpose of these presentations is to illustrate the relationship of k_{eff} to fissile inventory. Due to the limited availability of critical benchmarks applicable to the HTGR fuel cycle, the reader should not assume that the associated computed margins (e.g., 0.05 or 0.10) can be technically defended as providing adequate margins of subcriticality.

All computations of this section were performed using an ORNL configuration-controlled, prerelease version of SCALE 6.1 and ENDF/B-VII neutron cross section libraries. The library formats used were either the continuous-energy format ("CE_V7") or the 238-energy-group multigroup format ("V7-238").

4.2 URANIUM HEXAFLUORIDE (UF_6)

4.2.1 k-infinity as a Function of Enrichment for Unmoderated UF_6

A material model for pure UF_6 was developed, limited solely to the isotopes of ^{234}U, ^{235}U, ^{238}U and ^{19}F. The unmoderated UF_6 model had an F:U atom ratio of six and no impurities or residual HF content. As the ^{235}U content was varied from natural isotopic content up to 100%, the ^{234}U:^{235}U atom ratio was also varied so as to represent uranium isotopic ratios associated with an idealized enrichment cascade operation.

The k-infinity (k_∞) results are illustrated by Figure 4.1.

Figure 4.1 indicates that for the enrichment range of the current LWR fuel cycle (~5% ^{235}U or less), critical conditions are not physically possible with unmoderated UF_6 regardless of material inventory or geometry. One may regard the critical mass to be infinite, but it is more appropriate to view the concept of critical mass as "not applicable" for unmoderated UF_6 in the LWR enrichment range.

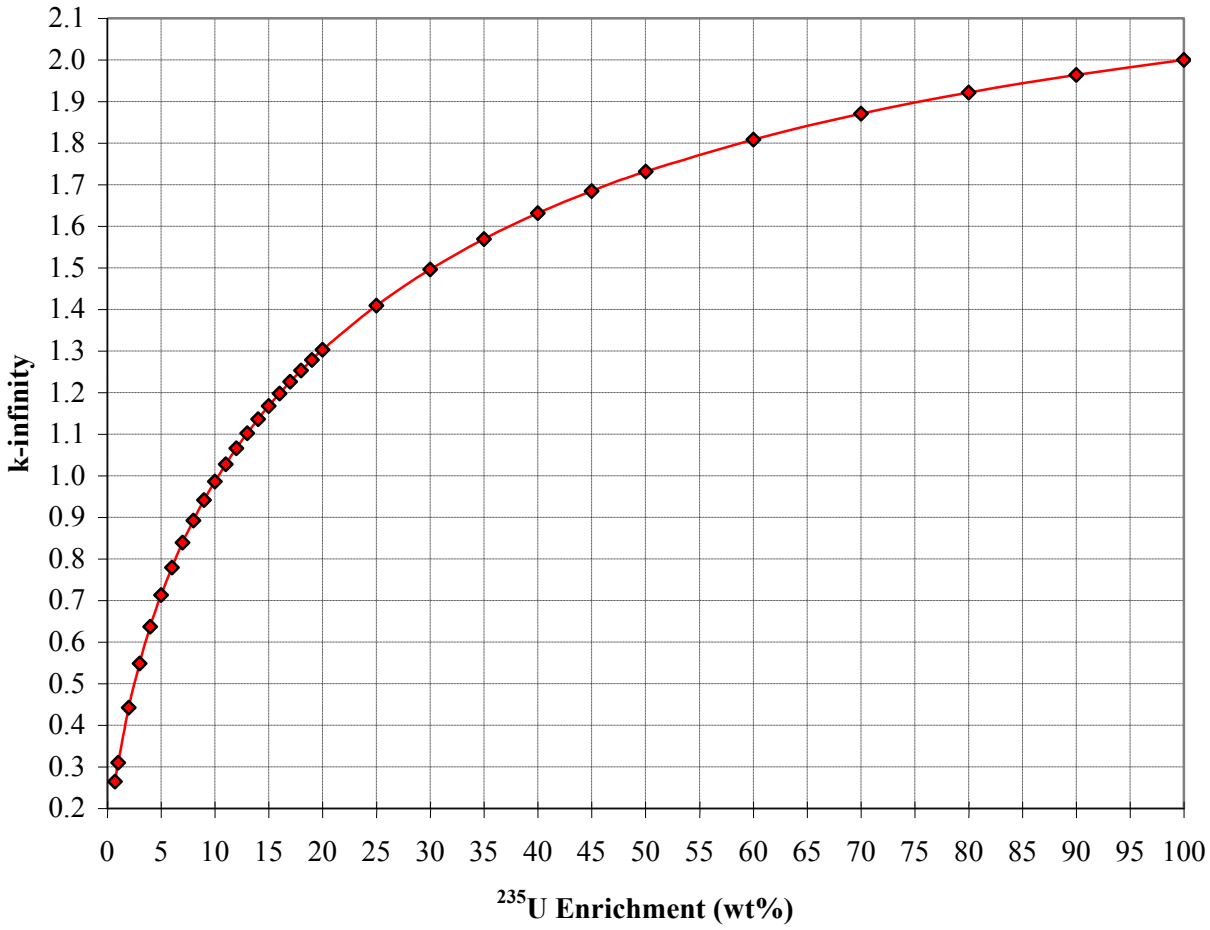

Figure 4.1. Computed k_∞ as function of ^{235}U enrichment for unmoderated UF_6.

The current enrichment services industry handles and transports enriched UF_6 in bulk-quantity containers with designations such "30B" (~2.5 metric ton capacity) and "48X" (~10 metric ton capacity).[6,19,20,21] Provided that the UF_6 remains unmoderated and is at LWR enrichment levels, there is no criticality potential for a single UF_6 container. When many such containers are collocated (such as typically done for storage or transport), negligible criticality risk exists, even if moderator materials are present between the UF_6 containers.

However, at enrichments characteristic of the HTGR fuel cycle, the k_∞ for UF_6 may exceed unity and critical mass requirements are finite. Enrichment services for the HTGR fuel cycle will require application of design and administrative criticality controls for inventories of unmoderated UF_6. The technical analyses justifying these controls will necessarily involve computational analyses, with associated demonstrations that computed margins of subcriticality are adequate.

Using the computed data illustrated by Figure 4.1, a computed k_∞ value of unity is obtained at approximately 10.3% enrichment. A historical report for gaseous diffusion plant operations, K-1663,[65] identifies 7% ^{235}U as a subcritical enrichment limit for unmoderated UF_6.

If an HTGR fuel cycle is deployed using fuel enriched to the 5% to 10% range, use of a defined UF_6 subcritical enrichment limit (at or above the particular maximum HTGR enrichment) would present

significant design and operational incentives. Such a limit would avoid some potential design and operational impacts related to UF_6 handling and transport methods.

Reliance on the noted historical report (for a 7% enrichment limit) is probably not acceptable from current safety or regulatory perspectives. Few details as to how the limit was derived are documented in the report, and contemporary reliance on such a subcritical limit should be justified by contemporary criticality analysis methods. Within current industry-consensus standards for criticality safety (i.e., the ANSI/ANS-8-series standards), there is no subcritical enrichment value for unmoderated UF_6.

For these reasons, four of the data points of Figure 4.1 are retained for further analysis as HTGR application models: unmoderated UF_6, in infinite mass/geometry, at ^{235}U enrichments of 5, 7, 9, and 10.3%.

4.2.2 Idealized Spherical Geometries for Unmoderated UF_6

Computations were performed to investigate criticality parameters for simple-geometry systems of unmoderated UF_6 at greater than 10.3% enrichment. The theoretical (maximum) density[66] for natural-enrichment UF_6 was assumed to be 5.06 g/cm^3. This density value was slightly adjusted to obtain theoretical UF_6 density values as a function of ^{235}U enrichment.[67,68] The modeled geometry for the UF_6 was spherical, with a close-fitting, 30 cm water reflector surrounding the sphere.

Figure 4.2 illustrates the computed results.

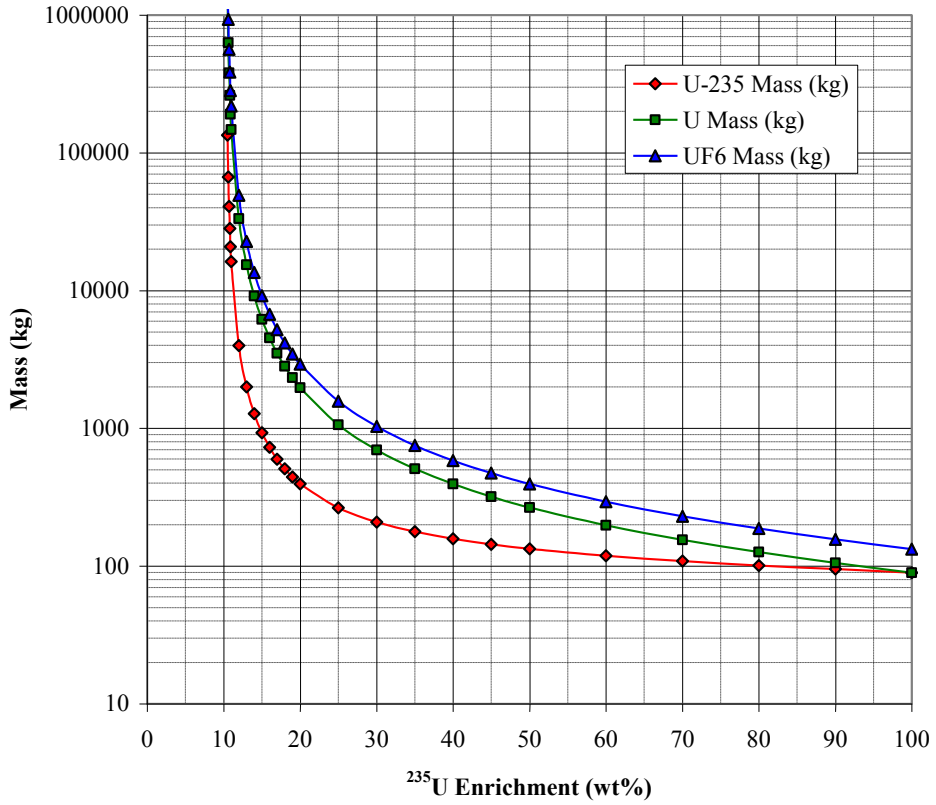

Figure 4.2. Data for spheres of unmoderated, water-reflected UF_6 as a function of ^{235}U enrichment for a computed k_{eff} value of 1.00.

Figure 4.2 illustrates the expected asymptotic behavior: as the ^{235}U enrichment is reduced from high levels and approaches the limiting critical enrichment, critical mass requirements increase to infinity.

The model used for Figure 4.2 includes what is (for most process situations) a highly conservative neutron reflector condition—a contacting, thick layer of water. Figure 4.3 examines the relationship of UF_6 mass to enrichment for three different reflector conditions: water-reflected (same data as Figure 4.2), concrete-reflected (a thick, contacting layer), and unreflected.

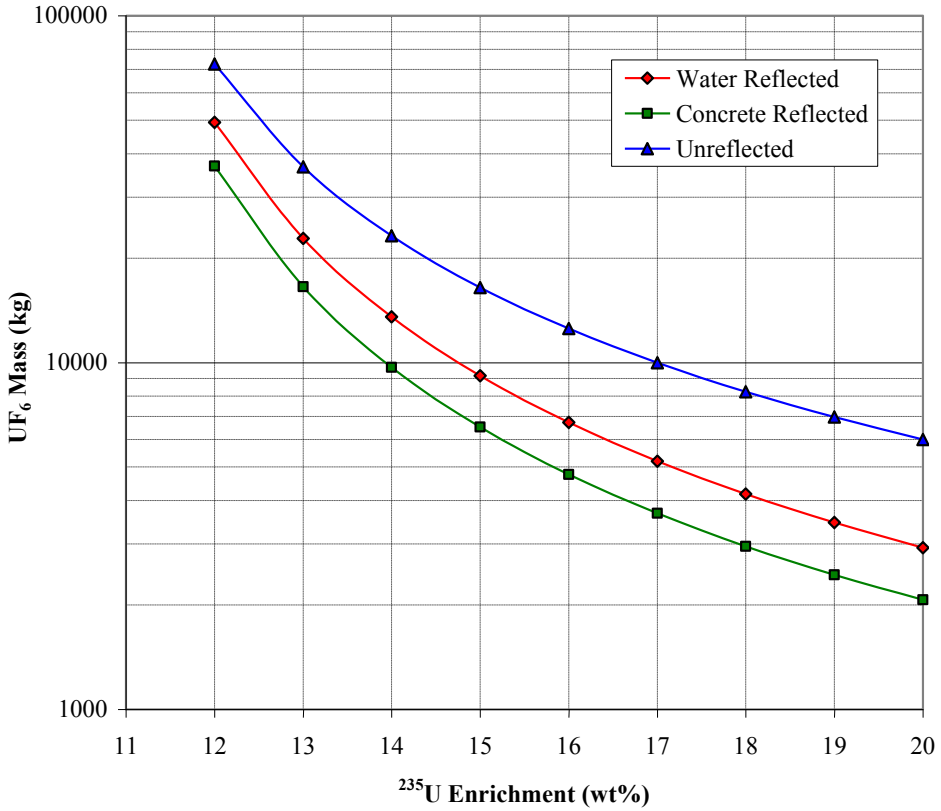

Figure 4.3. Data for spheres of unmoderated UF_6 as a function of ^{235}U enrichment and various reflector conditions, for a computed k_{eff} value of 1.00.

As the concrete model, the SCALE Standard Composition Library model of "Regulatory Concrete (NRC)" (input descriptor "REG-CONCRETE) was used. This concrete model reflects a typical concrete as may be manufactured using river rock as the coarse aggregate, silica sand for the fine aggregate, and Portland cement. The concrete density is 2.3 g/cm^3, and the hydrogen content (1 wt %) is equivalent to a water content of ~9 wt %.

Data of Figure 4.3 support a couple of observations. First, a fully water-reflected condition may not be an overly conservative condition for criticality safety analysis, since concrete is a significantly better neutron reflector than water for unmoderated UF_6. Partial reflection by concrete (due to facility construction) is a routine reflector condition.

Second, Figure 4.3 includes UF_6 mass values that are less than the design capacity of typical containers (e.g., 30B and 48X cylinders) currently used for enriched UF_6 handling and transport. The 30B cylinders are rated for loadings of ~2282 kg UF_6, and the 48X cylinders are rated for loadings of ~9540 kg UF_6.

Detailed criticality safety analyses will be required to authorize use of current industry-standard UF_6 cylinders for enriched uranium, in enrichment facilities that may produce UF_6 at enrichments in the 10% to 20% range. Such analyses must not only evaluate the intended enrichment level for particular cylinder models but must also evaluate credible misloading operations.

Four of the water-reflected UF_6 sphere configurations are retained for further analysis, at enrichments of 12, 15, 20, and 90% enrichment. The 90% enrichment case is a comparison case, used to simulate certain critical experiments involving highly enriched, unmoderated UF_6 described in report Y-DR-128.[69]

4.2.3 Relationship of Computed k_{eff} and Mass for Unmoderated UF_6

The primary objective of nuclear criticality safety computations is to assist in assuring that planned or credible fissile configurations are reliably subcritical. For this purpose, some upper limit (or limits) for computed k_{eff} values are derived using nuclear criticality safety validation methods. Such a limit is commonly referred to as an "upper subcritical limit" or "upper safety limit" and is designated by the symbol "k_{USL}."

A value or values for k_{USL} for unmoderated UF_6 is not derived by this paper, but calculations were performed to assess the potential impact of k_{USL} selection upon UF_6 inventory limits. Above, Figure 4.2 provided UF_6 inventory values for a computed k_{eff} value of 1.00. Similar calculations were performed to determine UF_6 inventories for computed k_{eff} values of 0.95 and 0.90. The results are shown by Figure 4.4. Note the significant mass differences of the curves for the differing k_{eff} values.

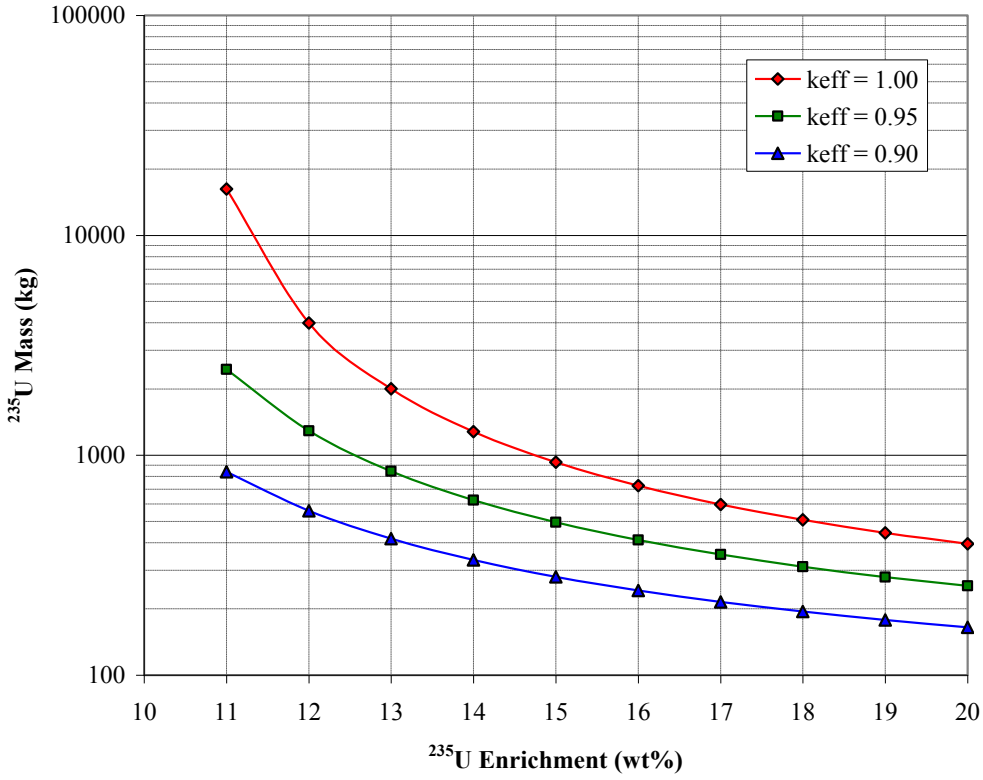

Figure 4.4. Data for spheres of water-reflected, unmoderated UF_6 spheres as a function of ^{235}U enrichment for computed k_{eff} values of 1.00, 0.95, and 0.90.

Similar information is presented in a different format by Figure 4.5.

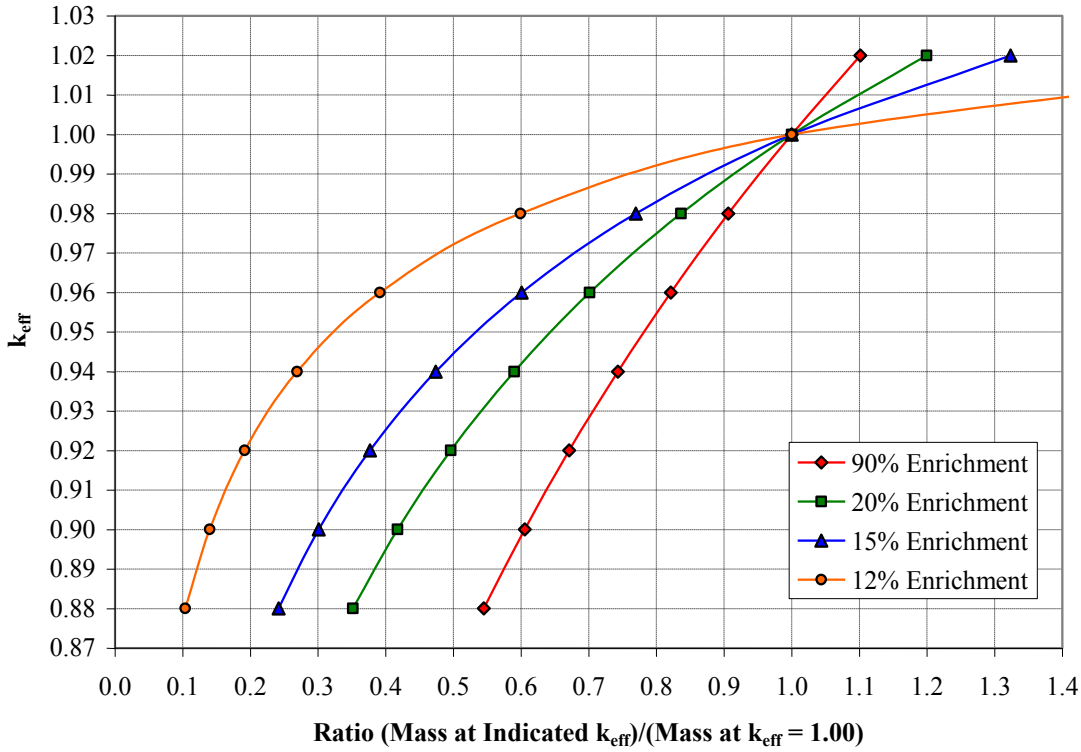

Figure 4.5. Mass ratio data for spheres of water-reflected, unmoderated UF_6 at various ^{235}U enrichments.

Figure 4.5 helps illustrate the impact of k_{USL} value on operational limits. If $k_{USL} = 0.96$ for 20% enrichment UF_6, then the allowed mass is 70% of what may be considered a "best-estimate" of critical mass requirements. If $k_{USL} = 0.92$, the allowed mass drops to 50% of estimated critical mass requirements. The impact increases as lower enrichments are considered.

4.2.4 Impact of Neutron Cross Section Uncertainties on Computational Results for Unmoderated UF_6

For low-enrichment, unmoderated UF_6 systems, the influences of neutron cross section uncertainties on computed k_{eff} values, derived mass estimates, and derivation of a limiting critical enrichment value are significant.

The SCALE TSUNAMI sequences were used to generate k_{eff} sensitivity data files (SDFs) for the application models, then the TSUNAMI-IP routine was used to predict the uncertainties in the computed k_{eff} values induced by uncertainties in cross section data. The most current and complete set of neutron cross section uncertainty data (the 44GROUPCOV covariance data file of SCALE6.0/6.1) was used for this evaluation. Although TSUNAMI-IP reports the uncertainty in computed k_{eff} values at the one-standard-deviation level, this uncertainty value does not necessarily represent a conventional statistical confidence level (e.g., application of a two-standard-deviation margin of TSUNAMI-IP results may not correspond to a 95% probability that the k_{eff} uncertainty is bounded).

One of the application models identified by Section 4.2.2 is a water-reflected sphere of UF_6 at 12% enrichment, having a computed k_{eff} value of 1.000. The uncertainty of this computed k_{eff} value, based on a one-standard-deviation uncertainty of neutron cross section data, is 2.75%. As shown by Figure 4.5, this k_{eff} uncertainty results in a very large fractional uncertainty in mass. If the selected value of k_{USL} corresponds to two standard deviations, the allowable mass of UF_6 is only 30% of the best-estimate critical mass value.

The k_{eff} uncertainty for low-enriched, unmoderated UF_6 systems has a similar impact for estimation of the limiting critical enrichment of UF_6. For the k_∞ case with a ^{235}U enrichment of 10.3%, a one-standard-deviation uncertainty for the calculated k_{eff} value is 2.80%. If a subcritical limit for unmoderated UF_6 was derived with primary reliance on estimated uncertainties in neutron cross section data, the result may differ little from the 7% value proposed in 1966.[65]

The two primary contributors to the calculated k_{eff} uncertainty values for the low-enriched, unmoderated UF_6 application models are uncertainties in ^{235}U and ^{238}U (n,γ) cross section data between 1 keV and 100 keV. Neutron capture cross sections for ^{19}F are relatively insignificant compared to capture cross sections for ^{235}U and ^{238}U, and neutron leakage from large geometry/large mass UF_6 systems is limited. Thus, neutron capture cross sections for ^{235}U and ^{238}U play a dominant role in determining computed k_{eff} values for these systems. Within the noted energy range, the ^{238}U (n,γ) cross section uncertainties range from about 10% to 35%. For ^{238}U, the peak energy-dependent sensitivity to (n,γ) cross sections occurs at about 10 keV, where the uncertainties in the ^{238}U capture cross sections range from 1.7 to 3.3%.

4.2.5 48 Inch (10 and 14 Ton) UF_6 Cylinders

The largest currently used cylinders for enriched UF_6 each have a nominal internal diameter of 48 in. and overall lengths of $9^1/_2$ or 12 ft, accommodating nominal UF_6 loadings of ~10 and ~14 tons. Currently, the maximum permitted enrichment for transport in the 48 in. cylinders is ~5% ^{235}U. Plans and safety evaluations exist for on-site use of these cylinders (at enrichment facilities) for ^{235}U enrichments up to 10%.[70,71]

A limited computational investigation was performed for a model 48X (10 ton) cylinder containing 20% enrichment unmoderated UF_6. Although it is unlikely that the 10 or 14 ton cylinders will be authorized for 20% enrichment material, these large cylinders are currently used for enriched UF_6 and would be involved in future enrichment services for the HTGR fuel cycle. The scenario analyzed here is the potential misloading of a 48X cylinder with an enrichment higher than intended.

The 48X cylinder model is based on ANSI N14.1-2001.[5] The model is a simple right-circular cylinder with an internal diameter of 48 in., an internal length corresponding to the minimum cylinder volume (108.9 ft^3), and a carbon steel wall thickness of 5/8 in.

The first case simulates a cylinder immediately after transfer of UF_6 to the cylinder. The cylinder is filled 95% full with liquid UF_6 at a density of 3.256 g/cm^3, with a temperature of 121°C. The cylinder axis is horizontal and the liquid geometry is a cylinder segment. The UF_6 material model includes admixed HF such that the H:U atom ratio is 0.088. This amount of hydrogen moderation is insignificant but is typically included in criticality safety models for UF_6 cylinders since the H:U value is the regulatory limit for moderator content in the large UF_6 cylinders. As a reflector condition, the cylinder is within a concrete box having wall thicknesses of 30 cm. The lateral interior walls and ceiling of the concrete reflector are located 30 cm from the cylinder walls, and the floor of the concrete reflector is located 6.35 cm (2.5 in.) from the cylinder.

A second case was performed with all conditions as described for the first 48X cylinder case, except that the cylinder contents are modeled in a solid condition (4.951 g/cm^3) at room temperature. The internal volume of the cylinder volume is ~62.5% filled. The UF_6 geometry is again modeled as a simple cylinder segment (the upper surface of the solidified UF_6 is modeled as flat).

The concrete reflector model used for these first two 48X cylinder cases could be viewed as overly conservative. A third 48X cylinder case was performed, identical to the second case, except that the only reflector is the bottom reflector. Equal or greater neutron reflection would be a normal condition for 48X cylinders, so this third model is nonconservative.

Figure 4.6 illustrates the geometry models for the three 48X cylinder cases and the computed k_{eff} results. The indicated k_{eff} uncertainty (±0.0002) is the statistical (Monte Carlo) uncertainty of the KENO-V.a result and is unrelated to the computed k_{eff} uncertainty associated with cross section covariance data. For the second and third cases, the modeled geometry of the solidified UF_6 within the cylinder may be nonrealistic. The subject of solid UF_6 configuration within a cylinder is discussed in the following section.

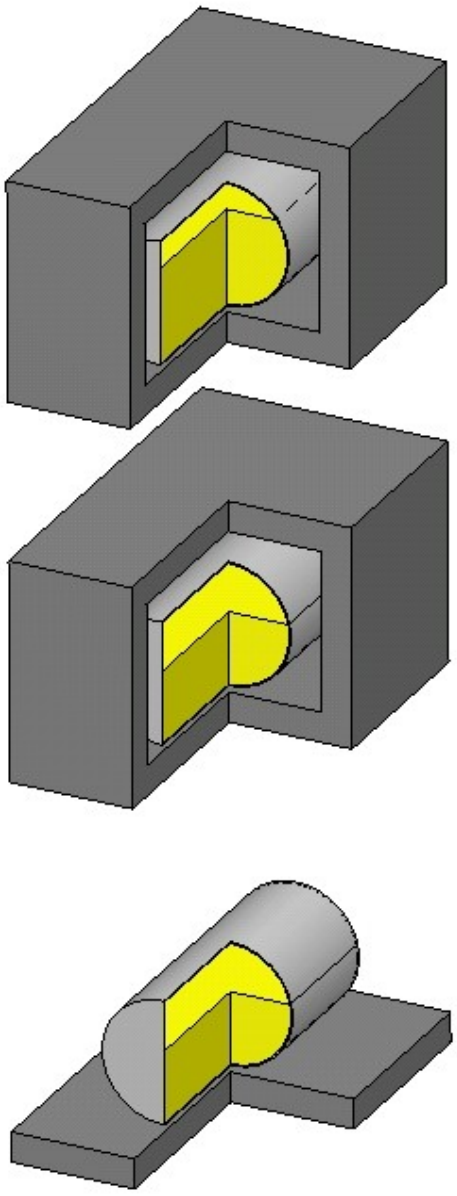

Case 1
48X Cylinder with liquid UF_6
Offset concrete reflector on all sides

k_{eff} = 0.9586 ± 0.0002

Case 2
48X Cylinder with solid UF_6
Offset concrete reflector on all sides

k_{eff} = 1.0209 ± 0.0002

Case 3
48X Cylinder with solid UF_6
Bottom concrete reflector only

k_{eff} = 1.0006 ± 0.0002

Figure 4.6. 48X cylinder models. All three models contain the same mass of 20% enrichment UF_6, with admixed HF such that the H:U atom ratio is 0.088. The right quarter of each model is removed.

Results for the 48X cylinder calculations suggest that inadvertent loading of a 48X (10 ton) UF_6 cylinder with UF_6 near 20% enrichment may result in a criticality accident.

Due to the large size and capacity of the 48 in. UF_6 cylinders, no application models for this type of container are developed. The simple-geometry UF_6 models described in prior sections should be adequate for comparison to critical benchmarks.

4.2.6 Individual 30 Inch ($2^1/_2$ Ton) UF_6 Cylinders of Unmoderated UF_6, With or Without Transport Overpacks

A more in-depth examination of the 30 in. UF_6 cylinder is performed here, because this container is likely to be used for future UF_6 transport, handling, and storage with ^{235}U enrichments greater than 5%.

The calculations performed and models developed are similar to those needed to obtain licensing for transport of 30B containers between facilities (public-sector transport). Also included are calculations and modeling simulating water intrusion into a 30B container. The derived 30B application models are also considered applicable to on-site use of the container at enrichment and fuel manufacturing facilities.

Single-cylinder and array models of 30B containers, with and without overpacks, are similar to those presented in report ORNL/TM-11947, "Criticality Safety Review of $2^1/_2$-, 10-, and 14-Ton UF_6 Cylinders."[72] The primary modeling differences are that this paper evaluates enrichments greater than 5% ^{235}U and the effects of water intrusion.

Physical overload of a UF_6 cylinder is possible and has infrequently occurred in past U.S. enrichment operations.[73] For any UF_6 cylinder at the rated maximum loading, the cylinder volume is about 95% filled when all contents are in a liquid state. If liquid UF_6 is added to a cylinder that already contains some inventory of UF_6 solid, an overload condition may result. When such a cylinder is later heated to liquefy the contents for material removal, the cylinder may hydraulically rupture. The consequences of such an accident are potentially severe (personnel fatality, radiological material release), so much care is taken to avoid UF_6 cylinder overload. The maximum physical amount of UF_6 that may be within a 30B cylinder under worst-case overload conditions is ~3600 kg UF_6. Here, overload of UF_6 cylinders is recognized as physically possible but very unlikely, based on the small number of gross overloading events for UF_6 cylinders (four) identified by Reference 73 as occurring in U.S. and Canadian facilities through 1986. Subsequent analysis considerations of this paper assume that any 30B cylinder contains no greater than the authorized UF_6 loading of ~2282 kg.

The distribution of solid UF_6 within a 30B (or other large) UF_6 cylinder is not well characterized and may differ from cylinder to cylinder. There are several reasons for this uncertainty:

- Although UF_6 solid has a much greater density that UF_6 liquid, this does not necessarily result in uniform buildup of crystalline UF_6 solid in the lower regions of a UF_6 cylinder. The thermal conductivity of solid UF_6 is low, and convection currents in the UF_6 liquid allow the liquid phase to lose heat more rapidly. As UF_6 crystals are formed, they may adhere to adjacent tank walls, while the UF_6 liquid level continues to decrease.
- UF_6 in the vapor state may freeze onto cylinder surfaces above the liquid level.
- UF_6 attached to the cylinder walls may or may not subsequently detach due to cylinder handling or environmental (temperature) factors.
- The mass of UF_6 in the larger cylinders is sufficiently large that several days may be required for all UF_6 loaded into a cylinder to fully solidify. At the enrichment facilities, cylinders may be transported from loading stations to storage locations prior to complete solidification of the contents. This may result in forces that rearrange masses of solidified UF_6 within cylinders containing a semisolid mix of both solid and liquid phases.

To investigate possible distributions of solid UF_6 within large cylinders, a video inspection was performed of the interior of a 48X cylinder in 1993. The video is currently maintained by the Depleted UF_6 Management Information Network at internet url: http://web.ead.anl.gov/uranium/guide/video/inside.cfm.[74]

The upper surface of the UF_6 was found to significantly deviate from a flat surface. Figure 4.7 depicts an approximate cross section view of the cylinder contents obtained from the website. Although most of the inventory appeared to be a dense agglomerate of UF_6, loose (particulate) UF_6 was observed, as well as layers of UF_6 adhering to interior side walls of the cylinder above elevations of the primary material mass. UF_6 "snow" was also observed. This was interpreted as indicating the cylinder contents were not yet at complete thermal equilibrium, even though the cylinder was loaded one month prior to the inspection.

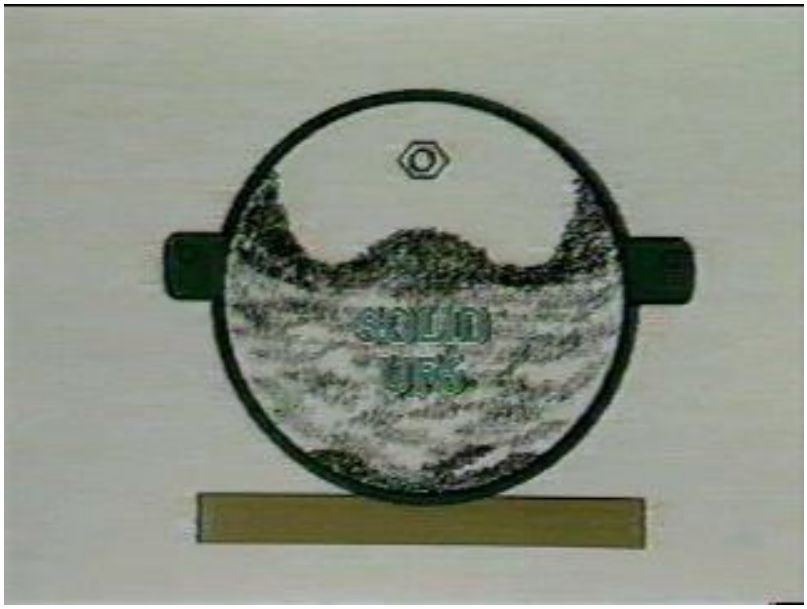

Figure 4.7. Graphical illustration of a cross section of a 48X cylinder indicating material distribution.[74] Items on the left and right of the cylinder indicate lifting lugs; the item within the upper portion of the cylinder represents the fill valve location.

For license of a package (container plus its overpack) for transport, 10 CFR[4] §71.55 (b) requires that a package must remain subcritical under conditions of "close full reflection of the containment system by water on all sides, or such greater reflection of the containment system as may additionally be provided by the surrounding material of the packaging." In demonstrating this requirement is met, "the most reactive credible configuration of the fissile material" must be considered.

Calculations were performed for individual 30B containers for

- four ^{235}U enrichments (5, 10, 15 and 20%);
- three reflector conditions (cylinder reflected by water, cylinder reflected by transport overpack, and cylinder reflected by a transport overpack and water); and
- four configurations of UF_6 within the container.

The 30B cylinder model used here is the same as that of ORNL/TM-11947.[72] It consists of a simple right-circular cylinder with walls of 0.5-in.-thick carbon steel and an internal volume (26.0 ft^3) matching the minimum allowable volume prescribed by ANSI N14.1-2001.[5]

The model for the 30B overpack geometry was also obtained from report ORNL/TM-11947. This model is based on the overpack description provided in 49 CFR[4] §178.358. Some design details of this model may have minor differences with certain specification overpacks for 30B containers,[19–21] such as type of

steel, but these differences should have very minor influence on the computed results presented here. The overpack consists of a phenolic foam layer, jacketed inside and outside by thin layers of carbon steel. The phenolic foam is a low-density material (~0.029 g/cm^3) which includes hydrogen (~0.001 g/cm^3) and natural boron (~0.001 g/cm^3). Figure 4.8 illustrates the model of a 30B UF_6 container with overpack. Radially, a very slight gap exists between the outside surface of the UF_6 cylinder model and the inner steel jacket of the overpack model. At either end of the UF_6 cylinder, there is a void region between the overpack and the cylinder. This gap simulates void space that exists due to inclusion of skirt rings on either end of the cylinder construction. The steel of these skirt rings is omitted from the cylinder models.

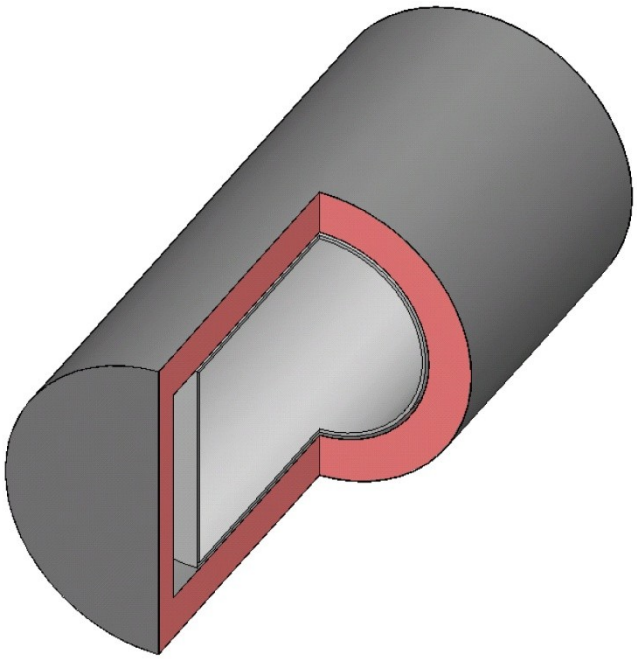

Figure 4.8. 30B cylinder and overpack model. A quarter section of the model is removed, and the cylinder contents are not shown.

For the water-reflected cylinder model, the thickness of water is 30 cm. For the model with both overpack and water reflection, the thickness of water about the overpack is 30 cm, and water is modeled as present in all void spaces within the overpack but external to the cylinder.

The UF_6 models included residual HF content, providing an H:U atom ratio of 0.088. The UF_6-HF mixtures were modeled at theoretical density and at lesser densities. The four modeled configurations (loads) for the material models are

- Load a—Material at 62.6% of theoretical density, cylinder volume 100% filled, right-circular-cylinder geometry;
- Load b—Material at 81.3% of theoretical density, cylinder volume 77.7% filled, cylinder segment geometry;
- Load c—Material at 100% of theoretical density, cylinder volume 62.6% filled, cylinder segment geometry; and
- Load d—Material at 100% of theoretical density, cylinder volume 62.6% filled, hollow cylinder geometry (uniform thickness of material in radial and axial directions).

Figure 4.9 illustrates the loading configurations.

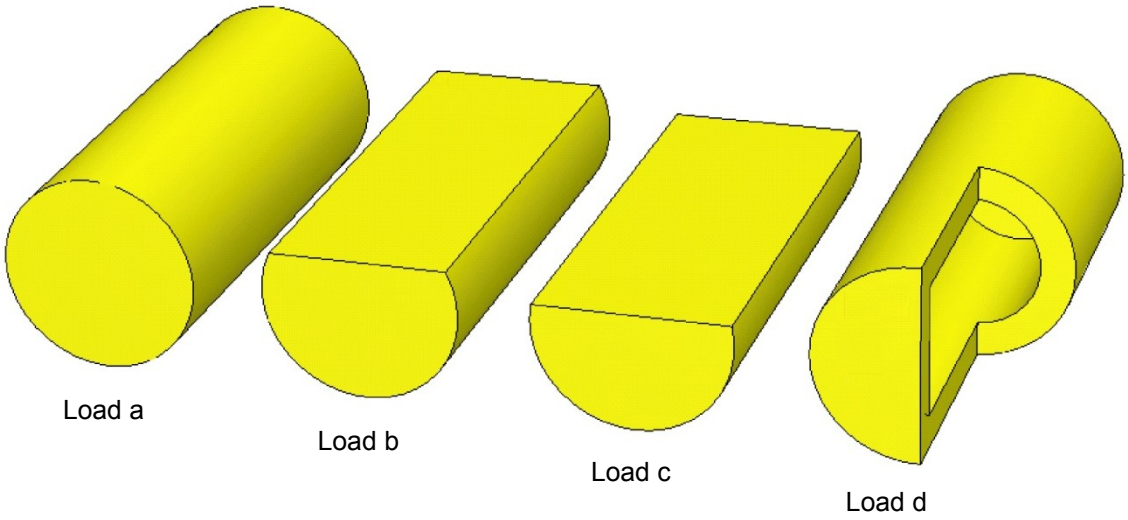

Figure 4.9. 30B cylinder loading models. A right-front quarter section is removed from Load d, so as to indicate the hollow cavity within the cylinder of UF_6.

Computed k_{eff} results for individual 30B cylinders and packages are provided by Table 4.1.

ORNL/TM-19947 provides computational results for certain cases of Table 4.1 (for 5% enrichment, for Loads a, c, and d). For these cases, ORNL-TM-19947 and Table 4.1 results are in close agreement.

All computed results of Table 4.1 are less than 1.00 as expected. The modeled UF_6 loading per package (~2282 kg) is less than the UF_6 mass values determined by Section 4.2.2 for $k_{eff} = 1.00$ for water-reflected spheres of UF_6.

The reflector model yielding the highest k_{eff} values is that of a simple water reflector. The overpack material density is very low, and insufficient steel is present in the overpack jacket materials to present significant neutron reflector effects.

The most reactive loading geometry is that of Load c. Of the four loading models, Load c provides the most compact configuration of the payload. Loading geometries similar to Load c could readily be postulated that would have higher computed k_{eff} values. For example, simple mounding of UF_6 along the length of the cylinder (near the cylinder centerline) would result in a more compact UF_6 configuration that may still be judged as credible. However, it is unlikely that computed k_{eff} values as high as 0.90 would result for any alternate single-cylinder material configurations.

The primary conclusion from Table 4.1 data is that margins of subcriticality are significant for individual 30B containers and packages containing UF_6 up to 20% enrichment, provided that the contents remain unmoderated.

Table 4.1. Computed k_{eff}[a] results for individual 30B cylinders or packages

	Single Cylinder Reflected by Water Only			
	Load a	**Load b**	**Load c**	**Load d**
Enrichment	k_{eff}	k_{eff}	k_{eff}	k_{eff}
5%	0.4521	0.4612	0.4723	0.4403
10%	0.5752	0.5947	0.6146	0.5500
15%	0.6662	0.6928	0.7189	0.6299
20%	0.7397	0.7726	0.8037	0.6950

	Single Cylinder Reflected by Overpack Only			
	Load a	**Load b**	**Load c**	**Load d**
Enrichment	k_{eff}	k_{eff}	k_{eff}	k_{eff}
5%	0.2926	0.3267	0.3539	0.2396
10%	0.4145	0.4620	0.4999	0.3386
15%	0.5098	0.5662	0.6102	0.4184
20%	0.5896	0.6519	0.7005	0.4871

	Single Cylinder Reflected by Overpack and Water			
	Load a	**Load b**	**Load c**	**Load d**
Enrichment	k_{eff}	k_{eff}	k_{eff}	k_{eff}
5%	0.3718	0.3921	0.4102	0.3549
10%	0.4989	0.5304	0.5585	0.4643
15%	0.5943	0.6337	0.6677	0.5467
20%	0.6729	0.7186	0.7566	0.6153

[a]Each k_{eff} result is converged to a statistical uncertainty of 0.0002.

Previously identified application models for unmoderated UF_6 in simple geometry are considered adequate to represent single-cylinder models of the 30B package.

4.2.7 Arrays of 30B Transport Packages

10 CFR[7] §71.59 provides standards for package arrays and defines how a package "Criticality Safety Index," or CSI, must be derived. Analyses must be performed for arrays of undamaged packages (commonly referred to as a "normal condition" or NC array) and packages in a condition as may result from a series of regulatory-specified impact, fire, and other challenges (the "hypothetical accident condition" or HAC array).

Specific content of interest from 10 CFR §71.59 is provided:

(a) A fissile material package must be controlled by either the shipper or the carrier during transport to assure that an array of such packages remains subcritical. To enable this control, the designer of a fissile material package shall derive a number "N" based on all the following conditions

being satisfied, assuming packages are stacked together in any arrangement and with close full reflection on all sides of the stack by water:

(1) Five times "N" undamaged packages with nothing between the packages would be subcritical;
(2) Two times "N" damaged packages, if each package were subjected to the tests specified in §71.73 ("Hypothetical accident conditions") would be subcritical with optimum interspersed hydrogenous moderation; and
(3) The value of "N" cannot be less than 0.5.

(b) The CSI must be determined by dividing the number 50 by the value of "N" derived using the procedures specified in paragraph (a) of this section.

10 CFR §71.59(c) places limits on the number of fissile packages that may be transported by a carrier. The sum of CSI values present on the carrier is limited to a maximum of either 50 or 100, depending on the certain aspects of the conveyance. For most UF_6 shipments, a CSI maximum of 100 is applicable.

Array calculations provided in this section are similar to those that may be used by an applicant to meet array requirements of 10 CFR §71.59 for transport of unmoderated UF_6 in 30B packages, at ^{235}U enrichments greater than 5%.

For purposes of these calculations, it is assumed that even though 30B overpacks do suffer some damage due to the challenges identified in 10 CFR §71.73, this damage does not result in any appreciable reduction in the spacing of UF_6 cylinders contained in proximate packages (i.e., the overpacks remain in place about the cylinders, mechanical damage to the overpacks is limited to localized dents or crushing). This assumption is consistent with testing done during initial development of the 30B overpack design.[13]

Infinite-array calculations are performed to examine the dependence of computed k_{eff} on the amount of interspersed hydrogenous moderation between packages. The interspersed moderation is simulated as water at various specific gravity values ranging from zero to unity. Calculations are performed for arrays of 30B cylinders without overpacks, and with overpacks. For the arrays without overpacks, the cylinder spacing is maintained as if overpacks were present. Bases for performing calculations without overpacks include: (a) the calculations provide insight to moderation effects without the complicating influence of a second moderator presence (hydrogen in the phenolic foam), and (b) the foam may suffer damage due to fire exposure or mechanical damage, in which case water could occupy regions within the foam.

Infinite-array calculations were performed using each of the load models discussed in Section 4.2.6. The most reactive material configuration was that of Load a, where the UF_6 uniformly fills the interior volume of the cylinder. All results presented below are of the configuration of Load a.

Figure 4.10 provides a KENO-3D graphical illustration of the model used for the infinite arrays of 30B cylinders without overpacks.

Figure 4.11 presents results for arrays of 30B cylinders without overpacks. The k_{eff} results at an enrichment of 5% are consistent with those reported in ORNL/TM-11947. The k_{eff} results for no moderator are consistent with the k_∞ results for Figure 4.1. For the lower ^{235}U enrichments, k_{eff} maxima are observed at very small density fractions of water.

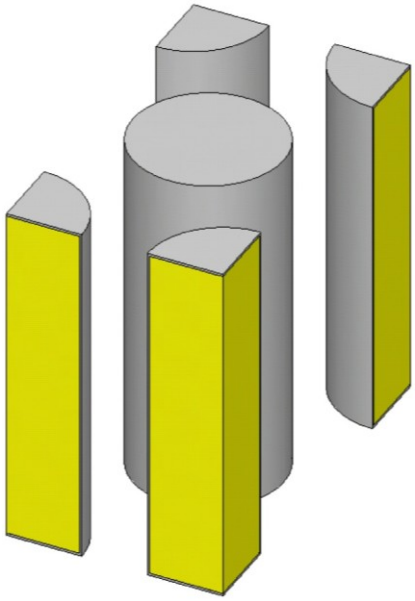

Figure 4.10. KENO-3D illustration of the unit used to simulate infinite arrays of 30B cylinders without overpacks. Mirror reflector conditions were applied to all six faces of the model to simulate an infinite array. (Vertical reflector faces were offset to match the overpack length.)

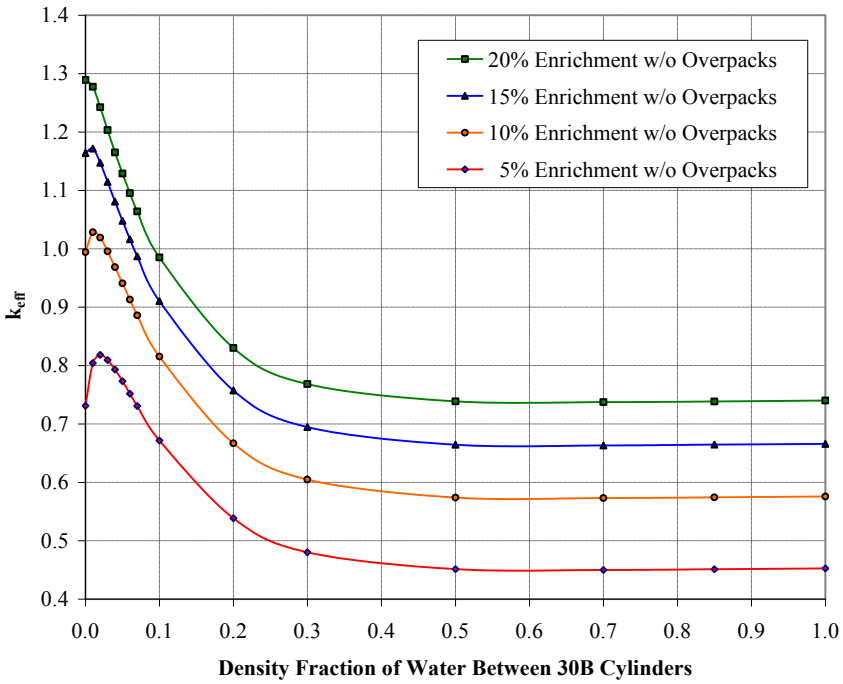

Figure 4.11. Computed k_{eff} results for infinite arrays of 30B cylinders without overpacks. Each k_{eff} result is converged to a statistical uncertainty of 0.0002. The water density for a density fraction of 1.0 is 0.9982 g/cm^3. The UF_6 distribution is that of "Load a."

Figure 4.12 illustrates the model used for infinite arrays of 30B cylinders with overpacks, and Figure 4.13 provides the computed k_{eff} results. As shown by Figure 4.13, for arrays with overpacks, all k_{eff} maxima values occur for a water density fraction of zero. This is partially due to presence of hydrogen in the phenolic foam of the overpack at a density of ~0.001 g/cm^3, which is similar to the hydrogen content provided by water at a density fraction of ~0.01.

Additional results (not shown on Figure 4.13), were obtained for models including low density water interior to the overpacks but exterior to the cylinders. Any inclusion of water within the overpacks resulted in computed k_{eff} values less than shown by Figure 4.13.

To investigate the influence of boron in the phenolic foam of the overpacks, selected cases from Figure 4.13 were executed with the boron omitted from the model. The results are compared on Figure 4.14. Even though the boron density in the foam is very low (~0.001 g/cm^3 natural boron), the influence on neutron interaction between cylinders is significant.

Based on results of the infinite array calculations, the optimum interspersed water moderation between 30B packages (cylinders with overpacks, with boron modeled in the foam) is zero. A conservative load model is that of Load a, for UF_6 uniformly distributed within the cylinder volume.

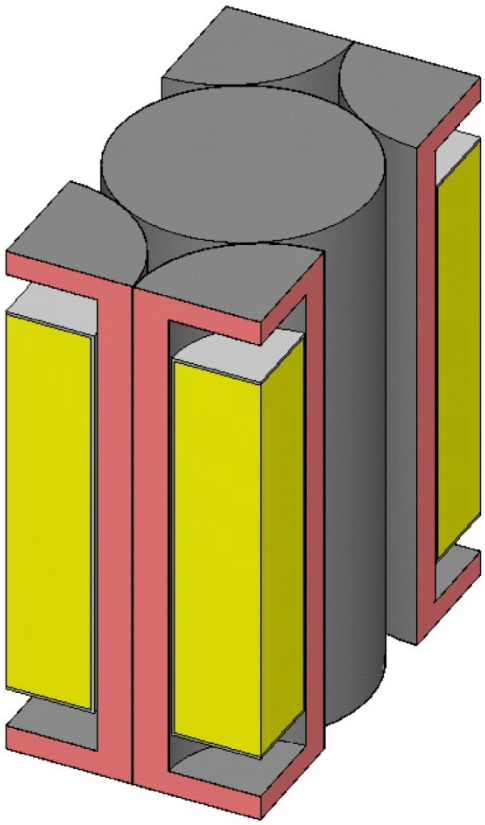

Figure 4.12. KENO-3D illustration of the unit used to simulate infinite arrays of 30B cylinders with overpacks. Mirror reflector conditions were applied to all six faces of the model to simulate an infinite array.

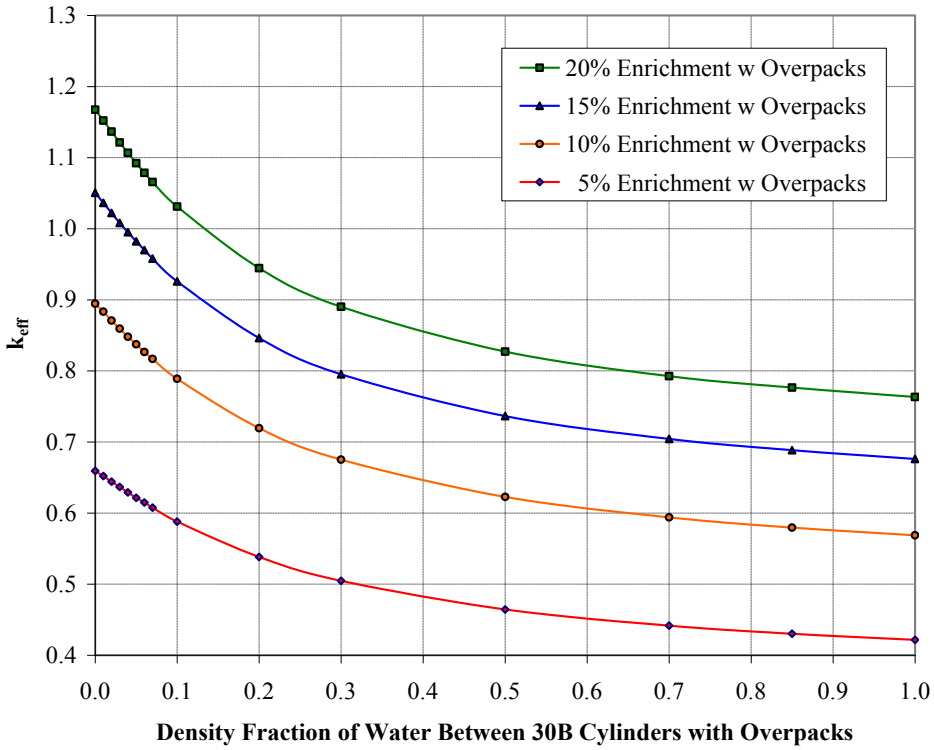

Figure 4.13. Computed k_{eff} results for infinite arrays of 30B cylinders with overpacks.

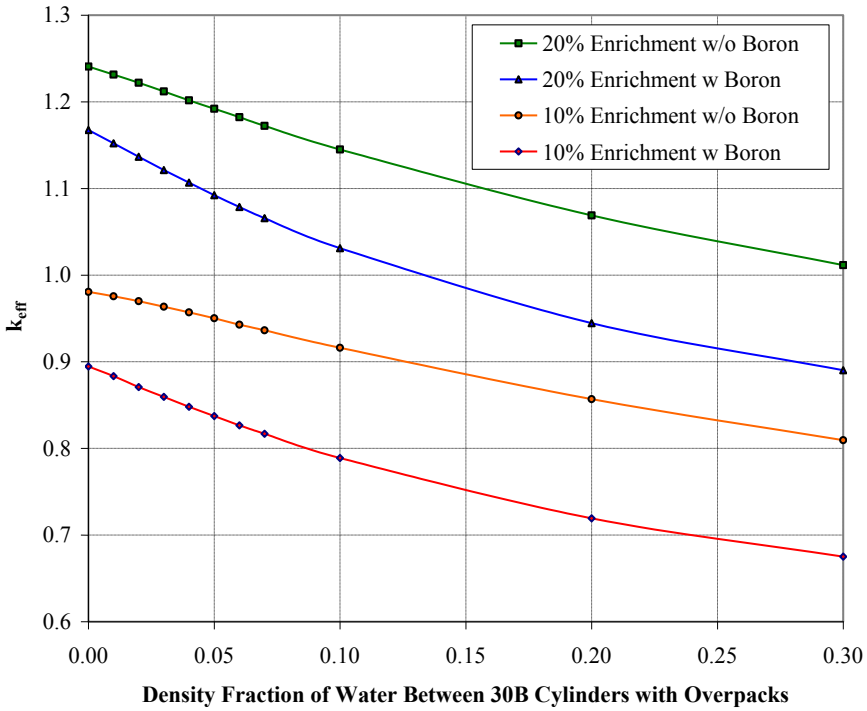

Figure 4.14. Computed k_{eff} results for infinite arrays of 30B cylinders with overpacks, illustrating the effect of boron in the phenolic foam.

To simulate the calculations an applicant might use to derive a Criticality Safety Index (CSI), two finite-array 30B package array models were developed. The size of these arrays (50 or more packages) corresponds to a number of packages that would support a CSI value of 5, provided that (a) other criteria for package design and testing are satisfied and (b) the applicant could provide an adequate supporting validation and demonstration of adequate safety margin. Both arrays place the packages in a compact arrangement on a triangular pitch and surround the array with a 30-cm-thick water reflector. The 2 × 25 array is shown by Figure 4.15, and the 3 × 19 array is shown by Figure 4.16.

Table 4.2 provides the results for the water-reflected 2 × 25 and 3 × 19 arrays of 30B packages.

As application models, the 3 × 19 array with enrichments of 15% and 20% are selected.

4.2.8 Individual 30B Packages with Water Intrusion into the UF_6 Payload

Some non-zero criticality risk is associated with the current use of 48- and 30-in.-diameter cylinders for UF_6 enriched up to 5%. If water were to in leak into such a cylinder, it is possible that mixture of the water with the fissile contents may result in a critical configuration. The level of this risk is difficult to quantify and depends on many factors.

The primary factors determining the risk are

(a) the likelihood that water will enter a cylinder in sufficient quantity; and
(b) the likelihood that adequate mixing of the water and the fissile material occurs and that the resulting configuration of the reaction products is conducive to criticality.

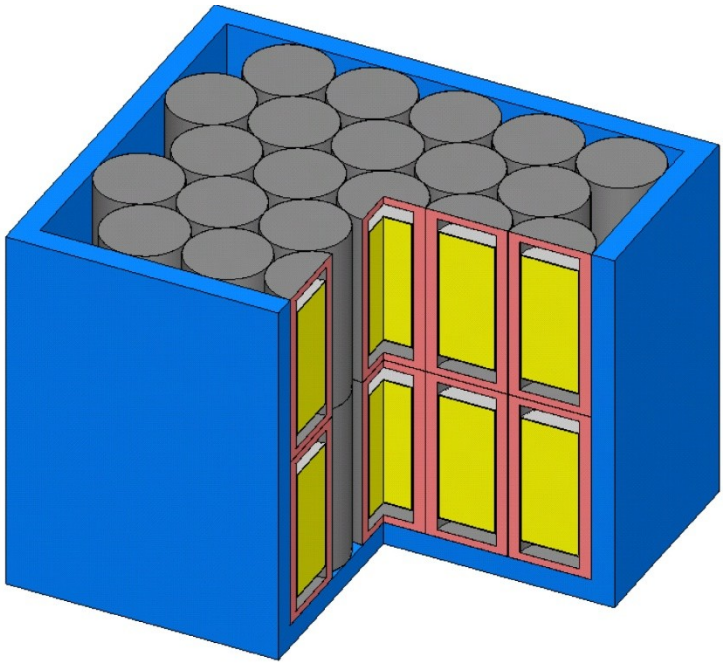

Figure 4.15. KENO-3D graphic of a 2 × 25 array of 30B packages. The top water reflector is omitted, and a quarter section is removed.

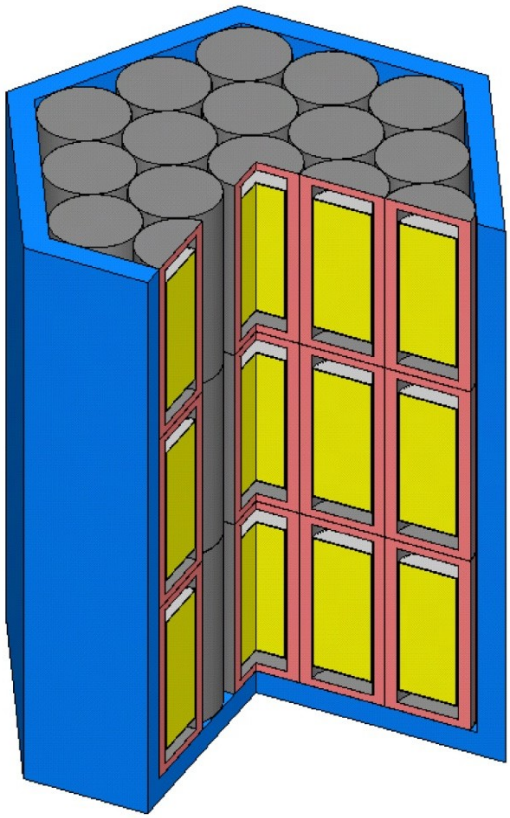

Figure 4.16. KENO-3D graphic of a 3 × 19 array of 30B packages. The top water reflector is omitted, and a quarter section is removed.

Table 4.2. Computed k_{eff} results[a] for 30B package arrays

Enrichment	2 × 25 Array k_{eff}	3 × 19 Array k_{eff}
5%	0.5049	0.5115
10%	0.6924	0.7001
15%	0.8232	0.8312
20%	0.9247	0.9341

[a]Each k_{eff} result is converged to a statistical uncertainty of 0.0002.

Examples of mechanisms that might contribute to water entry include

- transport accidents that involve mechanical puncture of a cylinder or fire-induced hydraulic rupture of a cylinder, accompanied by source of water such as rainwater, water from river or lake bodies, or water from firefighting activities;
- facility events that may be considered severe, such as tornado or high wind events that induce cylinder puncture followed by rainwater or facility water sources such as broken lines; and
- facility events that may be considered benign, such as corrosion or handling damage that causes containment failure of a cylinder, followed by rainwater or other water entry.

The probability of these mechanisms depends on a number of factors, some of which are under operational or regulatory control, some which rely on the level of commerce and similar factors (e.g., frequency of transports, condition of roadways/bridges, traffic conditions), and some which rely on forces of nature.

If water were to enter a cylinder, achievement of critical configuration would require that

- some threshold amount of water must enter,
- adequate distribution/mixing of the water and fissile material must occur, and
- the resulting mixture geometry must be sufficient to support criticality.

Mixing of the water and fissile material could occur due to chemical reaction, by intrusion of water into porous or fractured UF_6 solids, or a combination of these actions. The extent to which mixing may occur depends on factors that are poorly known and may vary from cylinder to cylinder. Likewise, the geometry that may be attained by the moderated mixture can only be assumed. The threshold amount of water of concern is difficult to predict, because a realistic estimate depends on level of mixing of water and fissile material and the resulting geometry. Absolute lower bounds on the amount of water required for criticality are possible but may be nonrealistic.

The risk of criticality due to water intrusion into large cylinders of enriched UF_6 is at least "low." Such cylinder use has extensively occurred in domestic and international commerce for decades with no criticality accident to date.

Regardless of the level of current risk or how well that risk is quantified, the current risk is accepted for enrichments up to 5%. This is demonstrated by the Code of Federal Regulations approvals for 30B specification packages and by NRC approval of Certificates of Compliance for performance packages using either 48- or 30-in.-diameter cylinders.

It is beyond the scope of this assessment to re-evaluate risks for, or the acceptability of, bulk shipments of UF_6 enriched to 5% ^{235}U. However, a primary objective of this work is to assess potential challenges to

criticality safety margins that are associated with nuclear fuel cycle changes from a maximum enrichment of 5% to the HTGR limit of 20%.

Thus, a qualitative assessment of the potential increase in risk for water-induced criticality in an enriched UF_6 cylinder is performed, assuming that the primary fuel cycle change is use of the 30B package for enrichments in the range of 5% to 20% ^{235}U. Further, it is assumed that all other probability factors associated with the currently accepted criticality risks (for water intrusion) remain constant.

To perform this qualitative assessment,

- three differing geometries of moderated fissile mixture within a 30B transport package are considered (ranging from potentially nonconservative to potentially overconservative),
- a range of moderation ratios (H:U or H:^{235}U atom ratio) are considered (ranging from undermoderated to overmoderated), and
- four enrichments (5%, 10%, 15%, and 20%) are considered.

To compare similar systems at differing enrichments, the metrics used (but considered separately) are (a) the amount of water required and (b) the amount of reacted U required. Possible variations in computational bias are ignored; all comparisons of systems are made at computed k_{eff} values of unity.

UF_6 solid, at room temperature, has been found in laboratory-scale experiments to be potentially resistant to water dissolution under certain conditions.[75] In particular, if the UF_6 and water are at room temperature, the UF_6 is in a monolithic mass, and the upper surface of the UF_6 is horizontal, an interface layer of reactant forms at the UF_6-water interface which can effectively prevent gross dissolution. Also, if a cylinder containing UF_6 is submerged with some small aperture (such as a open valve or other similarly small penetration through the containment wall), reactants may plug the opening and inhibit extensive dissolution.

The primary reaction of interest is exothermic and may be represented by

$$UF_6 + 4H_2O \rightarrow UO_2F_2{\cdot}2H_2O + 4HF$$

Using the method outlined in Ref. 76, solution specifications for $UO_2F_2{\cdot}2H_2O + 4HF + H_2O$ were derived as a function of H:^{235}U atom ratio for the four enrichments of interest. It was assumed that during the chemical reaction described above, none of the HF or H_2O is lost in vapor form.

For the container model, a horizontal 30B cylinder initially containing the cylinder's rated UF_6 loading limit is considered. The 30B cylinder is modeled as being within an overpack. Locations between the overpack and the cylinder are modeled as water-filled, and a water reflector surrounds the overpack. Although water is included in the model as a reflector, the primary neutron-reflecting material for the fissile solution is that of the solid UF_6.

The orientation of the 30B cylinder and absence of any other significant reflector external to the cylinder may be nonconservative for some water entry scenarios. However, the objective here is not to derive the minimum conditions for criticality in a 30B cylinder. Instead, the approach is to determine how sensitive critical requirements are to variation in ^{235}U enrichment assuming that comparable material configurations result.

The geometric configuration judged to present the least conservatism for criticality analysis is shown by Figure 4.17. The initial UF_6 configuration (prior to water entry) is that of "Load c" as described in Section 4.2.6: the UF_6 is at theoretical density and has a flat upper surface. Due to water entry into the

cylinder, it is assumed that a homogeneous solution of $UO_2F_2 \cdot 2H_2O + 4HF + H_2O$ results in a slab geometry on top of the UF_6.

Of the three solution geometries considered, the most conservative geometry is that of a hemisphere, as shown by Figure 4.18. This model presumes that a localized depression exists in the upper surface of the UF_6. As water enters the depression, the depression may enlarge due to UF_6 dissolution. Or, the depression may simply fill with solution generated by contact of water and UF_6 particulate from other regions within cylinder. This solution configuration is not the most conservative that may be postulated, it is simply the most conservative of the three models selected for analysis.

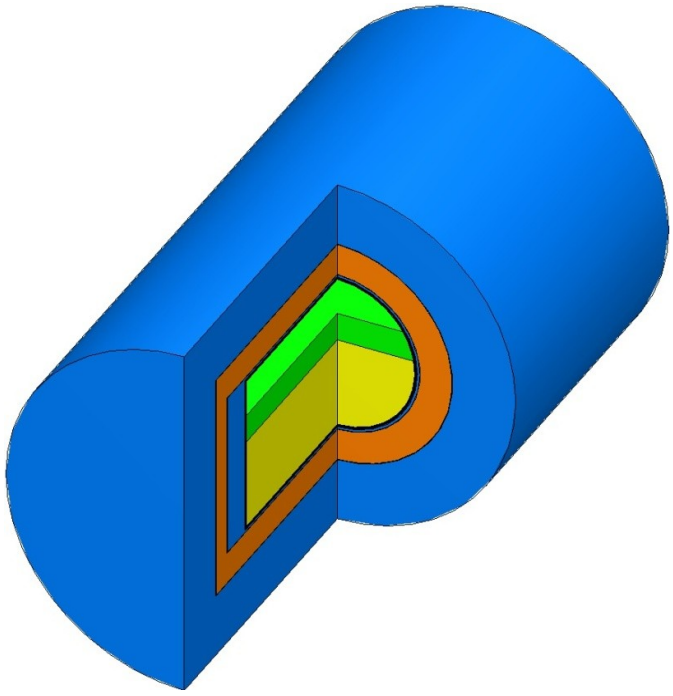

Figure 4.17. KENO-3D graphic of solution slab geometry in a 30B package. A quarter section of the model is removed.

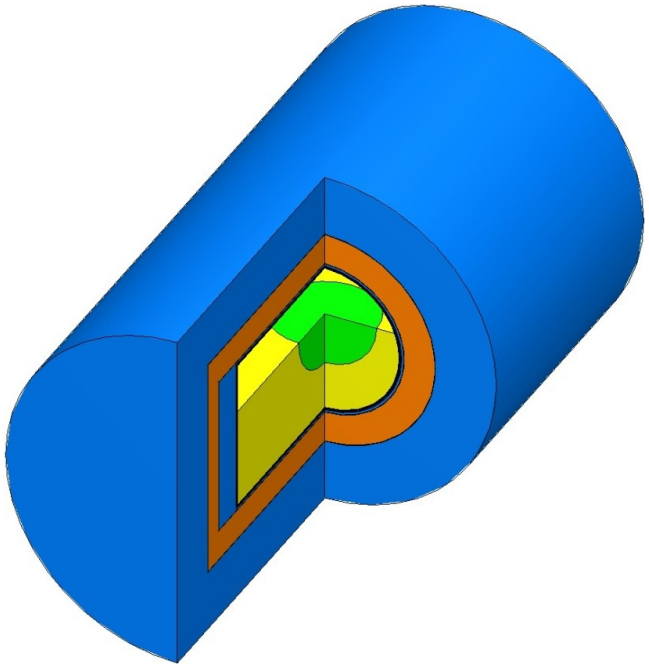

Figure 4.18. KENO-3D graphic of solution hemisphere geometry in a 30B package. A quarter section of the model is removed.

A third solution configuration is that of a hemicylinder, as shown by Figure 4.19. This configuration is judged to be the most realistic configuration, provided that the UF_6 cylinder remains horizontal, with no tilting or rotation of the cylinder axis.

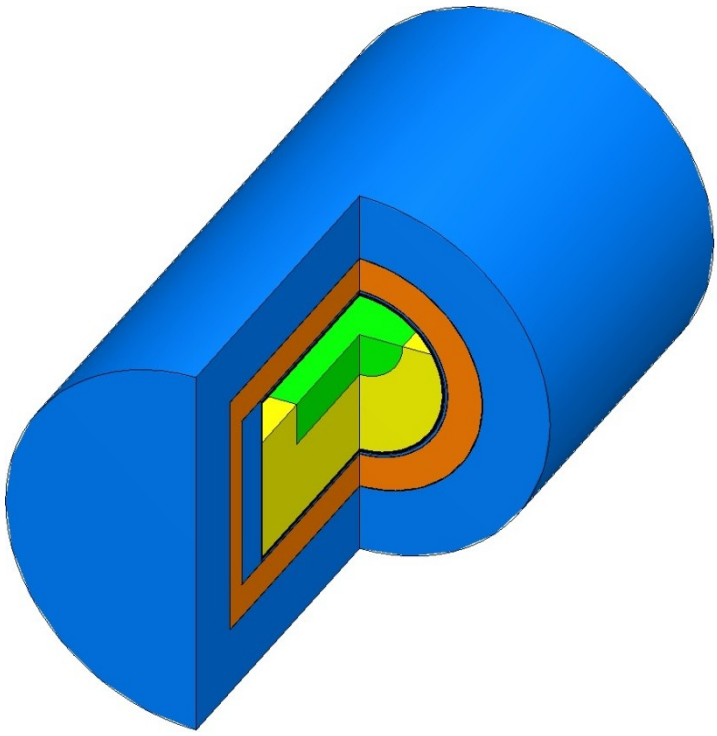

Figure 4.19. KENO-3D graphic of solution hemicylinder geometry in a 30B package. A quarter section of the model is removed.

For the solution hemisphere model, the origin of the hemisphere is located at the same elevation as the upper surface of the UF_6 solids and equidistant from either end of the cylinder.

For the solution hemicylinder model, the hemicylinder axis is at the same elevation as the upper surface of the UF_6 solids. The distance between either end of the solution hemicylinder and the inside (end) walls of the 30B cylinder is 12 in.

For realism, the total uranium inventory for each uranium solution-UF_6 solids systems is maintained equivalent to the modeled uranium content of the cylinder prior to water introduction. To achieve this balance, iterative application of the SCALE CSAS1 search routine was performed. With the initial UF_6 upper surface maintained, solution dimensions for computed $k_{eff} = 1.00$ were determined with the first use of CSAS1. Then, the amount of UF_6 solids was adjusted (by changing the elevation of the upper surface of the UF_6) to account for the inventory of uranium now in solution. The CSAS1 search routine was applied a second time, and a second rebalance of the UF_6 inventory was performed. A third (and final) use of the CSAS1 search sequence yielded solution dimensions that differed insignificantly from the second CSAS1 results.

Each final solution-UF_6 solids configuration has a computed k_{eff} value that is within 0.0002 of unity, and the total uranium inventory of the cylinder varies less than 0.1% from the initial UF_6-solids-only inventory.

Table 4.3 provides the solution moderation ratios and uranium densities for the models.

Table 4.3. UO_2F_2-HF-H_2O models

5% Enrichment			
H/U-235	**H/U**	**ρ_U (g/cm^3)**	**ρ_{235} (g/cm^3)**
160	8.1	1.518	0.076
200	10.1	1.360	0.068
300	15.2	1.078	0.054
500	25.3	0.763	0.038
700	35.4	0.590	0.029
1000	50.6	0.440	0.022

15% Enrichment			
H/U-235	**H/U**	**ρ_U (g/cm^3)**	**ρ_{235} (g/cm^3)**
53	8.0	1.522	0.228
100	15.2	1.078	0.162
200	30.3	0.665	0.100
300	45.5	0.481	0.072
500	75.8	0.309	0.046
700	106.1	0.228	0.034
1000	151.6	0.164	0.025

10% Enrichment			
H/U-235	**H/U**	**ρ_U (g/cm^3)**	**ρ_{235} (g/cm^3)**
80	8.1	1.518	0.152
100	10.1	1.359	0.136
200	20.2	0.893	0.089
300	30.3	0.665	0.067
500	50.6	0.440	0.044
700	70.8	0.329	0.033
1000	101.1	0.239	0.024

20% Enrichment			
H/U-235	**H/U**	**ρ_U (g/cm^3)**	**ρ_{235} (g/cm^3)**
40	8.1	1.517	0.303
50	10.1	1.358	0.272
100	20.2	0.893	0.179
200	40.4	0.530	0.106
300	60.6	0.377	0.075
500	101.0	0.239	0.048
700	141.4	0.175	0.035
1000	202.0	0.125	0.025

Figure 4.20 plots the water inventories required for computed k_{eff} values of unity, for the solution slab model. The assumed density of the water admitted to the 30B cylinder is 0.9982 g/cm^3.

On Figure 4.20, fewer data points are shown for the curve at 5% enrichment than for the other curves. The leftmost data point of each enrichment curve corresponds to a uranium concentration of ~1.5 kg U/liter, which is close to the solubility limit of uranium in the uranyl fluoride form. The H:^{235}U ratio at the solubility limit increases with decreasing enrichment. For the rightmost data point of the 5% curve, a physical limit of the model is encountered: the cylinder volume is 100% occupied by UF_6 and uranium solution, and no more water can be added to the model. These two factors (solution product density and geometric limit for the assumed model) result in a smaller H:^{235}U range of criticality concern for models with 5% enrichment.

The results of Figure 4.20 for uranium enrichment of 10% are consistent with conclusions of Ref. 71. The minimum water necessary for a computed k_{eff} of unity from Figure 4.20 is ~95 liters, whereas Ref. 71 determined the necessary water input was ~82 liters. The model of Ref. 71 includes a more effective reflector condition (no overpack, water reflector in direct contact with all external cylinder surfaces), so the difference in results appears reasonable.

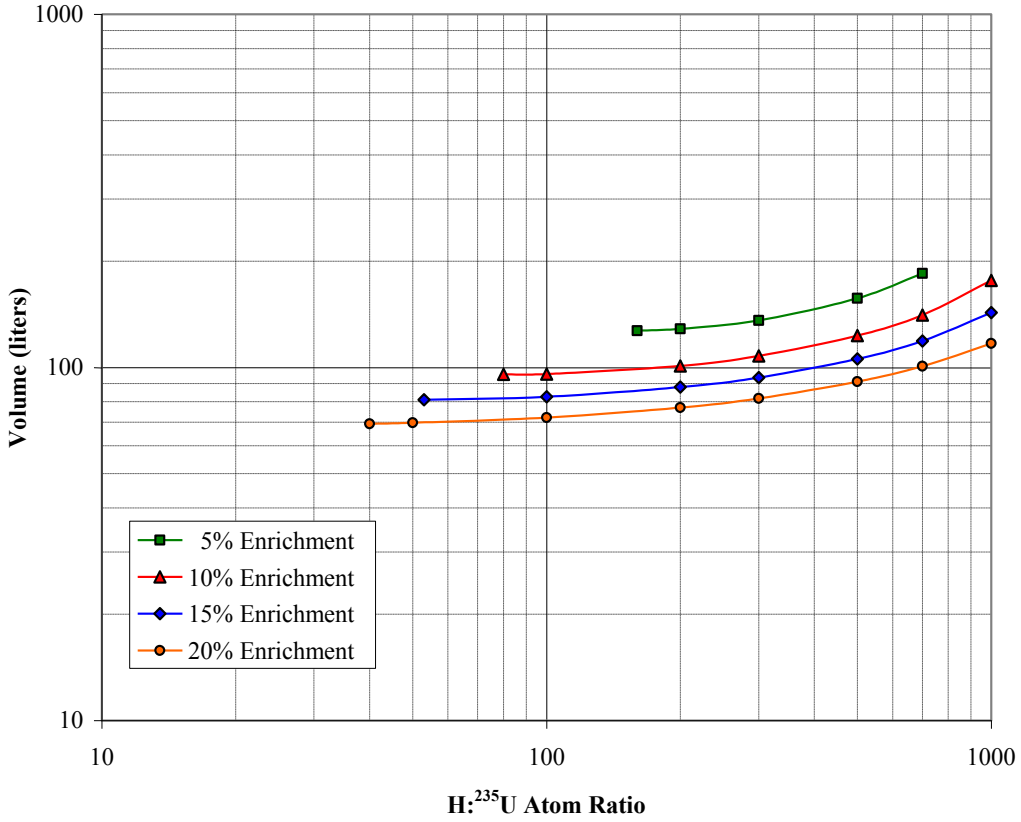

Figure 4.20. Solution slab model results: volume of admitted water for computed k_{eff} = 1.00.

The slab model maximizes the predicted amount of water intrusion required for critical conditions, because the solution geometry maximizes neutron leakage from the fissile solution.

Figure 4.21 shows the amount of uranium that must be dissolved to achieve a computed k_{eff}=1.000 value for the slab solution model.

The range of solution models used for Figure 4.21 did not extend to sufficiently high H:^{235}U ratios as to allow determination of minimum mass values for reactant uranium. The fact that the curve minima values occur at such high H:^{235}U ratios suggests neutron multiplication of the solution slab is strongly enhanced by having a large surface area in contact with the UF_6 inventory.

Figures 4.22 and 4.23 provide required water volumes and uranium dissolution masses, for the hemicylindrical solution model for computed k_{eff} values of unity. Figures 4.24 and 4.25 provide results for the hemispherical solution models.

Table 4.4 summarizes results for all models and enrichments.

As a higher ^{235}U enrichment or a more compact geometry for fissile solution is assumed, critical mass and volume requirements decrease significantly.

For an enrichment increase from 5% to 20%, the critical mass requirements decrease by about a factor of ten and the required water volume decreases by a factor of three.

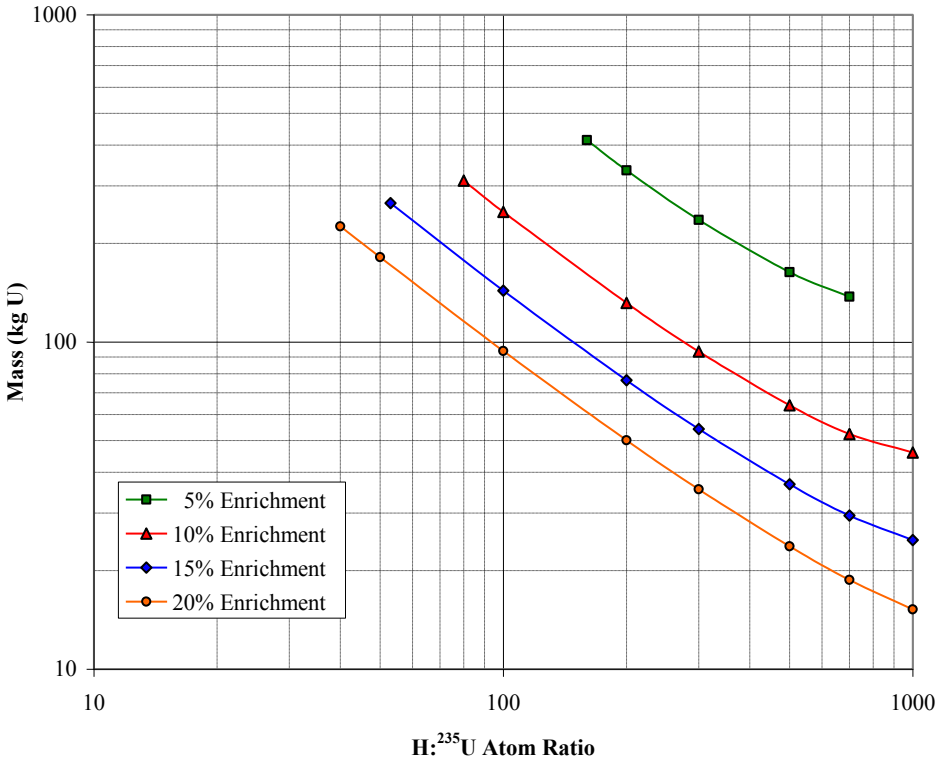

Figure 4.21. Solution slab model results: nass of reactant uranium for computed k_{eff} = 1.00.

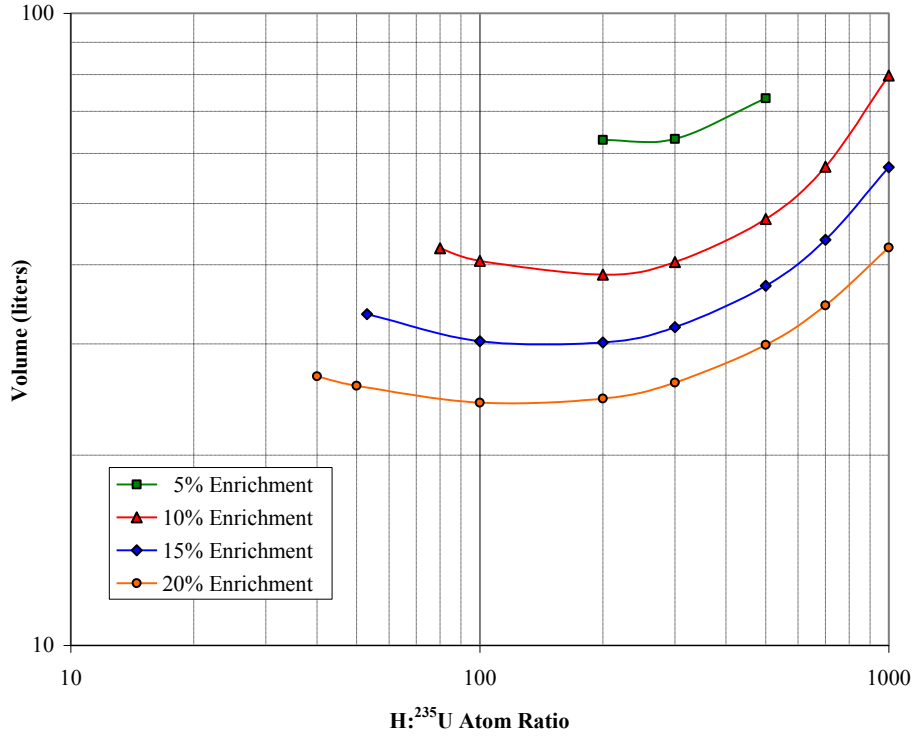

Figure 4.22. Solution hemicylinder model results: volume of admitted water for computed k_{eff} = 1.00.

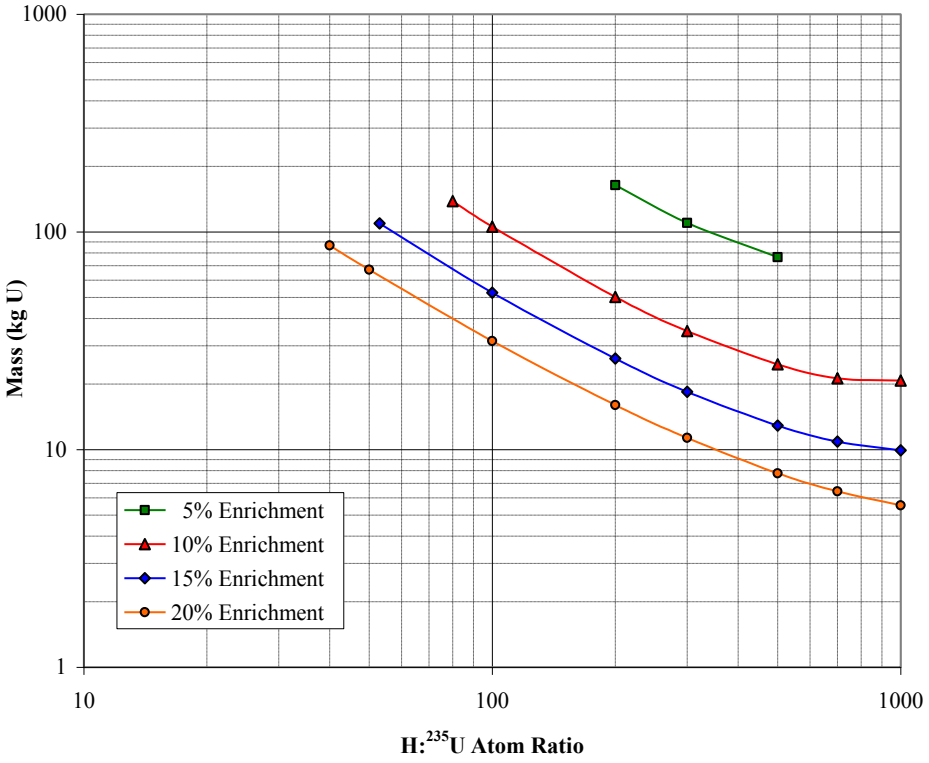

Figure 4.23. Solution hemicylinder model results: mass of reactant uranium for computed k_{eff} = 1.00.

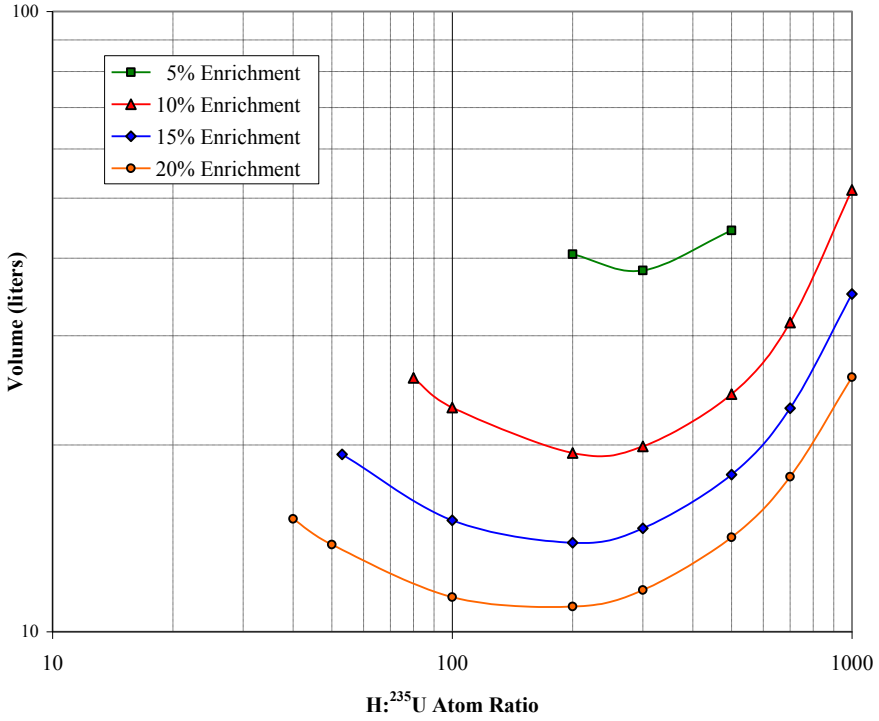

Figure 4.24. Solution hemisphere model results: volume of admitted water for computed k_{eff} = 1.00.

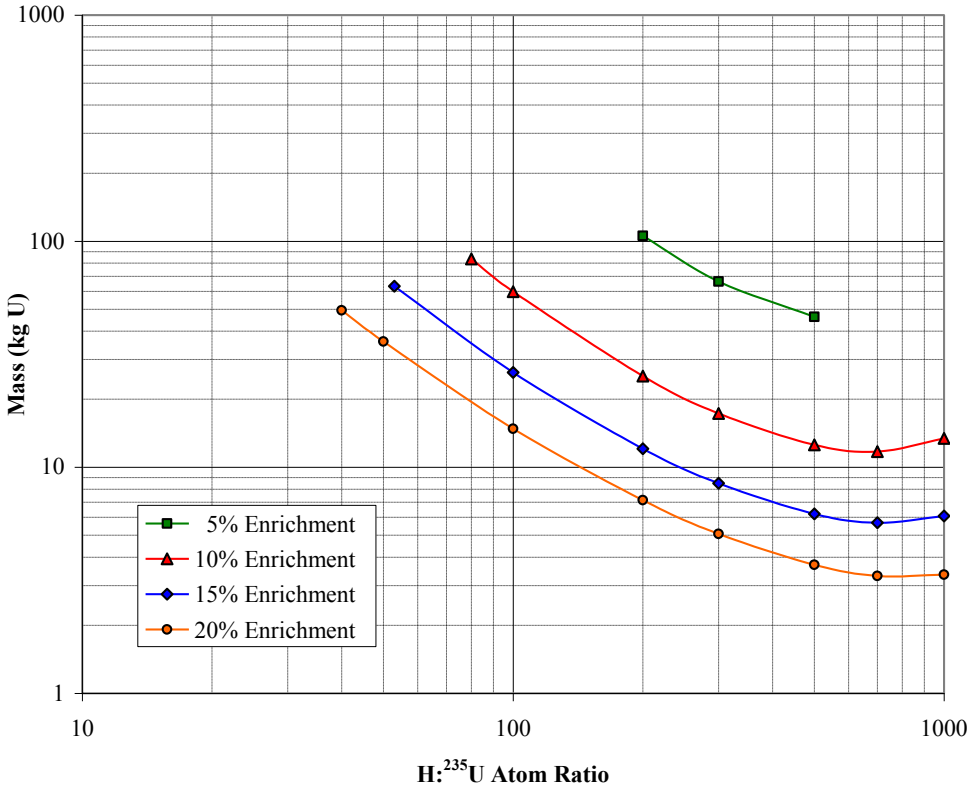

Figure 4.25. Solution hemisphere model results: mass of reactant uranium for computed k_{eff} = 1.00.

Table 4.4. Results summary for water intrusion into a 30B cylinder

^{235}U enrichment →	5%	10%	15%	20%
Solution model↓	**Minimum H_2O Input (liters) for Computed k_{eff} = 1.00**			
Slab	127	96	81	69
Hemicylinder	63	39	30	24
Hemisphere	38	19	14	11

^{235}U enrichment →	5%	10%	15%	20%
Solution model↓	**Minimum Reactant U (kg) for Computed k_{eff} = 1.00**			
Slab	~120[a]	~42[a]	~22[a]	~12[a]
Hemicylinder	~70[a]	21	10	~5[a]
Hemisphere	~40[a]	12	6	3

[a]Approximate values are projected minima based on trends.

If the hemisphere and slab configuration data are compared, the hemisphere configuration has mass and volume requirements that are reduced by a factor of three or more.

The relevance of Table 4.4 data for water volumes may vary based on the mishap scenario being considered. For example, consider a criticality scenario that involves a small penetration in the 30B cylinder wall above the UF_6 inventory, for a cylinder that is stored outdoors. The criticality scenario may require significant total rainfall amounts and time duration before a criticality risk could develop. For this scenario, the water volume requirement for criticality is important because the scenario of concern involves a definable (and slow) water input rate. Criticality safety evaluations may thus derive some control (such as periodic inspection of cylinders) to mitigate the scenario.

If the water intrusion scenario of concern involves potentially significant and unpredictable input rates and amounts of water, then the water volume data of Table 4.4 have a different relevance. Simply stated, the water input volumes of concern are less than the available void volumes within the UF_6 cylinders. Transport accident scenarios that exceed CFR package testing specifications fall into this category. Also, following a transport accident, the cylinder orientation may not be normal. This could enhance UF_6 dissolution and cause compact configuration of the reactant solution to be more likely.

Perhaps the most important observation from Table 4.4 data regards the uranium reactant masses. At 5% enrichment, several tens of kilograms of UF_6 must be dissolved or otherwise mix with moderator in order for a criticality risk to occur. While there is almost certainly some amount of fine particulate UF_6 within 30B cylinders (that may readily react with water or be suspended under forceful water entry), it is unlikely that any typical 30B cylinder has particulate inventories on the order of 40 to 120 kg U (60 to 180 kg UF_6). Thus, for a criticality risk to occur with a 30B cylinder loaded with 5% enrichment UF_6, the intruding water must dissolve a significant inventory of monolithic UF_6. For many water intrusion scenarios, experimental data of Ref. 75 could be used to justify that such extensive UF_6 reaction is improbable.

In contrast, at enrichments of 10% and higher, far less uranium must react with water to achieve a criticality risk. For each of the three geometric configurations modeled, the mass of reactant U at 20% enrichment is an order of magnitude less than required for 5% enrichment.

If water entry to a 30B cylinder of enriched UF_6 were to occur, the potential risk for a criticality accident is greater for enrichments in the 10% to 20% range, compared to the risk for 5% enrichment UF_6.

For application models, four cases are retained:

- Solution slab geometry with 10% enrichment and H:^{235}U = 100. This case most closely represents conditions evaluated by Ref. 70 and 71.
- Hemisphere geometry with 10% enrichment and H:^{235}U = 200. For 10% enrichment, this case represents the minimum H_2O input requirement.
- Hemisphere geometry with 10% enrichment and H:^{235}U = 700. For 10% enrichment, this case represents the minimum U reactant mass requirement.
- Hemisphere geometry with 20% enrichment and H:^{235}U = 500. This case involves only 660 g ^{235}U in solution.

4.2.9 Individual 12B Packages with Water Intrusion

The objective of this section is to briefly examine the "12B" UF_6 cylinder under conditions of water intrusion. Compared to the 30B cylinder, this cylinder is the next-smaller-size, currently authorized UF_6 cylinder design.

The 12B cylinder has a nominal inner diameter of 12 in. and has a rated UF_6 capacity of ~209 kg UF_6 (about 10% of the capacity of a single 30B cylinder). A similar geometric modeling approach was used as for the 48X and 30B cylinders. For simplicity, no UF_6 content was simulated. Instead, the entire cylinder volume was modeled as containing the same reactant solutions as used for the 30B-cylinder water-intrusion analysis. Also for simplicity, no overpack was modeled; a contacting water reflector was provided for all external surfaces of the 12B container model.

Figure 4.26 illustrates the computed k_{eff} results. The 12B cylinder design does appear capable of precluding critical conditions should water in-leak to a cylinder loaded with 5% enrichment UF_6. However, the cylinder geometry is not sufficiently limited to assure subcriticality for water intrusion to payloads in the 10% to 20% enrichment range.

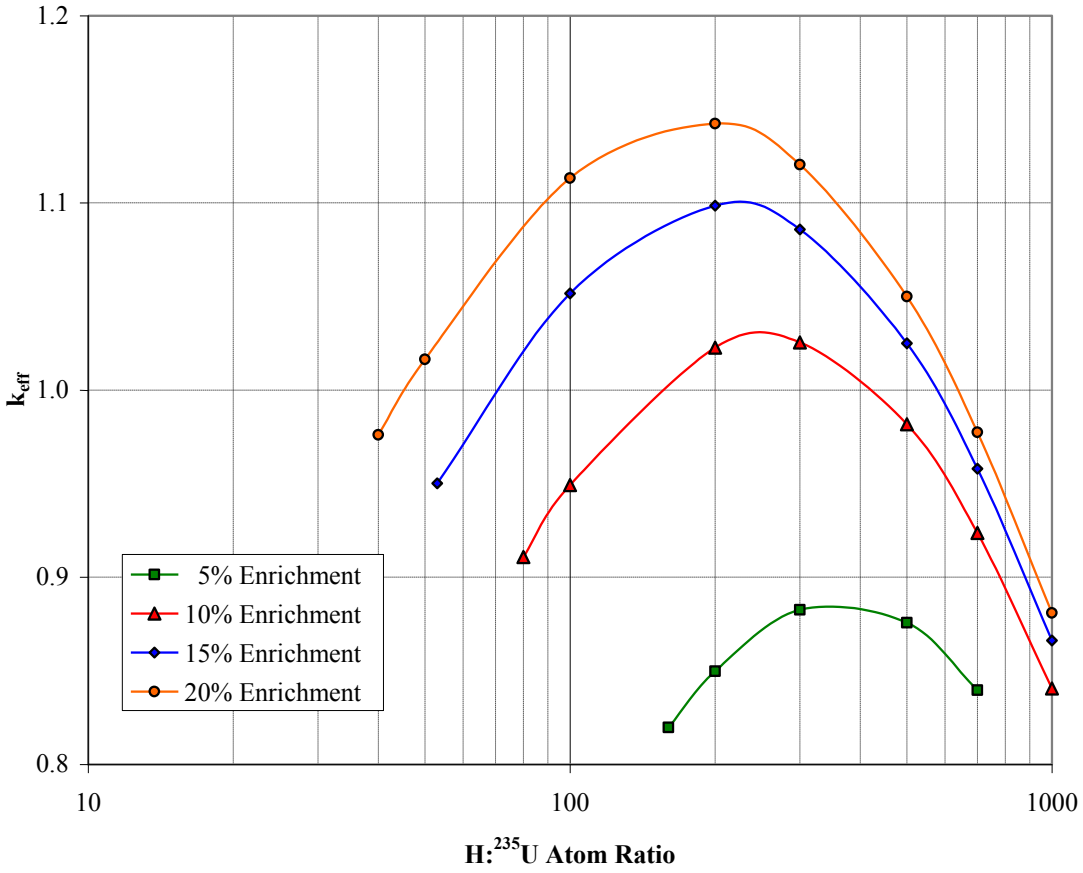

Figure 4.26. Computed k_{eff} results for the 12B cylinder for water-reflected conditions. The entire cylinder is filled with a solution of $UO_2F_2 \cdot 2H_2O + 4HF + H_2O$.

4.3 HOMOGENEOUS URANIUM SOLUTIONS

4.3.1 Uranyl Fluoride Solution in Simple Geometries

HTGR fuel manufacturing facilities will necessarily employ a variety of equipment to process and handle uranium in solution form. Criticality analyses for design and operation of fuel facilities will involve computational efforts simulating uranium solutions in both normal and potential off-normal configurations.

Likely, HTGR fuel manufacturing will involve both uranyl fluoride and uranyl nitrate solutions. Critical requirements for these two solutions, for identical enrichments, concentrations, and geometry, are similar. Typically, critical requirements for the fluoride form (mass and dimensions) are slightly less than for the nitrate form.

Solution models for UO_2F_2-H_2O solutions were derived using the methods and data documented in ORNL-TM-12292.[76] For a given geometry and uranium concentration, the UO_2F_2-H_2O solution models may yield appreciably different k_{eff} values than the previously described UO_2F_2-4HF-H_2O models. (The hydrogen density in pure water is about twice that present in pure HF. For a specified uranium concentration, the two models will have differing H:^{235}U atom ratios.)

Solution models were developed for the following enrichments:

- 2%, 3%, 4%, and 5% (representing the current LWR fuel cycle enrichment and solution benchmark data);
- 10%, 15%, and 20% (along with the 5% models, covers the HTGR fuel cycle range); and
- 50% and 100% (representing intermediate and high enrichment solution benchmarks).

Computed results for k-infinity (k_∞) for the solution models are provided on Figure 4.27. Note that as the enrichment value increases, the moderation ratio (H:^{235}U ratio) corresponding to the maximum k_∞ value decreases. For simple-geometry solution systems, minimum critical volume requirements typically occur near H:^{235}U values that correspond to k_∞ maxima.

Using each of the solution models, the sphere radius for a computed k_{eff} value of unity was determined. The reflector condition was a 30-cm-thick water reflector closely surrounding the sphere. Figures 4.28 and 4.29 show the derived uranium masses and solution volumes for the water-reflected spheres.

On Figure 4.28, note that irrespective of enrichment, the minimum mass values occur at H:^{235}U ratios of ~500. On Figure 4.29, note that for each enrichment, the minimum volume requirement occurs at an H:^{235}U value that corresponds to the maximum k_∞ for that enrichment. Similar relationships of k_∞ maxima, minimum volume and H:^{235}U ratio, and relationships of minimum mass to H:^{235}U ratio exist for other types of hydrogen-moderated solutions (e.g., uranyl nitrate, uranyl sulfate). However, these relationships do not necessarily hold true for fissile systems with two important binary moderators (e.g., moderated by both hydrogen and carbon).

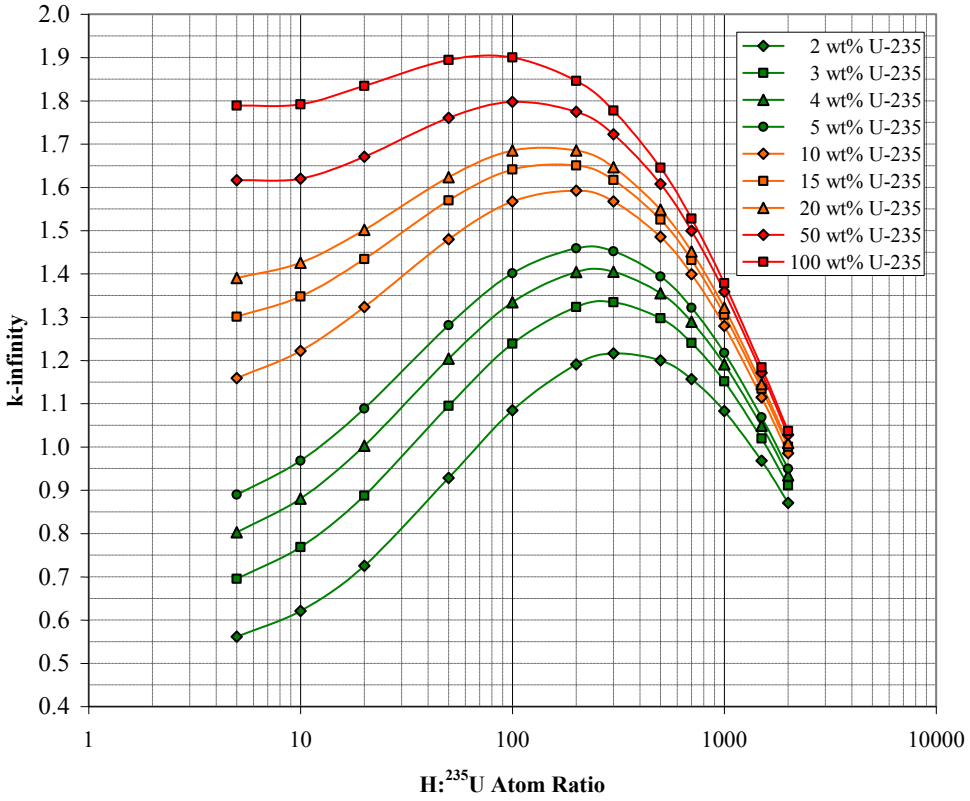

Figure 4.27. Computed k_∞ results for UO_2F_2-H_2O solutions.

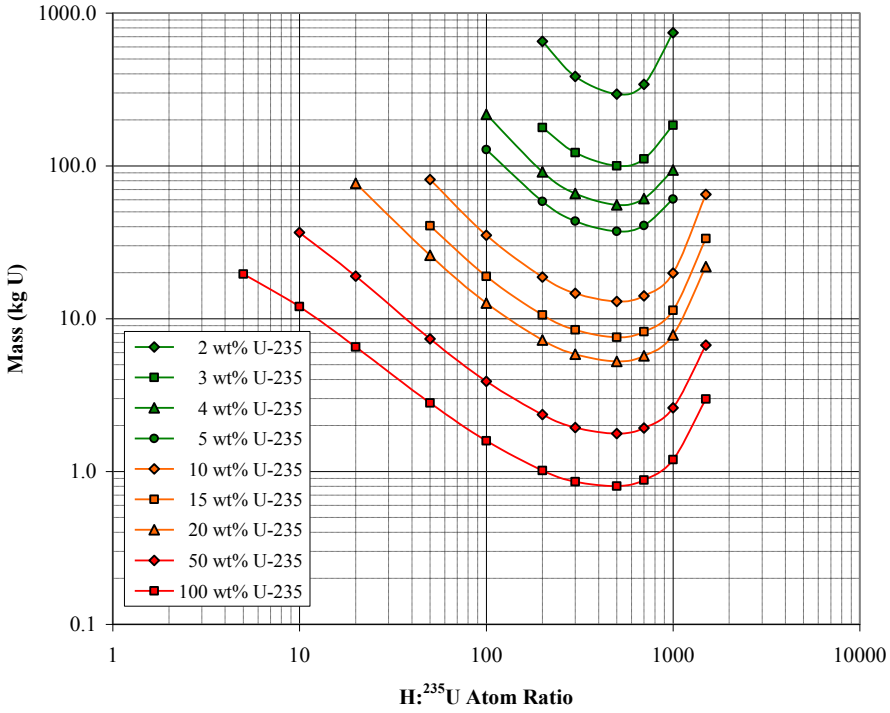

Figure 4.28. U mass for computed k_{eff} = 1.00, for water-reflected spheres of UO_2F_2-H_2O solutions.

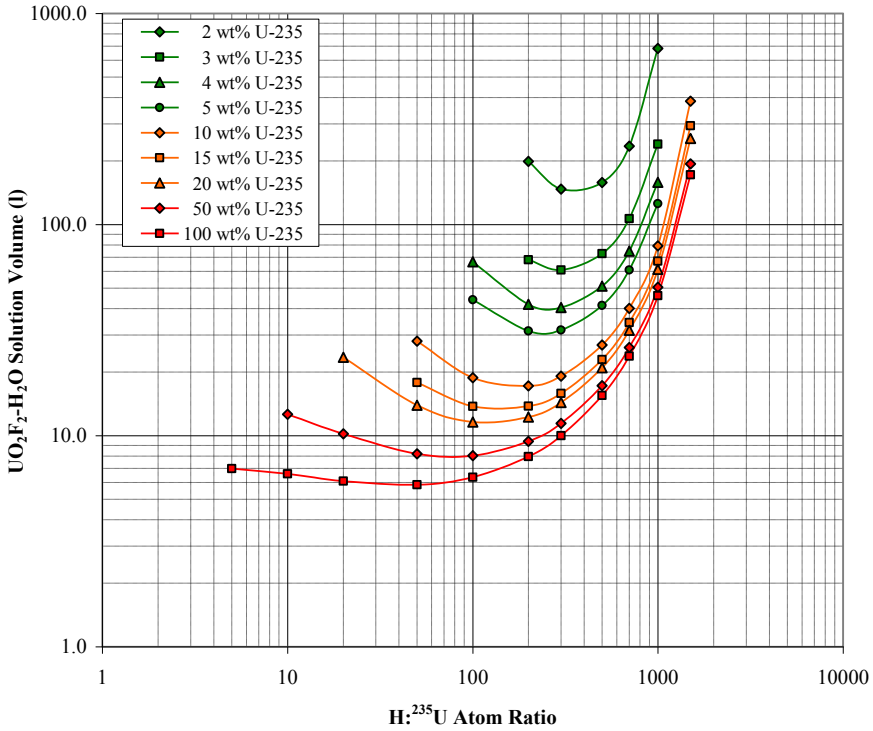

Figure 4.29. Solution volume for computed k_{eff} = 1.00, for water-reflected spheres of UO_2F_2-H_2O solutions.

Cylindrical vessels are commonly used for preparation and storage of concentrated fissile solutions. Figure 4.30 provides the solution diameter (for water-reflected conditions) for computed k_{eff} values of unity for uranyl fluoride solutions. For these models, the cylinder height is infinite.

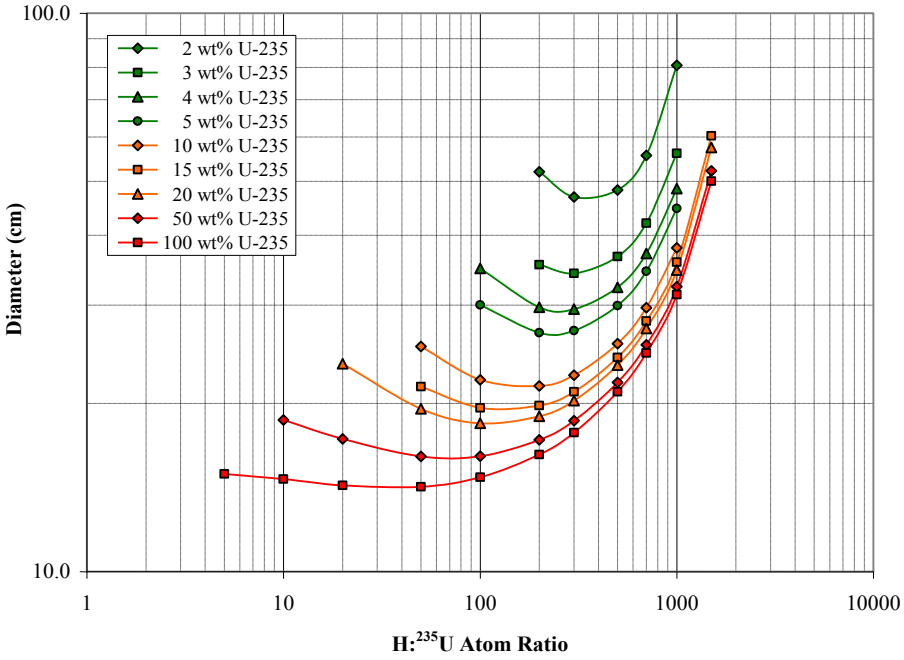

Figure 4.30. Solution diameter for computed k_{eff} = 1.00, for water-reflected infinite-height cylinders of UO_2F_2-H_2O solutions.

For each enrichment value, two cases are retained either as application models (to simulate HTGR fuel cycle configurations) or as comparison models (to investigate the applicability of solution benchmarks that are outside the HTGR enrichment range). Each pair of cases corresponds to (a) the H:^{235}U ratio for minimum fissile mass (i.e., H:^{235}U = 500 for all enrichments) or to (b) the H:^{235}U ratio for minimum solution volume. The H:^{235}U ratios selected to represent minimum volume requirements are

- H:^{235}U = 200 for enrichments of 2%, 3%, and 4%;
- H:^{235}U = 300 for enrichments of 5%, 10%, and 15%;
- H:^{235}U = 200 for enrichments of 20% and 50%; and
- H:^{235}U = 50 for 93% enrichment.

Although the preceding curves included data for 100% enrichment, a solution model at 93% enrichment is employed for comparison models. This ensures that the highest-enrichment comparison cases have an enrichment level (and ^{238}U content) that matches that of many available highly enriched uranium solution benchmarks.

4.3.2 Uranyl Nitrate Solution in Simple Geometries

The most likely form of moderated fissile material feed to the kernel manufacturing process is uranyl nitrate solution. For preparation and storage of the concentrated uranyl nitrate feed, cylindrical pipes, tubes, and vessels will be required.

Uranyl nitrate solution models were created, again using ORNL/TM-12292 methodology. The models contained no excess nitric acid (i.e., the N:U atom ratio was two). For the models, the only combinations of enrichment and H:^{235}U developed were

- H:^{235}U = 300 and 500 for enrichments of 5%, 10%, and 15%;
- H:^{235}U = 200 and 500 for 20% enrichment; and
- H:^{235}U = 50 and 500 for 93% enrichment.

The application models cover the minimum fissile mass and solution volume conditions for uranyl nitrate throughout the HTGR enrichment range. The comparison models at 93% enrichment simulate highly enriched uranyl nitrate solution benchmarks.

For each material model, the solution diameter yielding a computed k_{eff} value of unity was determined. The resulting diameters were comparable to (slightly larger than) the corresponding cylinder diameter values for uranyl fluoride solution as shown by Figure 4.30.

4.4 URANIUM GELS AND UNCOATED FUEL KERNELS

4.4.1 Introduction

In the initial processing steps for HTGR fuel manufacture, the fissile materials typically lack small-scale heterogeneity effects that require modeling in criticality safety calculations. Where inhomogeneous mixtures, materials of nonuniform density, or multiphase liquids may exist in these “ordinary” uranium processing activities, criticality analyses can usually account for such factors by use of homogeneous material models in a conservative fashion.

In manufacture of HTGR fuel, small-scale heterogeneity issues are first encountered when uranium feed solution from the initial processing steps, often mixed in a homogeneous or near-homogeneous blend with organics, is used to create small spheroids of uranium gels. Immediately upon creation, the gel particles are immersed in aqueous or organic liquids. At this point, and for immediately following process steps,

the fissile material within the spheroids is subject to both internal and external neutron moderation effects. The internal moderation of the particles changes as the porous spheroids are rinsed with cleaning liquids to remove reaction by-products and other unwanted content. External moderation can vary based on agitation of the spheroids within the surrounding liquid, or change of immersing liquid (e.g., from organic to aqueous).

Once all liquid treatments of the spheroids are complete, external moderator liquid is not present as a normal processing condition. The internal moderator content is reduced and eventually completely eliminated through drying and high temperature furnace treatments. For dry operations, criticality evaluations may still need to consider presence of moderator fluid as an abnormal condition.

The objective of Section 4.4 is to develop application models that simulate small-scale material heterogeneity effects for HTGR fuel operations that involve wet gel particles, uncoated fuel kernels, and all intermediate fuel forms.

4.4.2 Strategy for Material Models Development

Although final fuel kernels (uncoated particles) for various HTGR fuels have a fairly narrow range of key parameters (e.g., particle size, fissile mass per particle), there is a wide variability at the front end of the process for techniques and materials involved in creation of the fuel kernels. Consequently, the size and composition of wet gel particles and of partially dried gel particles are dependent on the final methods for fuel kernel manufacture as deployed on an industrial scale. The liquids that may be used to treat the gel particles and expected fissile concentration ranges for mixtures of gel particles may also vary from current laboratory-scale process methods.

For these reasons, a general modeling strategy is needed that will encompass the full range of potential internal and external hydrogenous moderation ratios that may occur throughout future fuel kernel manufacturing processes.

Although nonaqueous liquids may be used in gel particle manufacture, the primary moderator element of interest is certain to be hydrogen. The amounts of carbon present in the final fuel kernels and potentially present in organic moderators have a minor effect in comparison to the moderation ability of hydrogen. Thus, ordinary water is adopted as the material model for both internal and external fuel particle moderators.

The presence of other temporary constituents of the wet gel particles is ignored, and the wet gel particles are modeled as a homogeneous mixture of $UC_{0.5}O_{1.5}$ and H_2O. The internal moderation ratios modeled for the wet gel particles range from a maximum of about twice that anticipated for feed solutions, down to a moderation ratio of zero corresponding to the final cured fuel kernels.

Heterogeneous models of the wet (and dry) fuel particles and water were created. For this purpose, the spherical fuel particles were modeled with the densest packing possible (a three-dimensional triangular-pitch packing, where each sphere contacts 12 other spheres), with water filling the gaps between the particles. This packing fraction (~74%) exceeds the expected random packing fraction for spheres (~61%). Thus, for any given particle, the minimum average H:^{235}U ratio considered should lower bound realistic minimum values. For clarity, the term "average H:^{235}U ratio," when used here regarding heterogeneous fuel particle mixtures, refers to the H:^{235}U atom ratio considering both internal and external moderation of the particles.

Maintaining a triangular-pitch lattice of spheres, increased pitch values were modeled so that average H:^{235}U ratios extended to overmoderated levels (H:^{235}U up to 1500). By selecting a sufficient number of

values for both internal and average H:^{235}U moderation ratios, the entire spectrum of possible gel particle and hydrogenous liquid moderation ratios of criticality interest were addressed.

Material models were developed only for ^{235}U enrichments of 5%, 10%, 15%, and 20%. No comparison models above or below this enrichment range were developed, since there are no benchmarks that present heterogeneity of fissile particles and hydrogenous moderator on the scale to be investigated here.

As a modeling basis, preliminary fuel kernel parameters identified for the Next Generation Nuclear Plant (NGNP), as defined in report ANL-GenIV-075,[77] were used. The basic specifications for the final form fuel kernels are

- a stoichiometry corresponding to $UC_{0.5}O_{1.5}$,
- a material density of 10.5 g/cm^3, and
- a radius of 0.0175 cm.

The material modeling strategy for 10% enrichment fuel particles, ranging from dry kernels to well-moderated gel particles, is outlined.

(1) Using an idealized isotopic makeup for 10% enrichment uranium (^{234}U, ^{235}U, and ^{238}U), the ^{235}U mass of an individual particle was determined (2.09303×10^{-5} g ^{235}U).

(2) Internal moderation values selected were 0, 100, 200, 400, and 800. Ref. 35 identifies that the feed for gel particle formation should have a concentration of 2.6 to 2.9 moles per liter. For an ideal $UO_2(NO_3)_2$ solution, a concentration of 2.6 moles U/liter would have an H:U ratio of about 34 (H:^{235}U ratio of about 340, for 10% enrichment). The actual H:^{235}U ratio of the feed could be somewhat higher since the feed is acid deficient and organic additives are present. Thus, for modeling purposes, the maximum considered H:^{235}U ratio was set at about twice the ideal solution value. The H:^{235}U ratio of 400 corresponds to the expected initial moderation ratio as wet gel particles are initially formed, and the H:^{235}U values of 200 and 100 simulate partially dried fuel particles.

(3) For each fuel particle composition (H:^{235}U = 0, 100, 200, 400, and 800), pitches of fuel particles were determined for (a) touching fuel particles, and (b) nontouching fuel particles at preselected average H:^{235}U moderation ratios. The preselected average moderation ratios range from the minimum possible (that which occurs with touching particles) and includes any higher available average H:^{235}U ratios of values 10, 20, 50, 100, 200, 300, 500, 700, 1000, and 1500.

To model discrete fuel particle-water mixtures, the SCALE KENO-VI routine was employed, because the KENO-VI code allows modeling of a dodecahedral unit cell. The unit cell has 12 faces, with each face being a rhombus. The dodecahedral radius (r_{dode}) is the distance from the origin of the unit to a rhombus face. For a triangular-pitch, close-packed array of spheres, the sphere and dodecahedral radii are the same value. Dodecahedral unit cells can be stacked into an array, such that each sphere is touching 12 adjacent spheres. The dodecahedral unit volume is

$$4(2)^{0.5}(r_{dode})^3$$

and the sphere volume is

$$(4/3)\pi(r_{sph})^3 .$$

Thus, for spheres in contact (where $r_{sph} = r_{dode}$), the packing fraction (volume fraction occupied by the spheres) is 0.74048.

Table 4.5 provides modeling specifications for 10% enrichment uncoated fuel particles. As an example, six models were developed for particles having an H:^{235}U ratio of 200. All six models had the same

Table 4.5. Material and unit cell specifications for discrete models of 10% enrichment uncoated fuel particles in water

Discrete particle modeling parameters			
Particle H:^{235}U	Particle H_2O volume (cm^3)	Particle radius r_{sph} (cm)	Average H:^{235}U at contact
0	0.000000	0.017500	9.8
100	0.000080	0.029061	144.8
200	0.000161	0.035230	279.9
400	0.000321	0.043461	550.0
800	0.000643	0.054155	1090.2

Unit cell dimensions (Particles not in contact)	
Average H:^{235}U	Unit cell r_{dode} (cm)
20	0.01895
50	0.02229
100	0.02629
200	0.03187
300	0.03598
500	0.04217
700	0.04694
1000	0.05266
1500	0.06010

Full density water specifications

H_2O density (g/cm^3)	Atom density values	
	N_H [a/(bn-cm)]	N_O [a/(bn-cm)]
0.9982	6.67356E-02	3.33678E-02

Discrete particle atom density specifications						
Particle H:^{235}U	N_{235} (a/(bn-cm))	N_{238} (a/(bn-cm))	N_{234} (a/(bn-cm))	N_C (a/(bn-cm))	N_O (a/(bn-cm))	N_H (a/(bn-cm))
0	2.38877E-03	2.12062E-02	2.15174E-05	1.18082E-02	3.54247E-02	0.00000E+00
100	5.21627E-04	4.63073E-03	4.69868E-06	2.57853E-03	3.38170E-02	5.21627E-02
200	2.92781E-04	2.59915E-03	2.63729E-06	1.44728E-03	3.36199E-02	5.85561E-02
400	1.55947E-04	1.38442E-03	1.40473E-06	7.70883E-04	3.35021E-02	6.23789E-02
800	8.06046E-05	7.15565E-04	7.26066E-07	3.98448E-04	3.34372E-02	6.44837E-02

particle radius (0.035230 cm). When modeled in contact with water between particles, the average H:^{235}U ratio was 279.9. The particles were also modeled with increased unit cell radii (r_{dode}) so that particle-water models with average H:^{235}U values of 300, 500, 700, 1000, and 1500 were obtained.

Discrete-particle models similar to Table 4.5 data were also derived for 5%, 15%, and 20% enrichment fuel. At these other enrichments, the lowest average H:^{235}U values necessarily differed from that of Table 4.5 due to the variation in enrichment.

Fully homogenized models were also determined for all enrichments. These single-media models were obtained by multiplying the discrete-particle atom densities by the packing fraction of the particles, multiplying the water atom densities by (1 minus the particle packing fraction), and summing the resulting atom densities.

4.4.3 k-infinity Geometry Models for Heterogeneous and Homogeneous Models of Uncoated Fuel Particles and Water

For heterogeneous (discrete particle) models of fuel particles and water, a dodecahedral unit cell was described containing a single spherical particle surrounded by water. A KENO-VI array was constructed and then truncated by a cuboid to yield a building unit containing a total particle volume corresponding to 1000 spherical particles. This cuboidal unit (illustrating uncoated fuel particles in surface contact, packing fraction of 0.74048) is shown by Figure 4.31.

By use of mirror reflectors on all faces of the unit described by Figure 4.31, k_∞ models were obtained.

For homogeneous models of fuel particles and water, a simple cuboid of the single-media model was generated, and mirror reflectors were applied to all faces of the cuboid.

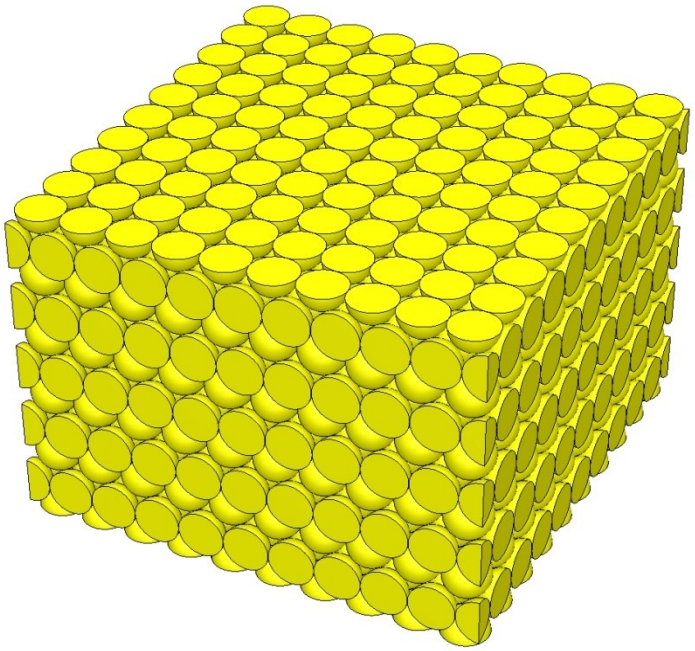

Figure 4.31. KENO-3D graphic of unit containing touching, uncoated fuel particle spheres in a triangular-pitch lattice. Water between the fuel particles is not shown. Similar models varied the spacing of the particles and/or the particle radius.

4.4.4 Cross Section Libraries and Treatments for k-infinity Calculations

The influence of cross section library selection and treatment options was investigated.

For all enrichments and moderation models, k_∞ calculations were performed using both the SCALE ENDF/B-VII continuous energy cross section library (CE_V7) and the 238-group multigroup cross section library (V7-238).

For all discrete particle models, problem-dependent V7-238 cross section adjustments were performed using the latticecell option for spheres in a triangular-pitch lattice ("latticecell sphtriangp"). Additional multigroup cross section treatments were tested for comparison, including

- celldata "multiregion spherical" treatment,
- celldata "latticecell sphtriangp" treatment with the "CELLMIX" option, and
- celldata "multiregion spherical" treatment with the "CELLMIX" option.

For the V7-238 "multiregion spherical" input, the fuel particle was simulated as a sphere surrounded by a layer of water. The water layer had a radius that maintained the moderator–to–fuel particle volume ratio of the dodecahedral unit cell model. A white boundary condition was specified for neutron return to simulate the effects of an infinite lattice of fuel particles.

The V7-238 "CELLMIX" option involves the described cross section pretreatments (latticecell or multiregion) plus an XSDRN-PM calculation to generate a homogenized, single-media mixture for the subsequent KENO calculations. This was done to determine the utility of the CELLMIX option for dimensional search calculations described later in this paper.

For multigroup calculations where the input material model was a homogenized, single-media mixture representing the fuel particles and moderator, the celldata treatment for infinite homogeneous media ("infh") was used.

4.4.5 k-infinity Calculational Findings and Results

Calculations that model discrete particles with intervening moderator liquid, performed using the continuous-energy cross section library, are assumed to provide the highest fidelity regarding the fissile configurations and source nuclear data. Computed results for discrete-particle models and the CE_V7 library thus serve as the reference comparison for other results.

Primary findings are summarized:

- For discrete particle models, the V7-238 results with celldata treatments "latticecell sphtriangp" and "latticecell sphtriangp" were in very close agreement with CE_V7 results for all enrichments and moderation values. V7-238–computed k_{eff} values were slightly greater than CE_V7 results, with a positive bias ranging from ~0.00% to ~0.20%.
- V7-238 results using the CELLMIX option, using either "latticecell sphtriangp" or "latticecell sphtriangp" celldata treatment, were in very good agreement with CE_V7 discrete-particle model results with minor exceptions. At average H:^{235}U = 1000 and 1500 values, the CELLMIX k_{eff} results showed a negative bias ranging from about –0.15% to –0.40%.
- Homogeneous material models (where user input was a single-media mix) yielded computed k_{eff} values as much as 1% less than discrete particle model results or CELLMIX results.
- The most reactive particle model was that of an unmoderated fuel kernel. All moderated fuel particle models (particle H:^{235}U values = 100 to 800) yielded highly consistent k_{eff} results, but these results were as much as 1% less than results for the unmoderated fuel kernel models.

Figure 4.32 provides example CE_V7 results for particle models with 10% enrichment. Homogeneous model results and results for particles having internal water moderation are consistent but generally less than results for particles with no internal moderation. At average H:^{235}U values of ~50 and less, all models yielded consistent results.

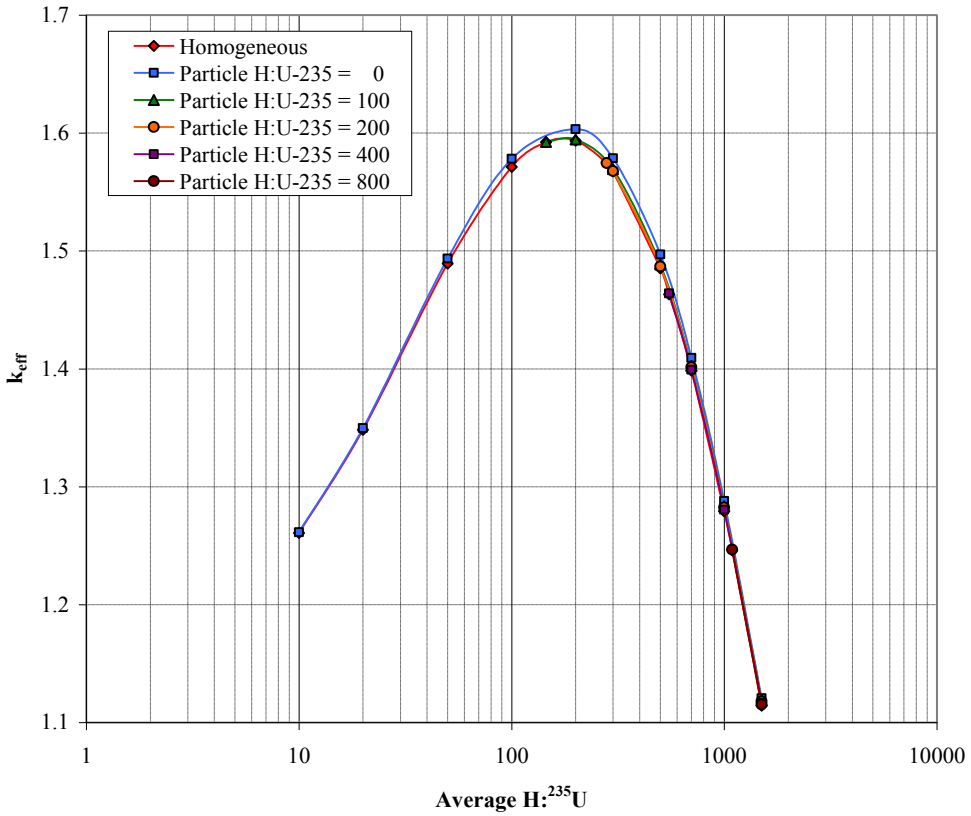

Figure 4.32. CE_V7 k_∞ results for uncoated, 10% enrichment fuel particles in water.

The results of Figure 4.32 suggest that use of a homogeneous model for fuel particles may be acceptable only if the fuel particles are well moderated, such as in the initial gel formation columns. However, in operations where the particles are being dried, or after particles have been cured, use of a homogeneous model is appropriate only for models where there is little moderation of the particles.

For each of the modeled HTGR enrichment values, Figure 4.33 compares CE_V7 results for discrete particle models with no internal moderation, and CE_V7 results for homogeneous material models. Good agreement of results is observed only at low average H:^{235}U ratios, where particles are closely spaced.

The results of Figure 4.33 reinforce the observation for 10% enrichment results, that use of homogeneous models for fuel particle and water mixtures is appropriate only at very low moderation ratios.

Figure 4.34 compares CE_V7 results to results for homogeneous UO_2F_2-H_2O solutions.

Even though Figure 4.34 indicates that particulate models have higher computed k_{eff} values than solution models, such does not necessarily mean that solution experiments cannot be used to validate process calculations for moderated particulates. What both Figures 4.33 and 4.34 do indicate is that when performing process calculations for particulate operations, simplified material models (homogenized or solution models) are potentially nonconservative for ^{235}U enrichments as high as 20%.

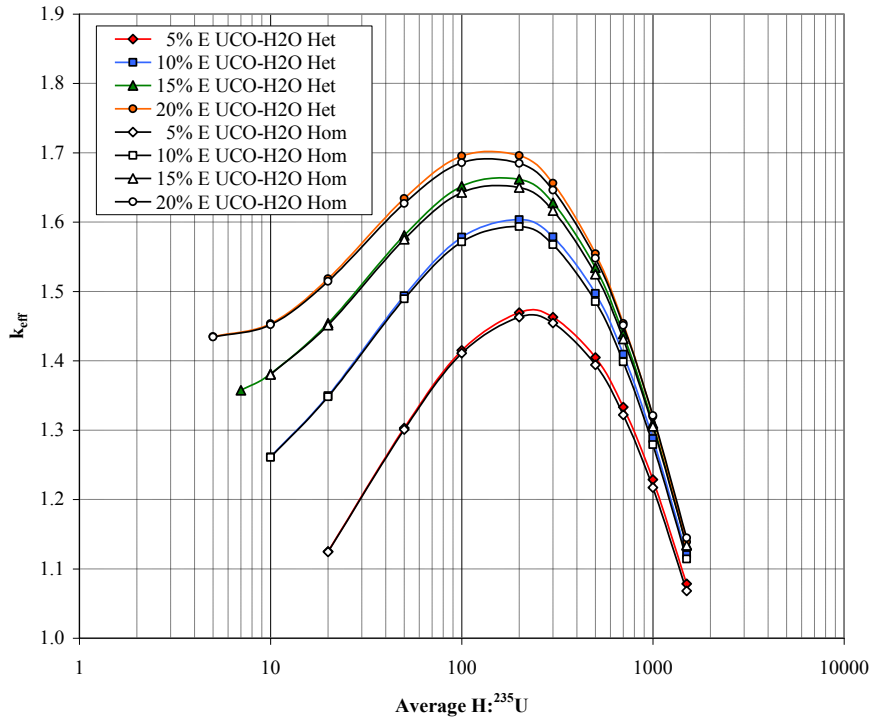

Figure 4.33. CE_V7 k_∞ Results for uncoated fuel particles in water—comparison of discrete-particle model and homogeneous results.

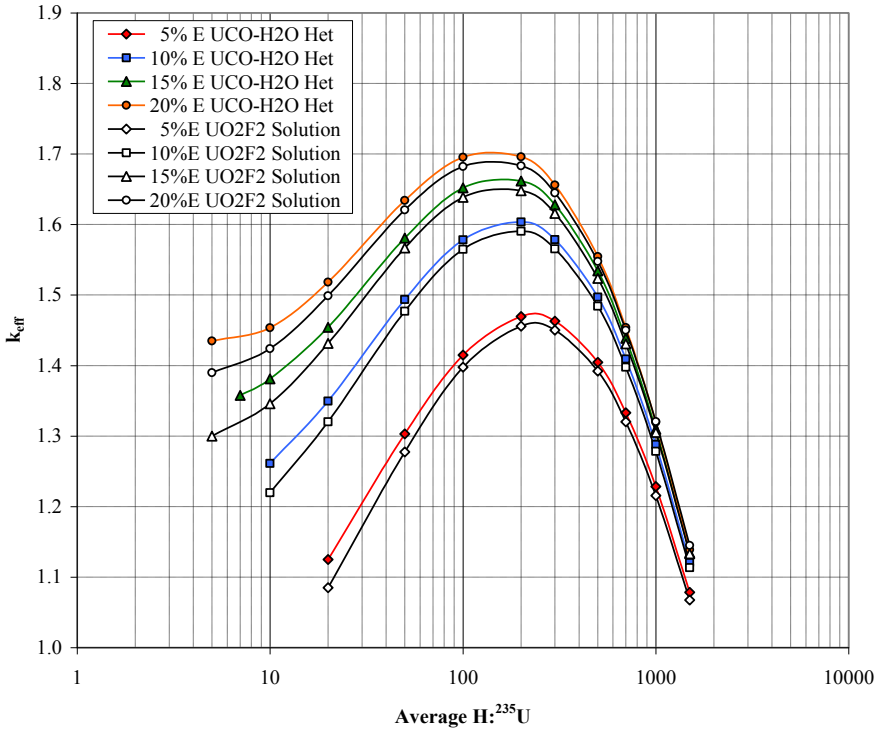

Figure 4.34. CE_V7 results for uncoated fuel particles in water—comparison of discrete-particle model and UO_2F_2-H_2O homogeneous solution results.

4.4.6 Finite Spheres of Uncoated HTGR Fuel Particles Mixed with Water

Finite, simple-geometry configurations (water-reflected spheres) with computed k_{eff} = 1.00 were desired as application models. However, the discrete-particle models described in Section 4.4.3 are KENO-VI models and thus cannot be used with the SCALE CSAS5 sequence to perform dimensional searches.

In Section 4.4.5, it was determined that use of the SCALE celldata "CELLMIX" option yielded computed k_∞ values that were comparable to results using discrete-particle models, provided that the H:^{235}U ratio of the models was less than 1000. Thus, mass estimates for computed k_{eff} = 1.00 were determined using the CSAS5S sequence in a dimensional search mode. In the celldata input, the fuel particles were described as small spheres in a triangular-pitch lattice, with moderator water between the particles. A separate material specification was input for the reflector water. The CELLMIX option provided a single-media, homogenized material for use by KENO-V.a during the dimensional search for sphere radius. In the KENO-V.a model, the water reflector thickness was maintained at 30 cm.

Figure 4.35 provides the derived uranium mass estimates for uncoated HTGR fuel particle-water mixtures, for computed k_{eff} values of 1.00. For data points with H:^{235}U values less than the minima values listed on Table 4.5, the water between the (touching) particles is at reduced density.

The uranium mass values of Figure 4.35 range from a few kilograms up to ~1000 kilograms. Since there are ~5 million particles per kilogram, discrete-particle models for systems of Figure 4.35 may involve up to 5 billion particles.

KENO-VI discrete particle models were created to match selected Figure 4.35 configurations. These models required use of nested KENO arrays of arrays. (For example, the 1000-particle unit of Figure 4.31 would be used as the unit for a 10×10×10 array, giving a unit containing one million particles. This larger unit would be used in a 10×10×10 array to form a unit containing one billion particles.)

However, the prerelease version of SCALE 6.1 was found incapable of modeling multiple-nested particle arrays of the necessary size if the basic building unit was a dodecahedral unit. Therefore, the basic building unit was changed to a cuboid as shown by Figure 4.36. A 10×10×5 array of these units was used to construct a unit that is equivalent to the 1000-particle unit shown by Figure 4.31. Testing of KENO-VI indicated that particle arrays containing as many as 10^{15} particles could be modeled and that k_∞ results of Section 4.4.5 (using a nonnested array of dodecahedral units) could be replicated using large multiple-nested arrays of the cuboidal units.

Based on Figure 4.35 data, eight application models were selected.

For each enrichment, a data point is selected at H:^{235}U = 300, which is near the minimum critical mass. The materials of these data points are representative of normal-condition process conditions (e.g., formation of gel spheres in columns, rinsing operations for gel spheres) or materials under process upset conditions where a near-optimum mix of water and fuel kernels may result (e.g., within drying equipment that contains layers of kernels on vertically stacked screens). The four minimum-mass application models are

- 5% enrichment, 19.0 cm radius sphere containing 2.09 kg ^{235}U;
- 10% enrichment, 16.2 cm radius sphere containing 1.42 kg ^{235}U;
- 15% enrichment, 15.3 cm radius sphere containing 1.24 kg ^{235}U; and
- 20% enrichment, 14.90 cm radius sphere containing 1.14 kg ^{235}U.

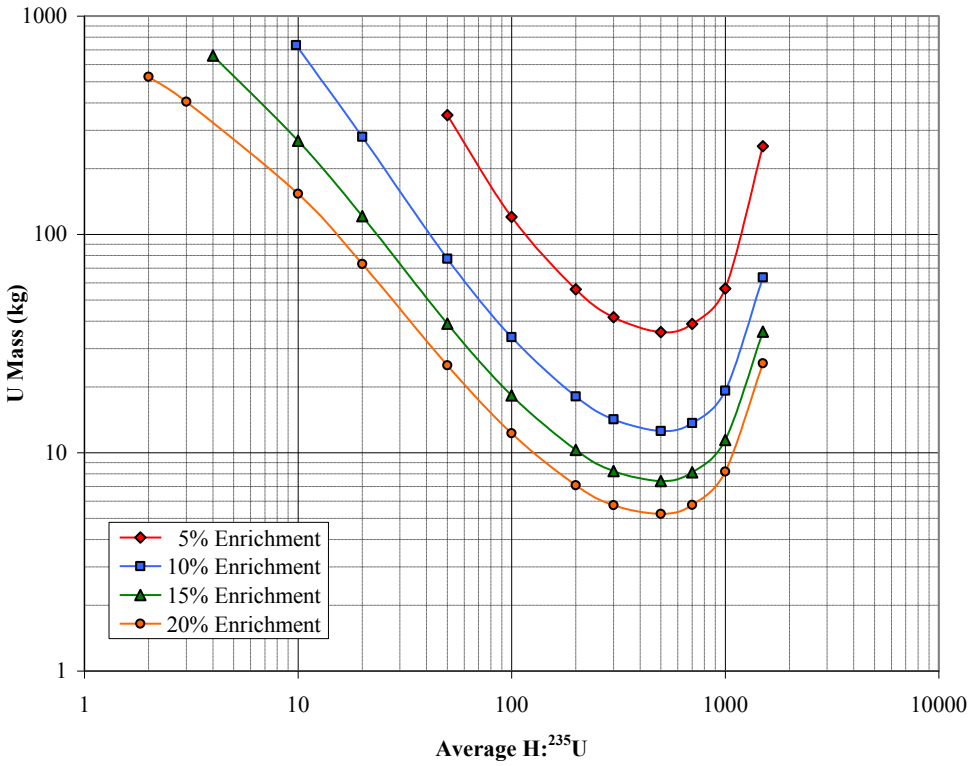

Figure 4.35. Uranium mass for computed k_{eff} = 1.00 for uncoated HTGR fuel particles moderated by water, for water-reflected spherical geometry.

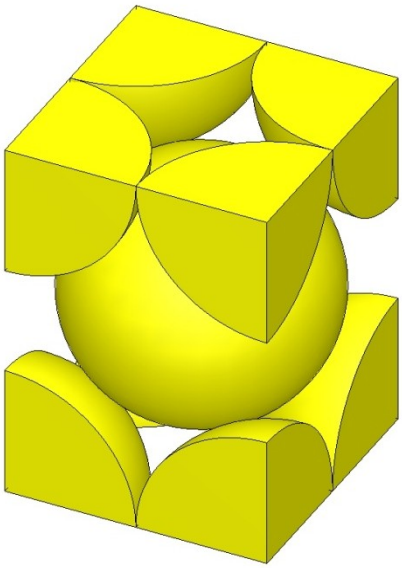

Figure 4.36. KENO-3D graphic of basic cuboid unit used to construct triangular-pitch particle arrays. The total inventory of the unit is equal to 2 particles.

For each enrichment, a data point is selected at an H:^{235}U value that represents a cured-particle packing fraction in a range (~0.55 to 0.70) that simulates closely spaced particles. This packing fraction range is significantly higher than packing fractions for optimum water moderation. These models simulate material mixtures that may result if water in-leaks into process vessels, feed hoppers, or storage containers loaded with kernels. These "poorly moderated" application models are

- 5% enrichment, 25.7 cm radius sphere containing 17.5 kg ^{235}U;
- 10% enrichment, 23.1 cm radius sphere containing 28.0 kg ^{235}U;
- 15% enrichment, 22.0 cm radius sphere containing 40.3 kg ^{235}U; and
- 20% enrichment, 18.9 cm radius sphere containing 30.7 kg ^{235}U.

For each application case, a CSAS6/KENO-VI discrete-particle model was created to verify that the model (with sphere dimensions based on CSAS5S/KENO-V.a runs using the CELLMIX option) would yield a computed k_{eff} value of approximately unity. The CSAS6/KENO-VI discrete particle models were then adapted for use with the TSUNAMI-3D_K6 sequence to obtain k_{eff} sensitivity data files.

4.5 COATED FUEL PARTICLE-WATER MIXTURES

4.5.1 Model Development

The models for the coated fuel particles, or TRISO particles, are based on preliminary fuel parameters from report ANL-GenIV-075.[77] This reference was used in Section 4.4 for development of uncoated fuel kernel models at 5%, 10%, 15%, and 20% enrichments. Those same fuel kernel models are employed for the TRISO particle models.

Specifications for the TRISO particle model are

- a kernel of $UC_{0.5}O_{1.5}$ with a material density of 10.5 g/cm^3, radius of 0.0175 cm;
- a layer of buffer (porous) graphite, density of 1.00 g/cm^3, radius of 0.0275 cm;
- a layer of inner pyrolytic carbon (IPyC, graphite), density of 1.90 g/cm^3, radius of 0.0310 cm;
- a layer of silicon carbide (SiC), density of 3.20 g/cm^3, radius of 0.0345 cm; and
- a final layer of outer pyrolytic carbon (OPyC, graphite), density of 1.87 g/cm^3, radius of 0.0385 cm.

Table 4.6 provides the lattice specifications and H:^{235}U atom ratios for models of TRISO particles immersed in water.

Figure 4.37 illustrates a 1000-TRISO-particle KENO-VI geometry unit.

For celldata processing of V7-238 cross sections, "latticecell sphtriangp" could not be used due to the multiple material layers of the particle model. Problem-dependent multigroup cross section adjustments were performed using the "multiregion spherical" method. For celldata input, each material layer of the TRISO particle was described, followed by a final sphere of water that maintained the correct water–to–fuel particle ratio. A white boundary condition was specified to simulate an infinite lattice of TRISO particles.

Table 4.6. Triangular lattice specifications and H:^{235}U atom ratios for TRISO particles in water[a]

5% Enrichment		10% Enrichment		15% Enrichment		20% Enrichment	
Unit cell r_{dode} (cm)	Average H:^{235}U	Unit cell r_{dode} (cm)	Average H:^{235}U	Unit cell r_{dode} (cm)	Average H:^{235}U	Unit cell r_{dode} (cm)	Average H:^{235}U
0.03860	214.777	0.03860	107.396	0.03860	71.603	0.03860	53.706
0.03991	300	0.04134	200	0.03991	100	0.04134	100
0.04268	500	0.04395	300	0.04395	200	0.04627	200
0.04514	700	0.04839	500	0.04735	300	0.05033	300
0.04839	1000	0.05213	700	0.05299	500	0.05691	500
0.05299	1500	0.05691	1000	0.05763	700	0.06224	700
		0.06344	1500	0.06344	1000	0.06885	1000
				0.07126	1500	0.07766	1500

[a]The unit cell for each spherical particle (particle outer radius of 0.03850 cm) is a dodecahedron. The value of r_{dode} is half of the center-to-center pitch of the particles.

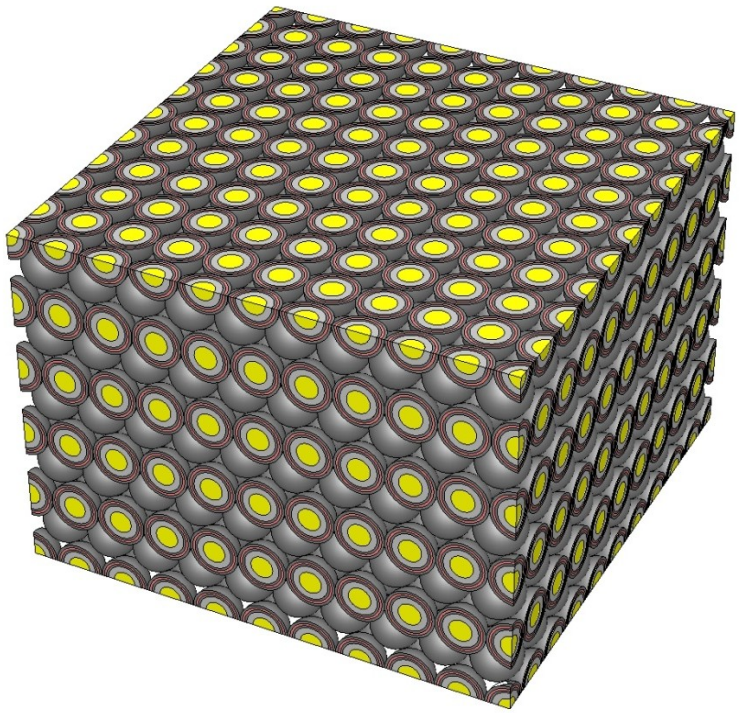

Figure 4.37. KENO-3D graphic of unit containing touching TRISO fuel particle spheres in a triangular-pitch lattice.
Water between the fuel particles is not shown. The total inventory of the unit is equal to 1000 particles.

4.5.2 k-infinity Results

Calculations of k_∞ were performed using both the CE_V7 and the V7-238 cross section libraries. The results were found to be in very close agreement. Figure 4.38 shows the CE_V7 results.

The results are very similar to results for CE_V7 calculations for uncoated fuel particles shown by Figure 4.34, except that the k_∞ maxima values are reduced, ranging from a decrease of $\Delta k_{eff} = 0.013$ for 20% enrichment to a decrease of $\Delta k_{eff} = 0.052$ for 5% enrichment. This decrease is likely due to the small thermal absorption cross section of silicon (~0.16 b) and the reduced volume fraction of fuel in the TRISO models due to presence of the particle coatings.

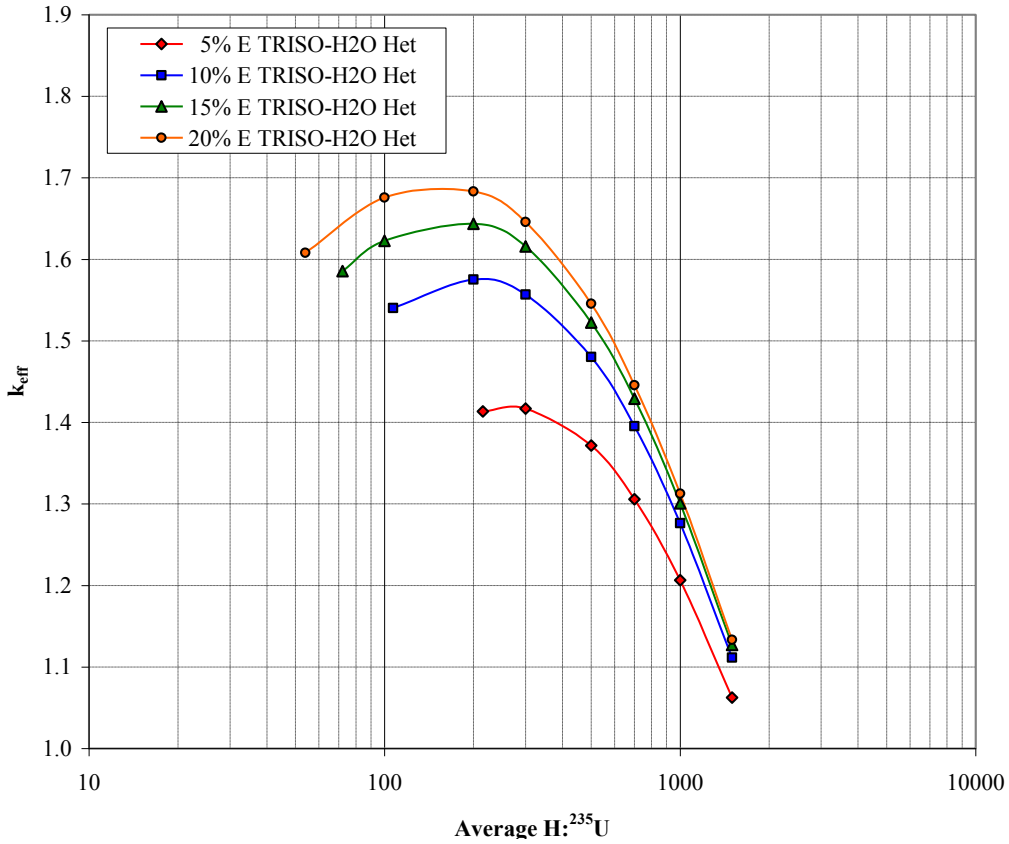

Figure 4.38. CE_V7 k_∞ results for TRISO fuel particles in water.

4.5.3 Finite Spheres of TRISO Fuel Particles Mixed with Water

Estimates for dimensions of water-reflected spheres of TRISO particles in water were determined in a similar fashion as for uncoated particles. The CSAS5S/KENO-V.a sequence was used in a dimension search mode, using a homogenized fuel model generated with the CELLMIX option. Figure 4.39 illustrates the uranium masses determined for computed values of $k_{eff} = 1.00$. For data points with H:^{235}U values less than the minima shown on Table 4.6, the water between the (touching) particles is at reduced density.

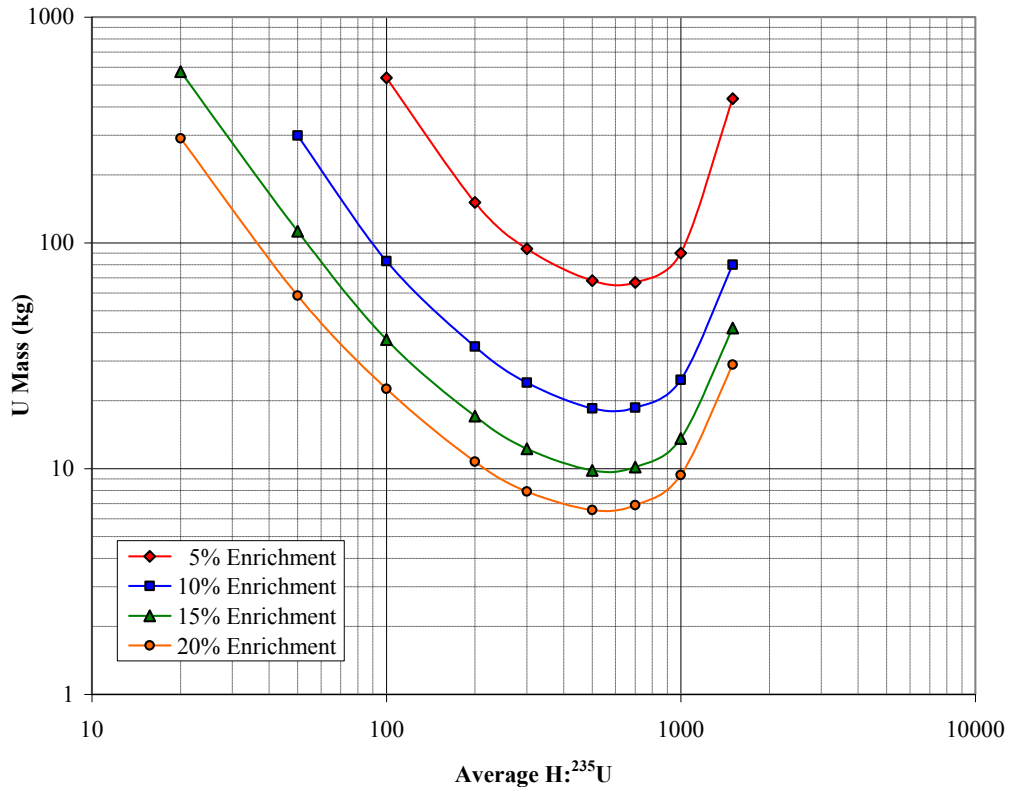

Figure 4.39. Uranium mass for computed k_{eff} = 1.00 for TRISO fuel particles moderated by water, for water-reflected spherical geometry.

There is an important criticality safety consideration regarding inadvertent water addition to inventories of TRISO particles. When uncoated fuel kernels are at packing fractions of ~0.5 to 0.7 (as may be expected for multikilogram inventories) and water occupies void spaces between particles, the resulting mixture is significantly undermoderated and thus critical mass requirements may be large. The "poorly moderated" application models for uncoated kernels involve ~20 to ~40 kg ^{235}U inventories.

Because of the large outside diameter of TRISO particles, the ratio of water to fuel, for water-flooded TRISO particles for the probable packing fraction range, is much larger. In fact, water addition to inventories of TRISO particles may result in H:^{235}U ratios that are near minimum mass requirements shown by Figure 4.39.

Four application models involve full-density water between the TRISO particles. These models simulate conditions such as (a) water in-leakage to process vessels, feed hoppers, or storage containers; (b) excess liquid addition or poor liquid distribution in large benders used for precoating of TRISO particles; or (c) excess binder resin addition or improper distribution in blenders used to mix TRISO particles with graphite and binder resin. The four models are

- 5% enrichment, 33.8 cm radius sphere containing 4.71 kg ^{235}U;
- 10% enrichment, 23.6 cm radius sphere containing 2.40 kg ^{235}U;
- 15% enrichment, 20.3 cm radius sphere containing 1.84 kg ^{235}U; and
- 20% enrichment, 18.7 cm radius sphere containing 1.58 kg ^{235}U.

Three additional application models involve water at reduced density between TRISO particles. These models might simulate normal-condition material mixtures as may result during precoating of TRISO particles in large blenders. These additional models are

- 10% enrichment, 88.0 cm radius sphere containing 183 kg ^{235}U, H_2O at 0.049 g/cm^3;
- 15% enrichment, 87.5 cm radius sphere containing 271 kg ^{235}U, H_2O at 0.037 g/cm^3; and
- 20% enrichment, 87.9 cm radius sphere containing 366 kg ^{235}U, H_2O at 0.025 g/cm^3.

For these application models, discrete-particle model CSAS6/KENO-VI cases were generated to confirm that the application models had computed k_{eff} values near unity. Then, the discrete-particle models were modified for use by TSUNAMI-3D_K6 to generate k_{eff} sensitivity data.

4.6 MIXTURES OF COATED PARTICLES, GRAPHITE, AND BINDER RESIN

4.6.1 Model Development

Application models were developed to simulate normal and off-normal conditions for operations that involve bulk blending of TRISO particles, graphite, and binder resin.

The previously developed models for TRISO particles were used without change.

Two ratios of graphite to fuel particles were used: one to simulate a ratio for fuel compacts (for prismatic HTGR fuel), and another to simulate a ratio for pebble fuel.

The graphite-to-fuel ratio of compacts was determined from fuel data provided in report ANL-GenIV-075;[77] the compact C:U atom ratio is ~65, exclusive of graphite contained in the TRISO particles. Including graphite within the particles, the C:U atom ratio is ~95.

For pebble fuel, the modeled C:U atom ratio is ~1205 excluding graphite in the TRISO particles, and the total C:U ratio is ~1235. The pebble graphite ratio is based on data for the Chinese HTR reactor, from report HTR10-GCR-RESR-001.[78] This C:U ratio applies only to the fueled region of the pebble.

A process parameter that is uncertain is the density of the loose graphite powder during the blending process. Density of the feed graphite powder could vary. During blending, the density of the powder (between fuel particles) will likely change due to compaction by the weight of the feed particles and effects of binder or other fluid addition. For modeling purposes, a graphite density of 0.865 g/cm^3 was assumed. This value is half of the graphite matrix density in final-form HTR pebble fuel (1.73 g/cm^3). Graphite powder at a density of 0.865 g/cm^3 contains appreciable void fraction, ~0.62 if a theoretical density for graphite particles of 2.3 g/cm^3 is assumed.

Another process parameter that is both uncertain and variable is the amount and distribution of hydrogen moderator present. Preliminary treatment of most of the feed graphite may involve mixture of the fine graphite powder with some resin such as phenol formaldehyde ($C_7H_6O_2$) or other materials. Separate pretreatment of the TRISO particles will be performed to coat each particle with a thin layer of graphite powder, using alcohol or other fluid to cause powder adhesion to TRISO particles. For final blending of precoated fuel particles and pretreated graphite, additional resins or binders may be added. To model the hydrogen content in mixtures of TRISO particles, graphite, binder resin, and other liquid that may be used, water at reduced density was employed. The range of water densities modeled within the graphite powder varied depending on the fuel type (pebble or compact) and the ^{235}U enrichment.

For pebble fuel mixtures (total C:U ~ 1235), the maximum water density modeled in the graphite ranged from ~0.04 g/cm^3 for 5% enriched fuel to ~0.16 g/cm^3 for 20% enriched fuel. Higher water contents were not considered because increased water densities would increase the H:^{235}U ratios above 1500.

For compact fuel mixtures (total C:U ~ 95), the mass and volume of graphite powder per TRISO particle is much smaller, so the maximum modeled water density in the graphite (for all enrichments) was ~0.62 g/cm^3. Higher water densities were not considered because reduction in the graphite-to-fuel ratio would be required to maintain a physically realistic mixture model. For compact fuel mixtures, the maximum H:^{235}U ratio ranged from ~1260 (for 5% enrichment) to ~315 (for 20% enrichment).

Because for each fuel mixture, the ratios of graphite-to-fuel particle and the graphite density were held constant; this resulted in a fixed particle spacing. The TRISO particles were modeled in a triangular lattice, with particle pitches of 0.278 cm for pebble fuel mixtures and 0.114 cm for compact fuel mixtures.

4.6.2 Computational Method and Results

Estimates for dimensions of water-reflected spheres of graphite, water, and TRISO particle mixtures were determined using the same technique described in Section 4.5.3 for spheres of water and TRISO particle mixtures.

Figure 4.40 shows the results for mixtures having a graphite-fuel ratio for pebble fuel. Because of the significant moderation by carbon (total C:U ~ 1235), the influence of water moderation is much less than for mixtures of TRISO particles and water.

Figure 4.41 shows results for mixtures having a graphite-fuel ratio for fuel compacts.

Two observations result from comparison of data of Figures 4.40 and 4.41:

- Since the carbon moderator ratio for pebble fuel is much greater than for compact fuel, dry mixtures of TRISO particles and graphite used for pebble manufacture have critical mass requirements that are an order of magnitude less than for dry mixtures used for compact manufacture.
- Conversely, addition of water moderator to the dry mixtures used for compact fuel results in critical mass requirements that are an order of magnitude less than for pebble fuel mixtures.

An additional observation results from comparison of Figures 4.41 and 4.39. If the 10, 15, and 20% enrichment curves of Figure 4.41 had been extended to higher H:^{235}U ratios, minimum mass requirements lower than the minima of Figure 4.39 (for TRISO-water mixtures) may have been determined. In performing criticality safety analyses for mixtures of TRISO particles, graphite, and moderator liquid, it should not be assumed that a more conservative material model is that of a TRISO particle-moderator liquid only.

Three selected application models have a graphite-to-fuel ratio typical of pebble fuel manufacture:

- 10% enrichment, 145 cm radius sphere containing 17.7 kg ^{235}U (H:^{235}U = 500);
- 15% enrichment, 119 cm radius sphere containing 14.8 kg ^{235}U (H:^{235}U = 300); and
- 20% enrichment, 18.7 cm radius sphere containing 13.1 kg ^{235}U (H:^{235}U = 300).

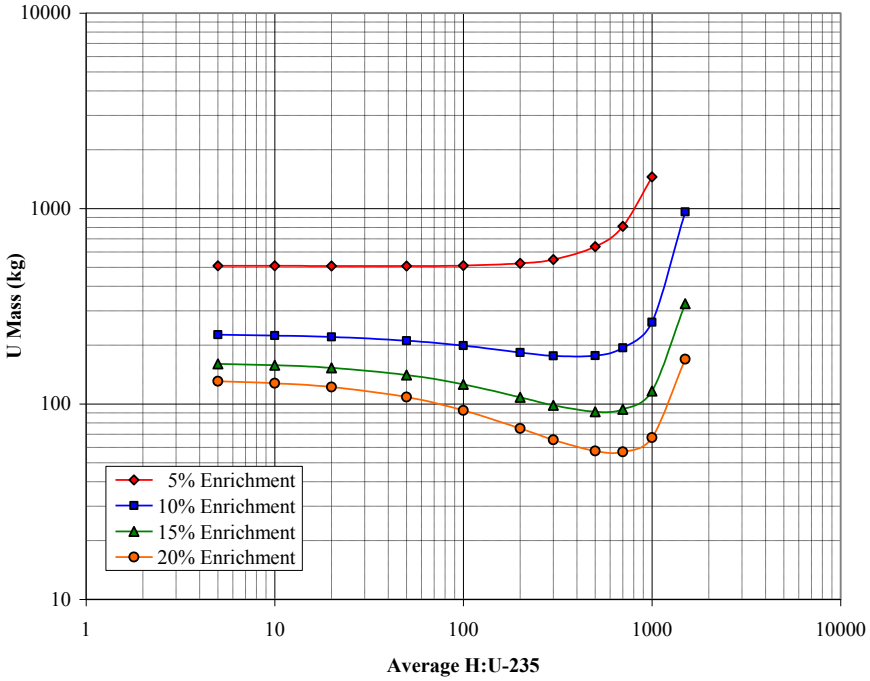

Figure 4.40. Uranium mass for computed k_{eff} = 1.00 for mixtures of TRISO fuel particles, graphite, and water, C:U ~ 1235, for water-reflected spherical geometry. A C:U atom ratio of ~1235 approximates the total carbon to uranium atom ratio of the fueled region of an HTGR fuel pebble.

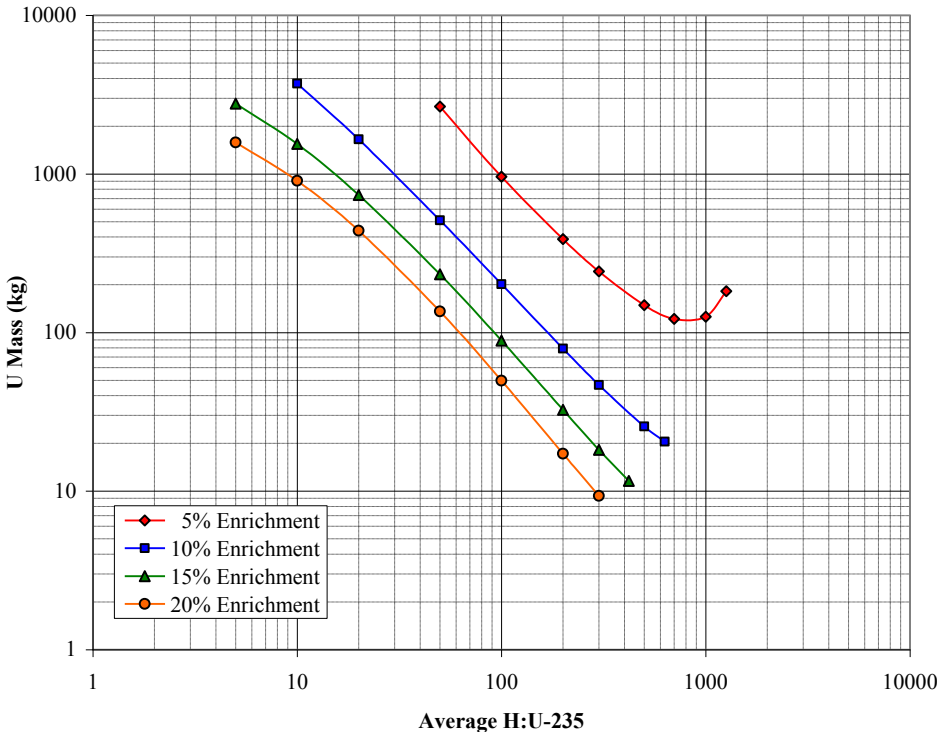

Figure 4.41. Uranium mass for computed k_{eff} = 1.00 for mixtures of TRISO fuel particles, graphite, and water, C:U ~ 95, for water-reflected spherical geometry. A C:U atom ratio of ~95 approximates the total carbon to uranium atom ratio of an HTGR fuel compact.

Three selected application models have a graphite-to-fuel ratio typical of compact fuel manufacture:

- 10% enrichment, 31.3 cm radius sphere containing 2.55 kg ^{235}U (H:^{235}U = 500);
- 15% enrichment, 28.0 cm radius sphere containing 2.73 kg ^{235}U (H:^{235}U = 300); and
- 20% enrichment, 22.4 cm radius sphere containing 1.87 kg ^{235}U (H:^{235}U = 300).

Since design or operational details are not presently known for potential future industrial-scale TRISO-graphite-resin blending operations, these application models are not designated here as representing materials for either normal or abnormal operating conditions.

Discrete-particle model CSAS6/KENO-VI cases were generated to confirm that the application models had computed k_{eff} values near unity, and TSUNAMI-3D_K6 was used to generate k_{eff} sensitivity data.

4.7 FRESH PRISMATIC FUEL COMPACTS

4.7.1 Background on Process Applications

Application models were developed to simulate normal and off-normal conditions for fuel compact inventories. These models may be applicable to activities such as

- collection of compacts as they are fabricated,
- heat treatment of compacts in ovens,
- storage of compacts, and
- shipment of compacts.

Collections of compacts considered include

- close-packed, dry arrangements ("unmoderated"),
- close-packed with gaps between compacts filled with water ("undermoderated"), and
- optimally spaced compacts in water so as to minimize critical mass requirements ("optimally moderated").

Compact collections might be randomly arranged, such as when compacts are dispensed from automated pressing operations into containers. Or, compacts might be placed into some ordered arrangement with spacing, such as depicted by Figure 4.42. In either case, inadvertent release or addition of water to the environment of the compacts could result in a highly effective moderation condition, as water fills the available volumes between compacts.

Compacts also may be placed into some ordered arrangement that results in a close-packed (e.g., triangular pitch, touching) configuration. This may occur in shipping containers or storage containers, either to efficiently utilize container capacity or to help avoid damage to the compacts.

4.7.2 Model Development

The modeling specifications for the compacts are based on the fuel compact description of report ANL-GenIV-075.[77] This description specifies 7256 TRISO particles per compact, and compact dimensions of 1.245 cm diameter and 4.93 cm height. The density of the graphite matrix between the particles is 1.1995 g/cm^3.

Individual compacts were not modeled. Instead, long cylinders (rods) of 0.6225 cm radius were used to simulate compacts placed end-to-end. For all models, these rods were arranged in a triangular-pitch lattice, with either water or void in the regions between the rods. Since configurations approximating

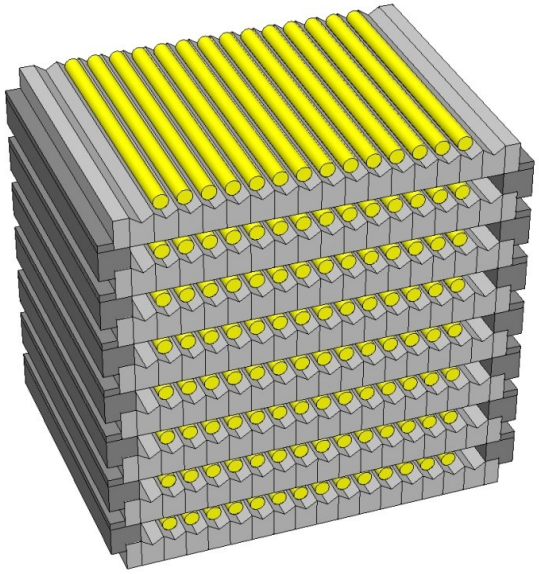

Figure 4.42. KENO-3D illustration of a stack of trays holding UO_2 pellets. This graphic illustrates a computer model for an example configuration at a LWR fuel fabrication facility. [Source: ORNL SCALE (KENO-VI) training course materials.]

minimum critical mass values were desired, the lattice models were truncated to a spherical geometry, with the resulting sphere surrounded by a thick radial reflector. Figure 4.43 illustrates an example model configuration.

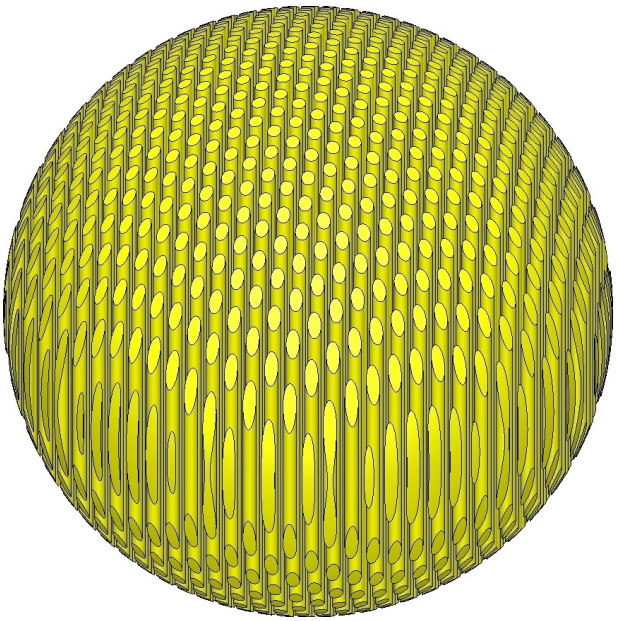

Figure 4.43. KENO-3D illustration of a fuel compact lattice truncated to a spherical geometry. The water moderator between rods (of end-to-end fuel compacts) and the reflector surrounding the spherical core are not shown.

Some compact/rod models involved discrete modeling of TRISO particles in a triangular-pitch lattice using CSAS6/KENO-VI within a graphite matrix. The particle lattices were truncated to a cylindrical shape matching the radius (0.6225 cm) of the compacts. Some particles near the surface of the compact were not whole particles, because the cylindrical boundary intersects some particles.

A KENO-3D graphic was generated to allow observation of the extent to which fractional particles are present in the model. The primary focus is on particles that are cut by the radial surface of the cylinder, because the modeled length of each rod is large compared to the compact diameter. Figure 4.44 shows the KENO-3D depiction of cut particles near the modeled radial surface of a compact/rod. Only a short section of the vertical height of a rod is shown.

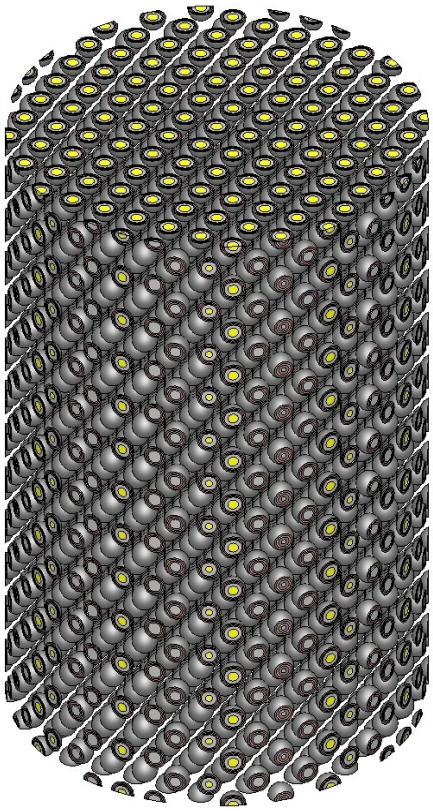

Figure 4.44. KENO-3D illustration of a vertical segment of a fuel compact/rod, showing cut TRISO particles on the radial surface. The graphite matrix between particles is not shown.

The SCALE desktop application GeeWiz was used to activate KENO-3D to perform volume calculations for each material in the compact segment illustrated by Figure 4.44. It was determined that the compact/rod model contains ~0.4% more $UC_{0.5}O_{1.5}$ per unit length than the specifications of report ANL-GenIV-075.[77]

Because the TRISO particles within a compact are not closely spaced, a similar discrete-particle compact model could be developed using a square pitch for the particles. Such a model was previously developed (also using the ANL-GenIV-075 TRISO particle and compact specifications) for the letter report "Source Term Uncertainties for High Burnup HTGR Fuel."[79] A similar volume determination was performed for the square-pitched particle/compact model. The square-pitch compact/rod model also had ~0.4% excess of $UC_{0.5}O_{1.5}$.

It is assumed that the modeling attributes of cut fuel particles has a negligible effect on computed k_{eff} results or k_{eff} sensitivity data. The slight excess of fuel (0.4%) is assumed to present minor impacts on computed k_{eff} results and negligible impact on k_{eff} sensitivity data.

When compacts are immersed in water, neutron reactions within the compacts are influenced on a small scale of heterogeneity due to TRISO particle configuration and graphite of the compacts. Neutron interactions between compacts are also influenced on a larger scale of heterogeneity due to water between the compacts. Thus, for multigroup calculations, use of the SCALE doubly heterogeneous ("doublehet") celldata treatment method is appropriate for conditions where water moderator fills spaces between compacts.

When the doublehet treatment is used, two material models/cross section sets are prepared for use by the k_{eff} calculation routines (e.g., CSAS6/KENO-VI). One material is the large-scale moderator (in this case, water between the compacts/rods). The other material is a homogenized single media representing all fuel and moderator materials within the compact/rod. Thus, doublehet calculations do not involve discrete particle models, and the cut-particle and mass excess attributes of the discrete-particle models do not apply.

An issue for the purpose of this paper is that the doublehet celldata treatment for multigroup cross section calculations has not yet been fully implemented in SCALE sequences. In particular, CSAS5S/KENO-V.a (for criticality searches) and the TSUNAMI-3D sequences (for k_{eff} sensitivity determinations) will not function if doublehet treatment for any input materials is prescribed.

The lack of doublehet implementation in CSAS5S/KENO-V.a is an issue of efficiency; a user can perform criticality searches by other more effort-intensive techniques. However, the inability to use doublehet treatment in TSUNAMI-3D sequences means that to obtain sensitivity data files for doubly heterogeneous systems, multigroup cross section treatments must be employed that only partially account for needed problem-dependent cross section adjustments.

To determine application configurations for compacts with optimum water moderation, a number of CSAS5/KENO-V.a k_{eff} calculations were performed for each HTGR enrichment value. Both the pitch of the fuel compacts/rods and the radius of the enveloping sphere were varied, while a water reflector condition was maintained. In addition to the doublehet celldata treatment, the CELLMIX option was invoked, so as to homogenize the water moderator and the fuel compacts into a single media. (This allowed the searches to be done with CSAS5/KENO-V.a rather than CSAS6/KENO-VI, minimizing the modeling effort.) The k_{eff} results were postprocessed to determine conditions (compact pitch and sphere radius), yielding approximate values for minimum fissile masses for a computed k_{eff} value near unity.

Similar sets of multiple CSAS5/KENO-V.a runs were performed to determine sphere radii and mass values for undermoderated configurations. In these models, the fuel compacts (again modeled as fuel rods) were placed in surface contact in a triangular-pitch rod lattice. Water filled the regions between the rods, a spherical surface truncated the overall rod array to a sphere, and a water reflector (30 cm thick) surrounded the spherical core.

A final set of CSAS5/KENO-V.a runs was performed for unmoderated compacts. The modeling approach was the same as for the undermoderated cases, except that no water was present between rods of compacts, and a 30-cm-thick layer of concrete (REG-CONCRETE) was used as the reflector.

For the optimally moderated and undermoderated models, off-normal conditions involving water introduction into and possibly around inventories of compacts, are simulated. Thus, water was used as the reflector model for the two types of off-normal condition models. The unmoderated models represent

normal storage or handling configurations, such as a large inventory of compacts stored within a concrete vault or a loaded shipping container. A structural reflector (such as concrete) is a more appropriate reflector model for normal-condition application models.

Table 4.7 summarizes parameters selected for the application models.

Table 4.7. Application model parameters for fuel compacts/rods

Condition	^{235}U Enrichment	Pitch (cm)	Radius (cm)	Mass (kg U)	Packing fraction
Unmoderated[a]	5%	n/a[d]	n/a[d]	n/a[d]	n/a[d]
	10%	1.245	258.40	2073	0.907
	15%	1.245	168.60	575.8	0.907
	20%	1.245	133.04	282.9	0.907
Undermoderated[b]	5%	1.245	65.654	272.1	0.907
	10%	1.245	52.791	141.4	0.907
	15%	1.245	48.572	110.1	0.907
	20%	1.245	46.338	95.6	0.907
Optimum moderation[c]	5%	1.365	55.015	133.169	0.754
	10%	1.505	36.828	32.859	0.621
	15%	1.645	31.063	16.502	0.519
	20%	1.725	27.698	10.638	0.472

[a]Close-packed rods, no water between rods, concrete reflector.
[b]Close-packed rods, water between rods, water reflector.
[c]Optimally spaced rods, water between rods, water reflector.
[d]The carbon moderation and enrichment levels are not adequate to support critical conditions.

For the optimum moderation cases at 10% to 20% enrichment, the packing fraction values (fraction of space occupied by compacts) are ~0.5 to 0.6. These packing fractions are potentially achievable by random (not ordered) accumulations of compacts.

4.7.3 Selection of Cross Section Treatment for Calculation of Sensitivity Data

Because the doublehet treatment cannot be used with SCALE TSUNAMI-3D sequences, some compromise must be made regarding the selection of problem-dependent cross section treatment method for TSUNAMI use.

To support this decision, a variety of k_{eff} calculations for each application model were performed, with results shown on Table 4.8. The results with the highest fidelity to nuclear data and to specific modeling of the intended applications are represented by the "CE_V7 Explicit" results. For these continuous-energy results, individual TRISO particles are described within the compacts. The V7-238 doublehet results apply the doubly heterogeneous cross section treatment, resulting in a single material model for the compacts (and a separate material model for intervening moderator) to be used in the k_{eff} calculations. Note the excellent agreement of the CE_V7 and V7-238 doublehet results. Unfortunately, neither of these modeling options can be used to generate k_{eff} sensitivity profiles with TSUNAMI.

Table 4.8. Comparison of explicit continuous-energy k_{eff} results to results for other application models for lattices of compacts

Condition	^{235}U enrichment	CE_V7 explicit	CE_V7 homogeneous[e]	V7-238 "doublehet"		V7-238 "multiregion" for particle treatment		V7-238 "latticecell" for rod treatment	
		k_{eff}	k_{eff}	k_{eff}	Δk_{eff} (%)[f]	k_{eff}	Δk_{eff} (%)[f]	k_{eff}	Δk_{eff} (%)[f]
Un-moderated[a]	5%	n/a[d]	n/a[d]	n/a[d]	n/a[d]	n/a[d]	n/a[d]	n/a[d]	n/a[d]
	10%	1.0010	0.9651	0.9995	-0.15%	0.9979	-0.31%	0.9671	-3.39%
	15%	1.0012	0.9727	0.9999	-0.13%	0.9987	-0.25%	0.9738	-2.73%
	20%	1.0013	0.9787	0.9997	-0.16%	0.9993	-0.20%	0.9792	-2.21%
Under-moderated[b]	5%	0.9996	0.9828	0.9998	0.02%	1.0099	1.04%	0.9840	-1.56%
	10%	1.0012	0.9866	1.0016	0.04%	1.0098	0.85%	0.9878	-1.35%
	15%	1.0012	0.9881	1.0014	0.02%	1.0092	0.80%	0.9894	-1.18%
	20%	1.0017	0.9900	1.0019	0.02%	1.0101	0.84%	0.9906	-1.10%
Optimum Moderation[c]	5%	0.9977	0.9871	0.9973	-0.04%	1.0076	1.00%	0.9883	-0.93%
	10%	0.9973	0.9927	0.9969	-0.04%	1.0046	0.73%	0.9937	-0.36%
	15%	0.9970	0.9973	0.9963	-0.08%	1.0029	0.59%	0.9980	0.10%
	20%	0.9977	1.0007	0.9969	-0.09%	1.0023	0.46%	1.0007	0.29%

[a]Concrete-reflector condition.
[b]Water-reflector condition, water in gaps between touching rods.
[c]Water-reflector condition, water in gaps between optimally spaced rods (minimum mass).
[d]The carbon moderation and enrichment levels are not adequate to support critical conditions.
[e]All materials within the compacts/rods are manually homogenized for material input description.
[f]The Δk_{eff} comparisons are to the CE_V7 explicit-model results.

Table 4.8 results for V7-238 with "multiregion" particle treatment appropriately simulate heterogeneity at the small-scale level. In these cases, "infinite homogeneous media" treatment for the intervening moderator was used, so large-scale heterogeneity effects on problem-dependent multigroup cross sections are ignored. The V7-238 multiregion results agree well with the CE_V7 results for unmoderated models, which is expected because there are no large-scale heterogeneity effects for the unmoderated models. The multiregion results differ from the CE_V7 results by ~0.5% to 1.0% for the undermoderated and optimally moderated models.

Table 4.8 results for V7-238 with "latticecell" rod treatment simulate only the large-scale heterogeneity effects. In order to employ the latticecell celldata option, the materials of the fuel compacts had to be manually homogenized as input. The agreement of latticecell results with CE_V7 results is very poor for the unmoderated models, as expected. The agreement for undermoderated models is not as good as the agreement using the multiregion method. For the optimally moderated models, the quality of the latticecell and multiregion results is about the same.

The primary factor controlling the quality of the latticecell results is not the cross section adjustments associated with large-scale heterogeneity results. Note that the CE_V7 homogeneous results (where the fuel compact model is manually homogenized in the same manner) agree very well with the latticecell results. This indicates the primary deficiency of the latticecell results is that manual homogenization of the compact models results in significant change to neutron physics within the compacts.

Based on these considerations, the CSAS6/KENO-VI models describing discrete particles within the compacts (applying multiregion cross section treatment at the TRISO particle level) were used to create TSUNAMI-3D_K6 inputs and obtain k_{eff} sensitivity data files for the application models of Table 4.8.

4.8 PEBBLE FUEL

4.8.1 Background Regarding Process Applications

Application models were developed to simulate normal and off-normal conditions for fuel pebble inventories. These models may be applicable to activities such as

- storage of pebbles, and
- shipment of pebbles.

Collections of pebbles considered include

- random-packed, unmoderated arrangements,
- close-packed, unmoderated arrangements, and
- close-packed unmoderated arrangements with the optimum amount of interstitial water so as to minimize critical mass requirements.

For random arrangements of pebbles, a packing fraction of 0.61 is assumed. This matches the benchmark-model specification for the HTR reactor as described in report HTR10-GCR-RESR-001.[78] A similar packing fraction would be anticipated within fuel fabrication facilities and at the reactor site, for large containers or vessels used to store pebbles.

Close-packed arrangements of pebbles with a packing fraction of 0.74 were also considered. This packing fraction would not occur unless intentionally created by automated or manual means. The most likely activity that would involve this packing fraction would be shipment of pebbles, if a transport container with a cuboidal payload region were developed. A potential motivation for such a container design is that with an ordered loading of pebbles, a fully loaded container would have a discrete, known number of pebbles. Also, the pebbles would be better protected during transport activities because movement of pebbles within the containers would be restricted.

The most likely normal-condition reflector for pebbles is structural reflection, such as the walls of the enclosing tank or container and nearby materials of facility construction. Also, pebble collections that might approach inventories of criticality safety concern are sufficiently large that under abnormal conditions of water admission to pebble collections, structural materials remain the dominant reflector. Thus, concrete is considered the primary reflector material of interest.

In comparing accumulations of fuel pebbles and compacts under off-normal conditions (primarily, water intrusion), a key difference is that for pebbles, optimum moderation occurs when the amount of water between pebbles is not at full density. Fully flooded pebbles will be shown to have much lower neutron multiplication than pebble collections having interstitial water at lower effective densities.

If water were to enter a pebble collection, as the water drains through the pebbles the volumes between pebbles may still primarily consist of void (air), with thin layers of water flowing across or adhering to the pebble surfaces. Thus, low-density water within pebble configurations may represent a realistic level of moderation.

4.8.2 Model Development

The overall modeling specifications for the pebbles are based on report HTR10-GCR-RESR-001;[78] the TRISO particle models are the same as previously developed based on report ANL-GenIV-075.[77] The pebble model involves 8335 TRISO particles per pebble. The fueled region of the pebble has a radius of 2.5 cm, with a graphite matrix density between the particles of 1.73 g/cm^3. Surrounding the fuel region is a graphite shell of outer radius 3.0 cm, also having a density of 1.73 g/cm^3.

It is noted that for the HTR reactor fuel, the fuel kernel has a radius of 0.025 cm, considerably larger than for the NGNP-based particle model used here (0.0175 cm). Consequently, the uranium mass per pebble in the models used here (~1.75 g U) is about one-third of that for HTR reactor pebbles (5 g U). For comparison, the ASTRA benchmarks of report IEU-COMP-THERM-008[80] have nearly identical overall pebble dimensions and 2.44 g U per pebble.

The pebbles were modeled in a triangular-pitch lattice, either touching (for a packing fraction of 0.74) or with a dodecahedral cell radius of 3.200 cm (for a packing fraction of 0.61). Thus, the pitch of the pebbles in close-packed configurations was 6.0 cm, and for random-packed configurations was 6.4 cm.

To estimate the mass of pebbles for computed k_{eff} values of unity, lattices of pebbles were modeled with CSAS6/KENO-VI. The lattices were truncated to a spherical geometry, and a 30-cm-thick reflector region of concrete ("REG-CONCRETE" at 2.3 g/cm^3) surrounded the sphere. As for the discrete particle models and the models for lattices of compacts, the spherical envelop results in some fraction of the lattice items (pebbles in this case) being sectioned.

Figure 4.45 provides a KENO-3D graphic of a sphere model, for pebbles placed in a triangular-pitch lattice.

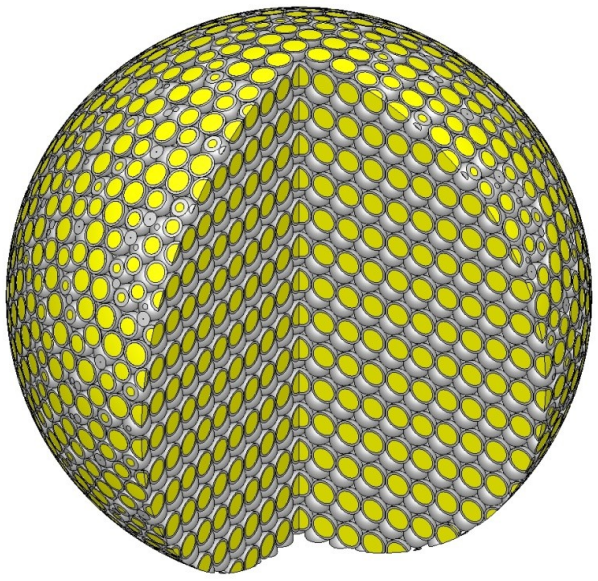

Figure 4.45. KENO-3D illustration of a fuel pebble lattice truncated to a spherical geometry. The low-density water moderator between pebbles and the full-density water reflector surrounding the spherical core are not shown. A quarter section of the model is removed to show the interior arrangement of pebbles.

The issues regarding use of doublehet cross sections adjustments for compacts also apply to development and use of models for pebbles.

Application models for pebbles in an unmoderated condition were first determined. For each enrichment, multiple CSAS6/KENO-VI runs were performed and results postprocessed to determine a fuel core radius for a computed k_{eff} value of unity. For these cases, problem-dependent cross section adjustments were performed using doublehet celldata treatment. This resulted in four application models (one for each enrichment) at a pebble packing fraction of 0.74, with an overall spherical geometry and a concrete reflector condition.

Also, similar calculations were performed for pebbles at a packing fraction of 0.61. These additional cases indicate the effect of the lower density associated with random packing of pebbles. Table 4.9 provides the resulting configurations for unmoderated pebbles at the two packing fractions.

Table 4.9. Unmoderated pebble configuration parameters[a]

^{235}U enrichment	Packing fraction = 0.74			Packing fraction = 0.61		
	Sphere radius (cm)	Approximate # of pebbles	Approximate U mass (kg)	Sphere radius (cm)	Approximate # of pebbles	Approximate U mass (kg)
5%	177.810	154176	269.0	221.449	245349	428.1
10%	126.348	55317	96.5	156.563	86703	151.3
15%	109.358	35867	62.568	135.116	55730	97.2
20%	100.303	27675	48.273	123.727	42792	74.6

[a]The overall shape of the pebble array is spherical, and a 30-cm-thick concrete reflector is modeled.

The increase in mass requirements associated with the lower packing fraction value is significant. However, this change in mass requirements is solely due to a density change—the proportions of graphite and fuel at both small scale (particle) and large scale (pebble) are the same for both packing fractions. Biases, uncertainties, and k_{eff} sensitivities should be very similar for the two packing fractions.

Using each of the four unmoderated pebble configurations with a packing fraction of 0.74, a series of cases was performed with the sphere dimensions maintained, but with addition of low-density water between pebbles. Figure 4.46 shows the results.

For the 5% enrichment fuel pebble configuration, any addition of interstitial water moderator reduces the neutron multiplication. At 10% enrichment, the k_{eff} increase due to optimum moderation is near-negligible.

The four unmoderated pebble configurations at a packing fraction of 0.74 (Table 4.9) were selected as normal-condition (storage and transport) application models.

Two pebble configurations were selected as abnormal-condition (water intrusion) application models:

- at 15% enrichment, sphere radius = 103.336 cm (~52.8 kg U), interstitial water moderator at 0.07 specific gravity; and
- at 20% enrichment, sphere radius = 90.385 cm (~35.3 kg U), interstitial water moderator at 0.10 specific gravity.

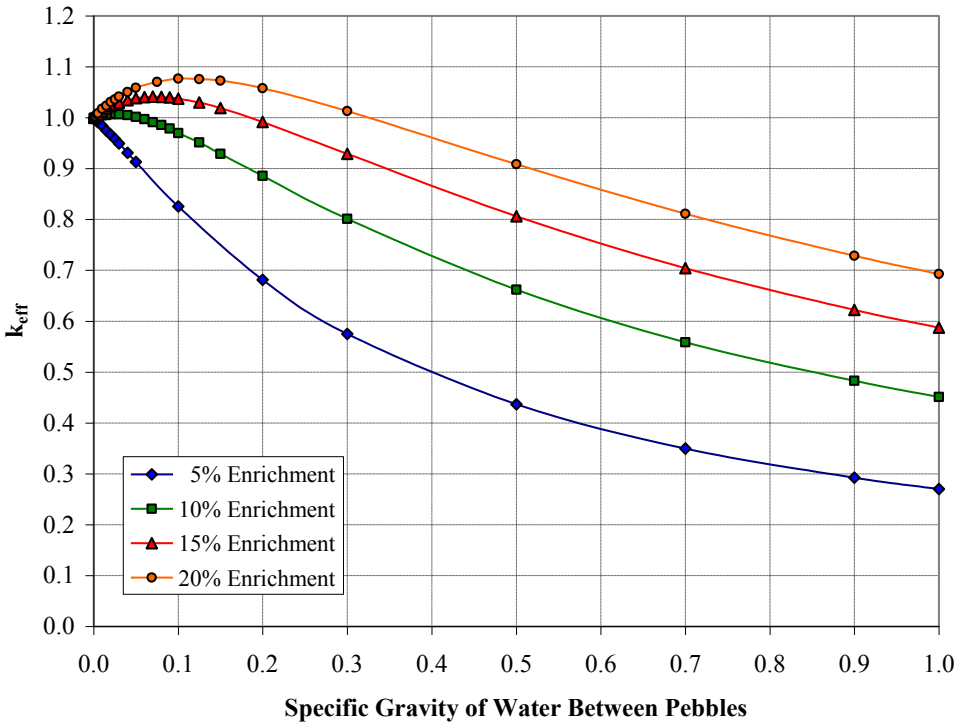

Figure 4.46. Computed k_{eff} as a function of specific gravity of water between pebbles. The modeled configurations are pebbles with a packing fraction of 0.74 and an overall spherical, concrete reflected configuration. At a specific gravity value of 1.0, the water density is 0.9982 g/cm^3.

4.8.3 Selection of Cross Section Treatment for Calculation of Sensitivity Data

CSAS6/KENO-VI k_{eff} calculations were performed to assist in determining a cross section treatment option for use in calculating k_{eff} sensitivity profiles. The k_{eff} results are shown on Table 4.10.

Figure 4.10 shows that for the V7-238 multiregion treatment at the particle level, results are in good agreement with the discrete CE_V7 results. Multiregion treatment results at the pebble level are generally poor.

Based on these results, the CSAS6/KENO-VI models with multiregion treatment at the TRISO particle level were used to create TSUNAMI-3D_K6 inputs and obtain k_{eff} sensitivity data files.

4.9 PRISMATIC FUEL ASSEMBLIES

4.9.1 Background on Process Applications

It is unlikely that any activities at fuel fabrication or reactor facilities will involve significant numbers of proximately placed prismatic fuel assemblies.

Table 4.10. Comparison of explicit continuous-energy k_{eff} results to results for other models for lattices of pebbles

Condition	^{235}U enrichment	Interstitial H_2O (sp. gr.)	CE_V7 explicit	CE_V7 homogeneous[a]	V7-238 "doublehet"		V7-238 "multiregion" for particle treatment		V7-238 "multiregion" for pebble treatment[a]	
			k_{eff}	k_{eff}	k_{eff}	Δk_{eff} (%)[b]	k_{eff}	Δk_{eff} (%)[b]	k_{eff}	Δk_{eff} (%)[b]
Unmoderated	5%	n/a	1.0032	0.9626	0.9995	-0.37%	1.0017	-0.15%	0.9599	-4.32%
	10%	n/a	1.0048	0.9696	0.9975	-0.72%	1.0016	-0.32%	0.9658	-3.88%
	15%	n/a	1.0053	0.9752	0.9999	-0.53%	1.0021	-0.32%	0.9710	-3.41%
	20%	n/a	1.0053	0.9752	0.9999	-0.53%	1.0021	-0.32%	0.9710	-3.41%
Optimum moderation	15%	0.07	1.0026	0.9998	0.9865	-1.61%	1.0018	-0.08%	0.9854	-1.72%
	20%	0.10	0.9901	0.9935	1.0001	1.01%	0.9885	-0.16%	0.9927	0.26%

[a]All materials within the fuel region of pebbles are manually homogenized for material input description.
[b]The Δk_{eff} comparisons are to the CE_V7 explicit-model results.

Unirradiated (fresh) fuel assemblies need to be protected from damage and thus would likely be placed into containers soon after compacts are installed. These containers would likely be designed to hold only one fuel assembly per container. If the container was designed to hold some small number of fuel assemblies, some separating materials would likely be used to prevent assembly contact and potential damage during container handling and transport.

Irradiated (spent) fuel assemblies at the reactor site, if in contact, would likely not be present in sufficiently large individual groups as to present a criticality issue because of decay heat removal needs.

Because out-of-reactor fuel assembly configurations are yet to be designed, it is difficult to postulate potential storage configurations involving large numbers of fuel assemblies for evaluation. Qualitatively, it can be stated that out-of-reactor fuel assembly configurations involving significant numbers of prismatic fuel assemblies will likely have design factors that, for reasons unrelated to criticality safety, serve to limit neutron multiplication. An example is the spent fuel storage configuration for the HTTR reactor, wherein individual vertical stacks of prism assemblies are located in steel tubes with intervening water for heat removal.

If there are future out-of-reactor prismatic fuel accumulations that have significant k_{eff} values (approaching or exceeding 0.90), an application model of an infinite-array (k_∞ model) is judged to be appropriate.

4.9.2 Model Development

The prism assembly model is adapted from Ref. 79, a letter report titled "Source Term Uncertainties for High Burnup HTGR Fuel." That model was developed primarily using report ANL-GenIV-075[77] as a basis. The model uses similar TRISO particle and compact models as previously employed in this paper.

Two unirradiated SCALE prismatic fuel models of Ref. 79 were obtained from the report authors. One model was a continuous-energy (CE_V7) model, in which the TRISO particles, graphite moderator of the compacts, and graphite of the fuel assembly were explicitly modeled. The other model was a V7-238 multigroup model that employed the doublehet treatment for problem-dependent multigroup cross section adjustments. In the multigroup model, the doublehet cross section treatment resulted in a single, homogenized material model for the fuel particles and graphite moderator of the compacts. Both models simulated half the height of a prismatic fuel assembly, with mirror reflectors on all faces to simulate an infinite lattice of fuel assemblies.

The two models were re-executed to verify agreement with computed k_{eff} results reported in Ref. 79. Then, the following changes were made:

- The fuel model was revised from an enrichment of 10.36% ^{235}U to 10% ^{235}U.
- All material temperatures were changed from reactor operating temperatures to room temperature (20°C, input as 293.15 K).
- The original models were revised to simulate a full-height fuel assembly.

The enrichment change resulted in a computed k_∞ change of $\Delta k_{eff} = -0.014$. The reduction to room temperature had a much more significant effect (as expected), with $\Delta k_{eff} = +0.117$.

Then, various tests of other modeling changes were performed, using CSAS6/KENO-VI k_{eff} calculations that were run to a high degree of convergence. The Monte Carlo standard deviation for each k_{eff} result was $\sigma = 0.00020$.

The 10% enrichment, CE_V7 model with TRISO particles in a square-pitch lattice was rerun, and an otherwise identical case with TRISO particles in a triangular-pitch lattice (as used for prior models in this paper) was executed. The results were statistically identical: k_{eff} = 1.19611 for the square-pitch result, and k_{eff} = 1.19618 for the triangular-pitch result.

The V7-238 doublehet model (10% enrichment) yielded a result (k_{eff} = 1.19699) that was in very close agreement with the two CE_V7 results. This agreement is similar to the agreement stated in Ref. 79, for calculations modeling reactor operating temperatures.

However, in reviewing the V7-238 doublehet model, a question arose regarding the input data for the doublehet treatment. The lattice of fuel rods (stacked fuel compacts) was described as a triangular-pitch lattice with a rod pitch of 1.8796 cm. This is the design or model spacing between adjacent rod locations in the prism model. However, this input pitch value for doublehet represents a much lower ratio of graphite-to-fuel than present in the assembly model.

Figure 4.47 shows a horizontal cross section of the prism assembly.

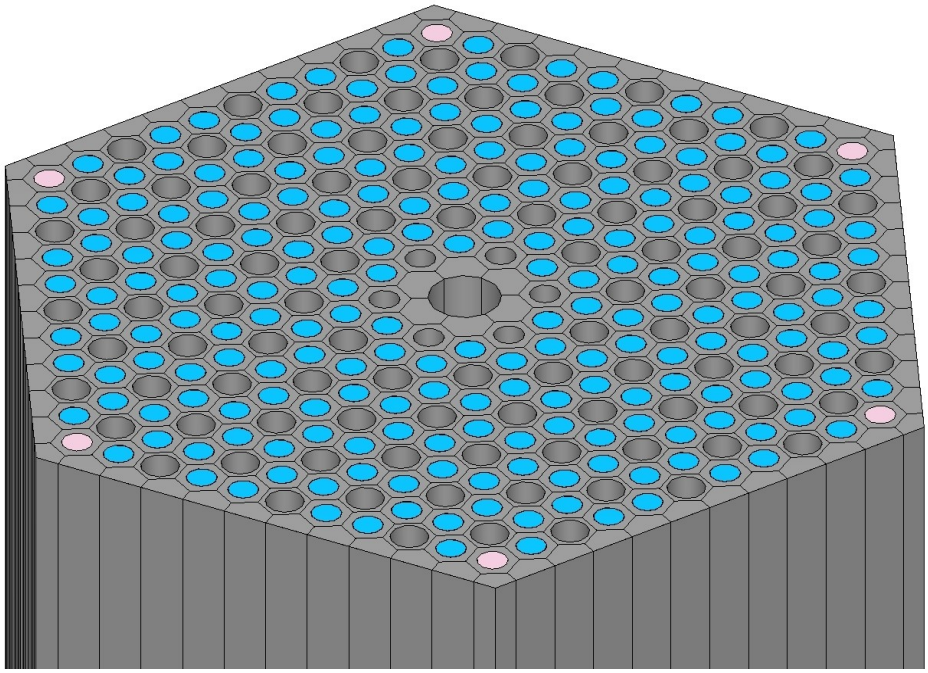

Figure 4.47. KENO-3D illustration of a horizontal cross section of the prismatic assembly model. Fuel rods/compacts are blue, burnable absorbers rods are pink, graphite of the block is gray. The central hole is the lifting hole; all other holes are flow channels for the gas coolant. The pitch between the centers of adjacent fuel rods is 1.8796 cm.

When triangular-pitched rods are specified in the doublehet treatment, the cross section adjustment methods assume an infinite lattice of fuel rods with the specified pitch, with moderator (graphite in this case) filling available areas between rods. Thus, each fuel rod has six adjacent rods, and the moderator-to-fuel ratio is determined by a hexagonal cell.

In the prism fuel assembly model shown by Figure 4.47, most of the fuel rods have only three adjacent fuel rods. Several fuel rods have only two adjacent fuel rods, and some of the rods have only one adjacent fuel rod. This reduction of adjacent fuel rods, accompanied by retention of graphite associated

with the coolant channels, results in an increase in the graphite-to-fuel ratio beyond that associated with a uniform, triangular-pitch rod array with a pitch value of 1.8796 cm.

The GeeWiz application was utilized to perform KENO-3D volume calculations, determining the total volume of all graphite regions of the fuel assembly excluding that present within the fuel rods. The graphite moderator volume per fuel rod was determined; the ratio of graphite to fuel rod is about 40% greater than represented by the original doublehet rod lattice input.

Based on the KENO-3D–derived graphite-to-fuel volume ratio, the equivalent pitch dimension that maintains the moderator ratio was determined to be 2.4694 cm. A V7-238 doublehet case result with a celldata rod pitch of 2.4694 cm yielded a computed k_{eff} value of 1.18563. The Δk_{eff} due to the use of an equivalent pitch in the doublehet input is $\Delta k_{eff} = -0.01136$. Options potentially yielding better agreement of doublehet and continuous-energy k_{eff} results (e.g., use of the SCALE MCDANCOFF routine to calculate a Dancoff factor for use in the doublehet input) were not investigated since the TSUNAMI sequences cannot utilize materials having doublehet treatment.

Similar to application model development for fuel pebbles and compacts, a compromise must be made in order to execute TSUNAMI-3D_K6 to obtain k_{eff} sensitivity data. Options are limited to

- use of a model that accounts for small-scale heterogeneity effects only (i.e., "multiregion spherical" treatment for the TRISO particles and graphite matrix of the compacts), or
- use of a model that accounts for large-scale heterogeneity effects only (i.e., "latticecell triangp" treatment for the fuel rods and graphite of the prism block).

The latter option requires that the inventory of the fuel compacts/rods be manually homogenized as inputs.

Computed k_{eff} results for each of these options significantly differ from the CE_V7 results:

- With the "multiregion spherical" treatment for small-scale heterogeneity effects, results were $k_{eff} = 1.23245$ (TRISO particles in square pitch) and $k_{eff} = 1.23260$ (TRISO particles in triangular pitch). These results differ from the discrete-model, CE_V7 results by $\Delta k_{eff} \sim +0.036$.
- With the "latticecell triangp" treatment for large-scale heterogeneity effects, results were $k_{eff} = 1.15778$ (using a rod pitch of 1.8796 cm) and $k_{eff} = 1.13973$ (using a rod pitch of 2.4694 cm, thereby preserving the average graphite-to-fuel ratio). In comparison to the CE_V7 results, values of $\Delta k_{eff} \sim -0.038$ or -0.056 are found.

4.9.3 Selection of Cross Section Treatment for Calculation of Sensitivity Data

To calculate k_{eff} sensitivity profiles for the prismatic fuel assembly, the "multiregion spherical" treatment was selected. In part, this decision was based on prior use of this treatment for the application models for fuel compacts and pebbles.

For discrete modeling of the TRISO particles in the fuel rods, a square-pitch lattice was used so as to benefit from improved computer run times.

A total of four application models were developed and sensitivity profiles determined. These models were identical except for the material input specifications for the fuel kernel model, which were varied to model 5%, 10%, 15%, and 20% enrichment fuel.

5. BENCHMARK EXPERIMENTS OF POTENTIAL UTILITY

5.1 INDUSTRY STANDARDS AND REGULATORY EXPECTATIONS FOR NCS COMPUTATIONAL METHOD VALIDATIONS

During the first two or three decades of criticality safety practice (1950s through early 1970s), computer methods for criticality safety purposes were either nonexistent or very limited. Direct or interpretative reliance on results of criticality safety experiments was the primary basis for safety of operations.

During the late 1960s and the 1970s, considerable development in user-deployable computational methods occurred. For various reasons, mostly unrelated to computational methods development, many critical experiment facilities ceased operations. These two factors eventually resulted in primary reliance on computational methods to determine criticality safety limits and to analyze the potential for an accident under off-normal conditions. That reliance continues to this day.

Due to concern for potential misapplication of computational methods, a national consensus standard for validation of nuclear criticality safety computational methods was issued in 1975. The content of this standard ("American National Standard for Validation of Computational Methods for Nuclear Criticality," ANSI N16.9-1975/ANS-8.11[81]) was merged into the primary U.S. standard for criticality safety, ANSI/ANS-8.1,[82] in 1983.

As reliance on computational methods continued to increase, much debate commenced within the criticality safety community during the 1990s regarding

- how to determine the applicability of benchmark critical experiments to the process conditions of concern, and
- given an application set of benchmarks, how to derive a maximum k_{eff} value that is reliably subcritical.

Guidance for the former issues, and numerical methods developed for the latter issue, were issued as an internal document at the Savannah River Plant in the late 1990s. Primary content of that document were updated and issued by the NRC in 2001 as "Guide for Validation of Nuclear Criticality Safety Calculational Methodology" NUREG/CR-6698.[83] Although NUREG/CR-6698 was issued for licensees and regulatory staff in the fuel cycle sector, it has gained use for evaluation and approval for transport packages and for out-of-core fuel handling and storage at reactor facilities.

In 2006, the NRC issued an interim staff guidance document, "Justification for Minimum Margin of Subcriticality for Safety," FCSS ISG-10.[83] Although ISG-10 endorsed use of the benchmark-applicability guidance of NUREG/CR-6698, it also recognized the utility of recently deployed computational methods for sensitivity and uncertainty (S/U) analysis methods presented by the SCALE code system. Although there are several aspects of validation that the SCALE S/U method may address, ISG-10 specifically cited the usefulness of S/U methods for determination of benchmark applicability. A specific recommendation of ISG-10 is that the "similarity coefficient," or c_k value, of a benchmark-application comparison using SCALE S/U methods, is indicative of the applicability of the benchmark. A c_k correlation of >0.95 represents a benchmark that provides a very high degree of similarity and is preferred for benchmark selection. A c_k value between 0.90 and 0.95 represents a high degree of similarity and may represent an acceptable benchmark. ORNL SCALE code developers recommend a c_k value of >0.90 for benchmark acceptance decisions and consider experiments with c_k values as low as 0.8 to be marginally useful for validation purposes.

Although S/U methods for criticality safety have received much development effort and are beginning to receive acceptance (nationally and internationally, with SCALE and other codes), no mention of S/U methods is provided in the recently issued (2007) United States consensus standard for criticality safety computational validation (ANSI/ANS-8.24-2007).[84] The standard does require that appropriate parameters for comparison of process applications and benchmarks be determined and used.

All the documents discussed in this section address the topics of benchmark selection and determination of an upper value of computed k_{eff} that is reliably subcritical (frequently termed as the "upper safety limit" and designated as k_{USL}).

The primary purpose of this paper is not to determine k_{USL} values. Any such values would be merely example values and not specifically used in any future evaluation. Instead, the primary objective is to determine if adequate benchmark data exists for development of k_{USL} values specific to HTGR fuel cycle needs.

5.2 BENCHMARKS FROM THE INTERNATIONAL HANDBOOK OF EVALUATED CRITICALITY SAFETY BENCHMARK EXPERIMENTS (IHECSBE)

All critical experiments of the IHECSBE (September 2009 edition) were screened to identify benchmark experiments judged as having potential utility for HTGR fuel cycle applications.

For this purpose, qualitative guidance for selection of benchmarks, as provided by NUREG/CR-6698 and ANSI/ANS-8.24-2007, were employed. Example criteria include

- similarity of fissile enrichment,
- similarity of fissile form (e.g., solution, compound),
- moderator type, and
- moderator–to–fissile nuclide ratio.

Appendix A provides a tabulation of the results of the screening. Each report of the IHECSBE judged to be of potential use, the number of benchmarks present in each report, the basis for report selection, and any additional pertinent notes are identified. In the IHECSBE, materials in the 10% to 20% enrichment range are categorized as "intermediate enrichment uranium," whereas this paper classifies these materials in the "low enrichment uranium" category. Appendix A uses the IHECSBE classification so as to properly identify report locations in the handbook.

Also, as requested by the sponsors of this paper, benchmarks that are of potential use for advanced LWR fuel cycle activities for enrichments in the 5 to 10 wt % range are noted. For this purpose, the area of focus was on front-end fuel cycle activities (prior to irradiation of the fuel).

Also included in the screening is the March 2010 edition of the International Handbook of Evaluated Reactor Physics Benchmark Experiments (IHERPBE). Three benchmark reports were identified as having potential HTGR utility. Two of these reports are distributed with the September 2009 edition of the IHECSBE (IEU-COMP-THERM-008 for the ASTRA reactor, and IEU-COMP-THERM-010 for the Chinese HTR-10 reactor); these reports are listed in Appendix A.

The third IHERPBE report, not issued with the IHECSBE and not included in Appendix A, applies to the Japanese HTTR reactor. This report (HTTR-GCR-RESR-001) has very limited utility as an HTGR criticality benchmark. The report states that significant simplifications were incurred to develop the model due to limited availability of dimensional and composition data. Modeling biases caused by these simplifications could not be estimated, and a significant positive bias is evident in various code results for

the model. The utility of the currently available HTTR model seems limited to performance of code-to-code comparisons and for investigation of physics parameters.

Key observations from this screening are as follows:

- In the 5 to 10% enrichment range, essentially all benchmarks are for uranium solutions and for UO_2 rod lattices in water.
- There are very few experiments involving
  - uranium in the 10 to 20% enrichment range,
  - uranium in the form of coated fuel particles (the limited experiments available are limited to final fuel forms),
  - significant amounts of graphite as a moderator,
  - both graphite and water as moderators, or
  - doubly heterogeneous moderator configurations.
- There are no experiments involving pure UF_6 or fully homogeneous simulations of UF_6.

5.3 CRITICALITY EXPERIMENTS NOT DOCUMENTED IN THE IHECSBE OR THE IHERPBE

A brief review of available critical experiment reports and bibliographies was performed to search for experiments of potential utility the HTGR fuel cycle. For this purpose, the primary bibliography document used was UCRL-52768,[85] "Nuclear Criticality Experiments from 1943 to 1978, An Annotated Bibliography: Volume 1, Main Listing." Results of the review are summarized below.

Legacy experiments have been performed for large assemblies of graphite and enriched uranium, typically with the uranium distributed as very thin foils. Most these experiments employed 93% enrichment uranium and were performed at various national laboratories (Los Alamos, Lawrence Livermore, Brookhaven, and Oak Ridge) in the 1950s and 1960s. Two configurations of the Lawrence Livermore "Snoopy" critical experiment (C:^{235}U ratio ~ 1200) were intended to be issued with the September 2009 edition of the IHECSBE as report HEU-MET-THERM-035. The report authors were contacted; they declined to release a draft version of the report.

Gas-reactor-related experiments were performed by companies involved in early development of such reactors (e.g., General Atomics). In most cases, the fissile material was highly enriched uranium. In general, detailed descriptions of such experiments were not published due to proprietary issues, or the experiments involved materials (e.g., thorium) that limit the utility of the experiments for HTGR fuel cycles based on low-enriched uranium.

Experiments related to space reactor development, in particular the "Rover" program, involved highly enriched uranium and carbon. These assemblies either employed prototype fuel assemblies immersed in water, or stacks of uranium metal, graphite, and hydrogenous moderator. About half of experiments involving Rover fuel are included in the IHECSBE, whereas Rover program experiments using other configurations are not in the IHECSBE.

Various intermediate-enrichment experiments were performed in Britain in the 1960s, involving uranium of enrichments of ~30% to 45%. A draft IHECSBE report (IEU-SOL-THERM-002[86]) was obtained. Based on evaluations described in the next section, these experiments are applicable to several HTGR fuel cycle application models. Additional British experiments (not currently planned for IHECSBE addition) address ~30% enrichment uranium in partially moderated configurations (UO_2-paraffin mixtures). These experiments may also be applicable to other HTGR applications for which benchmarks are lacking.

The only known critical experiments involving UF_6 in pure form were performed at the former Oak Ridge Critical Experiment Facility and are reported in Y-DR-128,[69] "Critical Experiments of UF_6 Cylinder Model 8A Containers." About half of these experiments are likely not acceptable for use; an ongoing IHECSBE evaluation effort for another set of critical experiments has determined that the composition of the concrete reflector blocks is too poorly characterized to allow accurate modeling. A significant additional uncertainty (not currently evaluated) involves the distribution of UF_6 within the cylinders. Finally, the very high ^{235}U enrichment (97.5%) reduces the potential utility for HTGR applications.

Experiments were also performed at Oak Ridge using seven close-packed water-immersed 30B cylinders containing 4.2% enrichment UF_6. These experiments only achieved a low observable level of neutron multiplication and thus are not usable as benchmarks.[13]

Based on this review, it is likely that several legacy critical experiment series did address criticality physics relevant to the HTGR fuel cycle evaluated here. However, detailed documentation of legacy critical experiments has (in many known cases) been lost or can no longer be located, and staff that performed the experiments are no longer available to assist in interpretation of records. Additionally, for experiments performed in the 1950s and 1960s (when NCS computer methods did not exist), the experimenters saw no need to record details now deemed necessary to characterize the uncertainty of computational models of benchmarks.

If appropriate resources are applied, some legacy experiments not presently in the IHECSBE may possibly be investigated, with documentation developed to yield benchmark-quality descriptions of utility to HTGR fuel cycle. The opportunity for such benefit may be quite limited.

6. EVALUATION OF BENCHMARK COVERAGE OF SELECT APPLICATIONS

6.1 PRELIMINARY EVALUATION OF APPLICATION AND COMPARISON MODELS

In Section 4, a total of 68 HTGR application models and 11 comparison models were developed. (For this count, all models at 5% enrichment are considered as application models, since pebble-fuel forms may be at enrichments between 5% and 10%.) For each model, a k_{eff} sensitivity data file (SDF) was generated using one of the SCALE TSUNAMI sequences.

A preliminary similarity comparison was done for these models for several reasons. First, the models were selected using engineering judgment, without forehand knowledge of potential k_{eff} sensitivity differences (or similarities) of the models. It is desirable to reduce the count of application models, where two or more models appear highly similar.

A second reason is to help determine what type of benchmarks are of likely utility, using models that lack the complexity or detail often encountered in IHECSBE benchmark details. As an example, developing models of the (non-IHECSBE) Y-DR-128 experiments involving highly enriched UF_6 would be time-consuming. By use of a simple, highly enriched sphere of UF_6 as a comparison model for the HTGR-enrichment UF_6 spheres, indication of utility of the Y-DR-128 experiments can be more easily gained.

A final reason is to provide insight as to the range of future critical experiments that may be desired. For instance, if no benchmarks are available for moderated, uncoated fuel kernels or for moderated TRISO particles, could a future experiment series with just one material provide benchmark coverage for both materials?

The matrix for c_k values is large (a 79 × 79 matrix), so a single spreadsheet is not included in this report. However, several application types had very low similarity to other application types. Where similarity is present between different types of applications (and also between application and comparison models), more limited c_k matrices are provided in Appendix B. For the tables in Appendix B, c_k values for two models that are "very highly similar" ($c_k > 0.95$) are highlighted in green. c_k values in the 0.90 to 0.95 range ("highly similar") are highlighted in yellow.

Many useful conclusions resulting from this preliminary examination are summarized:

1. (Table B.1) There are very high or high degrees of similarities for all unmoderated UF_6 models in the range of 9% to 20% enrichment. This suggests that if reliable benchmark data exist or are generated, a validation basis could be generated for unmoderated UF_6 loadings in the 30B cylinder for up to 20% enrichment. Also, the same benchmarks could support determination of a limiting subcritical enrichment value for unmoderated UF_6.
2. (Also Table B.1) Benchmarks involving highly enriched UF_6 do not have desired similarity to UF_6 at enrichments of ~10% and less. The Y-DR-128 experiments thus lack utility in justifying use of 30B cylinders at the upper end of HTGR enrichments, or in justifying a limiting subcritical enrichment value.
3. (Table B.2) The application models simulating water intrusion to a 30B cylinder (a combined system of solution and UF_6) have low similarities to either the UF_6 or the uranium-solution models.

4. (Table B.3) For any pair of solution-only models at enrichments of 10% through 93%, high or very high similarities exist. All models for 5% and 10% have high or very high similarities. Due to the significant availability of critical experiments for solutions with enrichments of ~5%, ~10%, and ~93%, adequate benchmarks should be available to cover HTGR configurations involving solutions.
5. (Table B.4) This table focuses on high-concentration solution models, as may be used to justify process equipment where criticality is prevented by limited geometry. The prior conclusions for Table B.3 remain applicable; benchmark coverage for HTGR solutions should not be an issue.
6. (Tables B.5 and B.6) Table B.5 focuses on configurations involving wet gel particles or uncoated kernels under water-moderated conditions. HTGR solution application models are provided for comparison. When gels or kernels are dispersed in water so as to be optimally moderated (to result in minimum-mass requirements for criticality), the models are similar or highly similar to solution models of the same enrichment. The same is shown by Table B.6 for coated fuel particles optimally mixed with water. For well-moderated systems involving wet gels, uncoated fuel particles, or coated fuel particles, solution benchmarks may provide an adequate validation basis.
7. (Also Tables B.5 and B.6) Where lesser moderation exists for fuel particles (such as containers or equipment containing dry kernels or coated fuel particles, with water entry), the models have very low similarity to solution models.
8. (Table B.7) For blending operations corresponding to pebble-fuel mix (high C:U ratio fuel), the blending models have high or very high similarity to HTGR solution models. Conversely, all pebble models (unmoderated or with optimum water moderation) have very low similarity to the HTGR solution models.
9. (Also Table B.7) Considering just the pebble fuel models, the only distinction is that the 5% enrichment models are not highly similar to the models for the 15% and 20% enrichments. However, the unmoderated model for pebbles at 10% enrichment is highly similar to pebbles of all enrichments (5% to 20%) and for both dry and optimally water-moderated conditions. Thus, benchmark data for this one condition (dry pebbles at 10% enrichment) could provide coverage for all pebble application models.
10. (Table B.8) For models where HTGR compacts are well moderated by water, the models have high or very high similarity to HTGR solution models. Less similarity to solution models is seen for compacts that are partially water-moderated. Very low similarity to solution models is seen for the dry compact models or for blending operation models (TRISO–graphite powder–water mixtures).
11. (Tables B.9 and B.10) Prism fuel assembly models are seen to have low similarity with any preliminary prism fuel form model (e.g., compacts, blending operation models). This is not fully explainable by the high C:U ratio of the prism assembly because very low similarities also exist to models for pebble fuel and preliminary forms. Benchmarks that may serve to validate calculations for assembled pebble fuel or any preliminary HTGR fuel form will likely not be applicable to prism fuel assemblies.

Based on the preliminary evaluation, 33 application models were retained for comparison to critical experiment benchmarks. These models are identified along with similarity results in Section 6.3.

6.2 BENCHMARK SET SELECTION

A set of 366 benchmarks was utilized to assess potential validation coverage for the HTGR application model set. Except for 13 solution experiment models (30% enrichment, based on Ref. 86), all models are documented in the IHECSBE.

The model set includes many, but not all, of the benchmarks tabulated in Appendix A and includes additional benchmarks not listed in Appendix A. Table 6.1 identifies the source IHECSBE reports and how many experiments were selected from each report. With limited exception, all acceptable experiment configurations listed in each report were used.

Table 6.1. IHECSBE benchmarks (366) used for similarity comparison to HTGR application models

Report	# of Expts
IEU-MET-FAST-007	1
IEU-MET-FAST-010	1
IEU-MET-FAST-012	1
IEU-MET-FAST-013	1
IEU-MET-FAST-014	2
IEU-SOL-THERM-001	4
IEU-SOL-THERM-002[a]	13
IEU-COMP-INTER-003	14
IEU-COMP-MIXED-002	9
Sum:	46

Report	# of Expts
HEU-COMP-THERM-002	3
HEU-COMP-INTER-004	1
HEU-SOL-THERM-001	10
HEU-SOL-THERM-013	4
HEU-SOL-THERM-014	3
HEU-SOL-THERM-016	3
HEU-SOL-THERM-028	18
HEU-SOL-THERM-029	7
HEU-SOL-THERM-030	7
HEU-SOL-THERM-039	6
Sum:	62

Report	# of Expts
LEU-COMP-THERM-002	5
LEU-COMP-THERM-009	26
LEU-COMP-THERM-010	30
LEU-COMP-THERM-017	29
LEU-COMP-THERM-018	1
LEU-COMP-THERM-019	3
LEU-COMP-THERM-020	7
LEU-COMP-THERM-022	7
LEU-COMP-THERM-023	6
LEU-COMP-THERM-024	2
LEU-COMP-THERM-025	4
LEU-COMP-THERM-026	4
LEU-COMP-THERM-032	7
LEU-COMP-THERM-042	7
LEU-COMP-THERM-070	12
LEU-COMP-THERM-075	6
LEU-COMP-THERM-085	13
LEU-SOL-THERM-001	1
LEU-SOL-THERM-002	3
LEU-SOL-THERM-003	9
LEU-SOL-THERM-004	7
LEU-SOL-THERM-005	3
LEU-SOL-THERM-006	5
LEU-SOL-THERM-007	5
LEU-SOL-THERM-008	4
LEU-SOL-THERM-009	3
LEU-SOL-THERM-010	4
LEU-SOL-THERM-011	13
LEU-SOL-THERM-016	7
LEU-SOL-THERM-017	6
LEU-SOL-THERM-018	5
LEU-SOL-THERM-019	6
LEU-SOL-THERM-020	4
LEU-SOL-THERM-021	4
Sum:	258

[a] A draft version of IEU-SOL-THERM-002[86] was used.

6.3 COVERAGE ANALYSIS RESULTS

6.3.1 Models Involving UF_6

Table 6.2 provides similarity results for final application models involving UF_6. Very few applicable experiments were found in the benchmark set. Almost all of the applicable benchmarks for Table 6.2 involved experiments with UF_4-CF_2 mixtures intended to simulate UF_6. All such available experiments are documented in the IHECSBE and were included in the 366-benchmark set. The likelihood of locating any non-IHECSBE experiments that are applicable to Table 6.2 models is low.

Table 6.2. Similarity results for application models and 366-benchmark set: models involving UF_6

Application model description	^{235}U (%)	Application Objectives	Number of Benchmarks Having Similarity		
			$0.90 \le c_k < 0.95$	$0.95 \le c_k < 1.00$	Total
Infinite system of unmoderated UF_6	10.3	Limiting critical enrichment of unmoderated UF_6	5	0	5
Close-packed, reflected array of 30B overpacks	15	Transport licensing, on-site storage	4	4	8
30B cylinder with H_2O intrusion, solution slab geometry	10	Determine risk of criticality due to water in-leakage	3	0	3
30B cylinder with H_2O intrusion, hemisphere geometry	20	Determine risk of criticality due to water in-leakage	8	0	8

6.3.2 Models Involving Solutions

As expected, excellent benchmark coverage for application models was found, as shown by Table 6.3.

6.3.3 Models Involving Fuel Particle Mixtures With Water

Table 6.4 provides results for application models involving mixtures of water and fuel particles. Excellent coverage is found for all cases involving minimum mass requirements (high H:^{235}U ratios). Although slightly reduced critical mass or critical dimensions may be calculated for particle-water mixtures (when compared to solution results), the particle sizes are so small that the criticality physics of the two material types remains very similar.

Table 6.3. Similarity results for application models and 366-benchmark set: models involving solutions

Application model description	^{235}U (%)	Application objectives	Number of benchmarks having similarity		
			$0.90 \le c_k < 0.95$	$0.95 \le c_k < 1.00$	Total
UO_2F_2 solution sphere, reflected, H:^{235}U = 200	10	Minimum volume conditions for hydrogen moderator	88	89	177
UO_2F_2 solution sphere, reflected, H:^{235}U = 500	10	Minimum mass conditions for hydrogen moderator	93	112	205
UO_2F_2 solution sphere, reflected, H:^{235}U = 100	20	Minimum volume conditions for hydrogen moderator	80	74	154
UO_2F_2 solution sphere, reflected, H:^{235}U = 500	20	Minimum mass conditions for hydrogen moderator	77	103	180
UO_2F_2 solution sphere, reflected, H:^{235}U = 200	15	Minimum volume conditions for hydrogen moderator	87	108	195

Table 6.4. Similarity results for application models and 366-benchmark set: models involving fuel particle-water mixtures

Application model description	^{235}U (%)	Application objectives	Number of benchmarks having similarity		
			$0.90 \le c_k < 0.95$	$0.95 \le c_k < 1.00$	Total
Gels/uncoated fuel kernels with H:^{235}U = 300	10%	Minimum mass conditions for gels or uncoated kernels in water	96	87	183
Gels/uncoated fuel kernels with H:^{235}U = 300	20%	Minimum mass conditions for gels or uncoated kernels in water	76	81	157
TRISO particles with H:^{235}U = 300	10%	Minimum mass conditions for TRISO particles in water	109	96	205
TRISO particles with H:^{235}U = 300	20%	Minimum mass conditions for TRISO particles in water	76	92	168
Uncoated fuel kernels with H:^{235}U = 20	10%	Evaluate water introduction into inventory of fuel kernels	20	0	20
Uncoated fuel kernels with H:^{235}U = 10	20%	Evaluate water introduction into inventory of fuel kernels	0	0	0
TRISO particles with H:^{235}U = 20	10%	Evaluate water introduction into inventory of TRISO particles	0	0	0
TRISO particles with H:^{235}U = 5	20%	Evaluate water introduction into inventory of TRISO particles	2	0	2

At low H:^{235}U ratios, the models simulate conditions where larger inventories of finished kernels or TRISO particles are stored. Since the particles are very closely spaced, water intrusion results in an under-moderated condition. There are few available experiments that involve both low enrichment and poorly moderated conditions within the 366-benchmark set. However, there are some experiments in the IHECSBE (noted in Appendix A but not in the 366-benchmark set) that may be applicable.

6.3.4 Models Involving Both Graphite and Water Moderation

Table 6.5 shows good benchmark coverage for blending operations where the C:U ratio is ~95 (as for mixtures used to form compacts). For off-normal events involving water entry or excess binder addition, hydrogen assumes a role as the dominant moderator, and the graphite merely functions as a diluent.

Table 6.5. Similarity results for application models and 366-benchmark set: models involving both graphite and water as moderators

Application model description	^{235}U (%)	Application objectives	Number of benchmarks having similarity		
			$0.90 \le c_k < 0.95$	$0.95 \le c_k < 1.00$	Total
TRISO-graphite mixture for compacts, H:^{235}U = 500, C:U = 95	10%	Evaluate excess binder addition or water introduction to blender	124	80	204
TRISO-graphite mixture for compacts, H:^{235}U = 300, C:U = 95	20%	Evaluate excess binder addition or water introduction to blender	82	98	180
TRISO-graphite mixture for pebbles, H:^{235}U = 300, C:U = 1235	15%	Evaluate excess binder addition or water introduction to blender	0	0	0
Compacts with optimum pitch in water	10%	Minimum mass requirements for compacts	117	88	205
Compacts with optimum pitch in water	20%	Minimum mass requirements for compacts	87	109	196
Close-packed compacts with interstitial water	10%	Water intrusion into storage/containers of compacts	71	0	71
Close-packed compacts with interstitial water	20%	Water intrusion into storage/containers of compacts	28	0	29

However, for blending operations with high C:U ratios (pebble manufacture), a binary moderator condition results. There may be few or no benchmarks in the IHECSBE or elsewhere that simulate such a mixture as the third model of Table 6.5, with C:U ~ 1200 and H:U ~ 300, plus the condition of low enrichment.

For formed compacts with a C:U ratio near that modeled (~95), there is appreciable void space between compacts, even if the compacts are closely packed. Good coverage is seen for water-immersed compacts that have optimum spacing, and acceptable benchmark coverage is still seen for close-packed compacts under water immersion conditions.

6.3.5 Models Involving Graphite and Limited or No Water Moderation

Table 6.6 lists the final application models involving only graphite as the moderator, or with some water moderator but with graphite remaining the primary moderator. As indicated, the 366-benchmark set lacked any experiments providing high similarity to these models. For most of the models of Table 6.6, all c_k values were less than 0.80. The maximum c_k value found for a Table 6.6 model was 0.83.

Table 6.6. Similarity results for application models and 366-benchmark set: models involving graphite and limited or no water moderation

Application model description	^{235}U (%)	Application objectives	Number of benchmarks having similarity		
			$0.90 \leq c_k < 1.00$	$0.95 \leq c_k < 1.00$	Total
Dry compacts	10%	Maximum storage inventory for dry compacts	0	0	0
Dry compacts	20%	Maximum storage inventory for dry compacts	0	0	0
Dry pebbles	10%	Evaluate intended storage conditions	0	0	0
Dry pebbles	20%	Evaluate intended storage conditions	0	0	0
Pebbles with optimum interstitial water	15%	Evaluate water in-leakage to storage	0	0	0
Pebbles with optimum interstitial water	20%	Evaluate water in-leakage to storage	0	0	0
Infinite array of prism fuel assemblies	10%	Storage	0	0	0
Infinite array of prism fuel assemblies	15%	Storage	0	0	0
Infinite array of prism fuel assemblies	20%	Storage	0	0	0

There are benchmarks in the IHECSBE or the IHERPBE (not included in the 366-benchmark set) that involve pebble fuel. Based on the preliminary similarity comparison of Section 6.3.1, those experiments likely are highly similar to all pebble models of Table 6.6. On the other hand, the number of available

pebble benchmarks is very small, which presents a challenge for statistical determinations of k_{USL}. Also as indicated by Section 6.3.1, the pebble experiments likely have low applicability to the dry compacts or prism fuel assembly models of Table 6.2.

6.4 UNCERTAINTY ANALYSIS RESULTS

6.4.1 Models Involving UF_6

Table 6.7 provides uncertainty results for the final application models involving UF_6. The computed k_{eff} values are TSUNAMI-3D forward-run results. The k_{eff} uncertainty values are "one standard deviation" values from TSUNAMI-IP, obtained using cross section covariance data from the SCALE6.0 "44GROUPCOV" data file. The primary uncertainty contributors are the two isotope and reaction pairs that contribute the most to the k_{eff} uncertainty result. For example, for the first model of Table 6.7, the greatest contributor to the 2.8% uncertainty (0.028) in the computed k_{eff} result is neutron capture in ^{235}U. The next-highest ranking contributor to the k_{eff} uncertainty is neutron capture in ^{238}U.

Table 6.7. k_{eff} uncertainty results for application models involving UF_6

Application model description	^{235}U (%)	Computed k_{eff}	k_{eff} uncertainty (%Δk/k)	Primary uncertainty contributors
Infinite system of unmoderated UF_6	10.30%	0.99912 ± 0.00015	2.800	$^{235}U(n,\gamma)$, $^{238}U(n,\gamma)$
Close-packed, reflected array of 30B overpacks	15%	0.83183 ± 0.00012	1.842	$^{235}U(n,\gamma)$, $^{238}U(n,\gamma)$
30B cylinder with H_2O intrusion, solution slab geometry	10%	1.00025 ± 0.00009	0.678	$^{235}U(n,\gamma)$, $^{238}U(n,n')$
30B cylinder with H_2O intrusion, hemisphere geometry	20%	1.00001 ± 0.00008	0.879	$^{235}U(n,\gamma)$, ^{19}F(elastic)

Table 6.7 indicates rather large uncertainties for computed k_{eff} values for the unmoderated UF_6 systems.

A basic means for potential use of the k_{eff} uncertainty data is to apply some multiple of the uncertainty values as a "penalty" adjustment for determination of k_{USL}. This penalty may be considered as a component of the "subcritical margin" (NUREG/CR-6698[83] terminology) or the "margin of subcriticality" (ANSI/ANS-8.24-2007[84] terminology).

6.4.2 Models Involving Solutions

Table 6.8 provides uncertainty results for the final set of application models for solutions.

For the solution models, the k_{eff} uncertainty values are within a "typical" range (less than 1%).

Table 6.8. k_{eff} uncertainty results for application models involving solutions

Application model description	^{235}U (%)	Computed k_{eff}	k_{eff} uncertainty (%Δk/k)	Primary uncertainty contributors
UO_2F_2 solution sphere, reflected, H:^{235}U = 200	10%	1.00002 ± 0.00019	0.757	^{235}U(chi), ^{1}H(elastic)
UO_2F_2 solution sphere, reflected, H:^{235}U = 500	10%	0.99994 ± 0.00019	0.713	^{235}U(chi), ^{1}H(elastic)
UO_2F_2 solution sphere, reflected, H:^{235}U = 100	20%	1.00007 ± 0.00018	0.803	^{235}U(chi), ^{1}H(elastic)
UO_2F_2 solution sphere, reflected, H:^{235}U = 500	20%	0.99995 ± 0.00019	0.758	^{235}U(chi), ^{1}H(elastic)
UO_2F_2 solution sphere, reflected, H:^{235}U = 200	15%	1.00006 ± 0.00019	0.736	^{235}U(chi), ^{1}H(elastic)

6.4.3 Models Involving Fuel Particle Mixtures With Water

Table 6.9 provides uncertainty results for application models with mixtures of water and fuel particles. Note that for well-moderated mixtures, the uncertainty values and contributors are similar to those for solutions. For poorly moderated mixtures, the dominant contributors to uncertainty involve cross section data for fast reactions [^{238}U(n,n')] and epithermal reactions [^{235}U(n,γ) and/or ^{235}U(n,γ)].

Table 6.9. k_{eff} uncertainty results for application models involving fuel particle-water mixtures

Application model description	^{235}U (%)	Computed k_{eff}	k_{eff} uncertainty (%Δk/k)	Primary uncertainty contributors
Gels/uncoated fuel kernels with H:^{235}U = 300	10%	1.00010 ± 0.00019	0.761	^{235}U(chi), ^{1}H(elastic)
Gels/uncoated fuel kernels with H:^{235}U = 300	20%	0.99963 ± 0.00018	0.811	^{235}U(chi), ^{1}H(elastic)
TRISO particles with H:^{235}U = 300	10%	0.99970 ± 0.00019	0.680	^{235}U(chi), ^{1}H(elastic)
TRISO particles with H:^{235}U = 300	20%	0.99995 ± 0.00019	0.754	^{235}U(chi), ^{1}H(elastic)
Uncoated fuel kernels with H:^{235}U = 20	10%	1.00039 ± 0.00018	0.680	^{238}U(n,n'), ^{235}U(n,γ)
Uncoated fuel kernels with H:^{235}U = 10	20%	1.00003 ± 0.00019	0.861	^{235}U(n,γ), ^{238}U(n,n')
TRISO particles with H:^{235}U = 20	10%	1.00022 ± 0.00037	0.556	^{238}U(n,γ), ^{235}U(n,γ)
TRISO particles with H:^{235}U = 20	20%	0.99964 ± 0.00031	0.780	^{235}U(n,γ), ^{238}U(n,γ)

6.4.4 Models Involving Both Graphite and Water Moderation

Table 6.10 provides uncertainty data for models with dual moderators of graphite and water. The k_{eff} uncertainty values are dominated by uncertainties for ^{235}U nuclear data.

Table 6.10. k_{eff} uncertainty results for application models involving both graphite and water as moderators

Application model description	^{235}U (%)	Computed k_{eff}	k_{eff} uncertainty (%Δk/k)	Primary uncertainty contributors
TRISO-graphite mixture for compacts, H:^{235}U = 500	10%	0.99963 ± 0.00021	0.612	^{235}U(chi), ^{235}U(nubar),
TRISO-graphite mixture for compacts, H:^{235}U = 300	20%	1.00006 ± 0.00019	0.700	^{235}U(chi), ^{1}H(elastic)
TRISO-graphite mixture for pebbles, H:^{235}U = 300	15%	1.00010 ± 0.00037	0.550	^{235}U(nubar), ^{235}U(chi),
Compacts with optimum pitch in water	10%	1.00461 ± 0.00039	0.595	^{235}U(chi), ^{235}U(nubar),
Compacts with optimum pitch in water	20%	1.00232 ± 0.00039	0.660	^{235}U(chi), ^{235}U(nubar),
Close-packed compacts with interstitial water	10%	1.00976 ± 0.00042	0.577	^{235}U(chi), ^{235}U(nubar),
Close-packed compacts with interstitial water	20%	1.01006 ± 0.00045	0.604	^{235}U(chi), ^{235}U(nubar),

6.4.5 Models Involving Graphite and Limited or No Water Moderation

Table 6.11 provides uncertainty results for models where graphite is the dominant or only moderator.

An observation is that although Section 6.3 identified poor benchmark coverage for graphite-moderated systems, the uncertainties in computed k_{eff} values for graphite systems are the smallest of all HTGR application models.

Table 6.11. k_{eff} uncertainty results for application models involving graphite and limited or no water moderation

Application model description	^{235}U (%)	Computed k_{eff}	k_{eff} uncertainty (%Δk/k)	Primary uncertainty contributors
Dry compacts	10%	0.99791 ± 0.00044	0.651	^{238}U(n,γ), ^{235}U(n,γ)
Dry compacts	20%	0.99928 ± 0.00039	0.646	^{238}U(n,γ), ^{235}U(n,γ)
Dry pebbles	10%	1.00101 ± 0.00049	0.580	^{235}U(nubar), C-graphite(elastic)
Dry pebbles	20%	1.00147 ± 0.00045	0.570	C-graphite(elastic), ^{235}U(nubar)
Pebbles with optimum interstitial water	15%	1.00145 ± 0.00045	0.518	^{235}U(nubar), C-graphite(elastic)
Pebbles with optimum interstitial water	20%	0.98845 ± 0.00039	0.548	^{235}U(nubar), C-graphite(elastic)
Infinite array of prism fuel assemblies	10%	1.23207 ± 0.00049	0.445	^{235}U(nubar), ^{238}U(n,γ)
Infinite array of prism fuel assemblies	15%	1.33818 ± 0.00049	0.431	^{235}U(nubar), ^{235}U(n,γ)
Infinite array of prism fuel assemblies	20%	1.40030 ± 0.00049	0.425	^{235}U(nubar), ^{235}U(n,γ)

7. AREAS OF CONCERN FOR DEMONSTRATION OF ADEQUATE CRITICALITY SAFETY MARGIN; SUGGESTED APPROACHES TO ADDRESS AREAS OF CONCERN

7.1 VALIDATION OF CALCULATION METHODS TO JUSTIFY UF_6 HANDLING AND TRANSPORT AT ENRICHMENTS GREATER THAN 5 WT % ^{235}U

Transition to a fuel cycle that requires handling, storage, and transport of bulk quantities of UF_6 at greater than 5% enrichment presents two specific criticality safety challenges: adequacy of benchmarks to validate safety computations, and potential increase in risk for a criticality accident due to water intrusion to a UF_6 cylinder.

The validation issue is addressed in the remainder of this section and the risk issue is addressed in Section 7.2.

Currently, benchmark coverage to support accuracy of computations involving bulk handling and transport of 5% enrichment UF_6 in 30- and 48-in.-diameter cylinders is limited. However, there is confidence that the minimum critical enrichment for UF_6 is greater than 7% enrichment, so accuracy of computational assessments of current activities is of little safety concern.

For use of 30 and 48 in. UF_6 cylinders at enrichments greater than 7%, the need for accuracy of computational methods becomes important, and it progresses in importance as greater enrichment increases are considered. For several neutron reactions of importance to unmoderated UF_6 at low enrichments, recognized uncertainties in current cross section data are significant. This includes inelastic scattering by fluorine at high energies, which is compounded by high uncertainties in the fast fission cross sections for ^{238}U in the same energy range. Nonproductive neutron capture by ^{235}U is also an important reaction with appreciable cross section uncertainties.

To justify increased reliance on nuclear criticality safety computations at 7% and greater enrichments, better or additional data is needed. That does not necessarily mean that critical experiments are needed. Even if desired, there are significant practicality issues associated with performing critical experiments with bulk quantities of low enrichment uranium. These issues involve accurately characterizing the UF_6 material distribution within the cylinder(s) and the availability of experimental facilities and approach-to-critical machines that can accommodate handling of the cylinders or manipulation of the material configuration within the cylinders.

One method to circumvent these issues would be to perform subcritical measurements within enrichment facilities while UF_6 remains in a liquid state. Capability to perform subcritical measurements of benchmark quality has been demonstrated; a few subcritical benchmarks are already in the IHECSBE. The technical challenges and risks associated with performing subcritical measurements of UF_6 are minor compared to those of performing critical experiments. Finally, an American National Standard[87] exists for performing in situ measurements without use of remote or shielded experiment control.

7.2 ADDRESSING THE INCREASED RISK OF CRITICALITY IN EVENT OF WATER INTRUSION INTO LARGE UF_6 CYLINDER CONTAINING GREATER THAN 5 WT % ^{235}U

Currently, the risk of a criticality accident associated with inadvertent water entry into 30 and 48 in. UF_6 cylinders is recognized. The overall risk depends on the probability and nature of an event that might

cause water introduction, combined with the probability that water introduction will yield a critical configuration. For the current enrichment limit of 5%, the second probability is actually quite low.

To achieve highly effective hydrogen moderation in the resulting uranyl fluoride solution requires that the solution attain a rather high total uranium concentration. This is improbable since the high concentration requirement means that a significant quantity of UF_6 must be dissolved. The inventory of particulate UF_6 within cylinders containing solidified UF_6 cannot be known precisely, but is unlikely to be present in sufficient amounts to foster dissolution of many kilograms of UF_6 and achievement of high uranium concentrations in solution.

As the UF_6 enrichment is increased, the amount of particulate UF_6 is not changed, but the amount of total uranium that must be dissolved to permit a critical configuration is significantly reduced. The uranium concentration required in solution decreases, and the required volume of solution also decreases. Nonuniformity in UF_6 distribution within the cylinder (i.e., localized depressions in the UF_6) may more readily foster a localized solution configuration that is conducive to a critical condition.

The industry lacks any practical option to use cylinders smaller than the 30 in. for transport at greater than 5% enrichment. Significant reductions in the physical volume required for solution criticality occur as enrichments increase beyond 5%. Moreover, the high hazard of UF_6 operations (associated with potential release of gaseous or liquid UF_6 during cylinder loading, unloading, and handling) is acerbated as the number of individual cylinder operations increases. The next smaller authorized UF_6 cylinder size less than the 30 in. cylinder is the 12 in. cylinder. The 12 in. cylinder contains only 10% of the capacity of a 30 in. cylinder and is not sufficiently small to preclude solution criticality in the upper range of HTGR enrichments.

The most readily available means to offset the increased risk for criticality in the 30 in. cylinder design (for enrichment increases above 5%) is to improve the resistance of the cylinder to water entry. Although potentially costly, this could be done without need to redesign equipment at current enrichment and fuel fabrication facilities. One means of improving cylinder resistance would be to adopt use of redesigned cylinders that have a thicker wall or a composite wall. The maximum operating temperatures for UF_6 cylinders is modest, so a composite-wall cylinder could be a steel-wall cylinder with a nonmetallic second layer. Even if a simple approach of using a thicker steel wall is adopted, the weight increase of the cylinder would be minor compared to the gross weight of a cylinder loaded with UF_6. Another means of providing a risk offset would be to develop a more robust overpack design.

7.3 ADDRESSING POSTULATED HTGR PROCESS APPLICATIONS THAT LACK ADEQUATE BENCHMARK COVERAGE: POORLY MODERATED MIXTURES OF PARTICULATES AND HYDROGEN MODERATOR

There are two general means to deal with deficient validation coverage for particulate mixtures moderated by hydrogen, within HTGR fuel fabrication operations:

(a) obtain necessary benchmark data (critical benchmarks or subcritical measurements) to gain the desired efficiency in operational capacity, and
(b) accept limitations in operational capacity.

Since particulate material types are not in final fuel form, individual equipment and container items can be sufficiently reduced in size, or batch handling limits for fissile mass can be reduced, so that safety of operations can be demonstrated.

For the HTGR enrichment range of 10% to 20%, designs of fuel fabrication facility equipment must necessarily be less than for current facilities that operate with a maximum of 5% enrichment. Even though the uranium masses necessary to perform critical experiments (or subcritical measurements) may be significant, the overall sizes of experimental assemblies of interest are not. Means do currently exist to manufacture the materials needed for measurements. As for UF_6 measurements, subcritical benchmark measurements could be performed at sites now performing lab-scale material manufacture. This approach avoids costs of material transport to or from experimental facilities, and allows for ready revision of material conditions as may be desired for measurement over the range of material conditions or forms.

The costs and effort associated with obtaining benchmark data for poorly moderated HTGR particulate materials are likely minimal compared to the capital and operating costs associated with more restrictive facility design and operation.

7.4 ADDRESSING HTGR FINAL FUEL FORM APPLICATIONS THAT LACK ADEQUATE BENCHMARK COVERAGE

This issue presents potentially significant challenges for resolution, because performing critical experiments with fissile material with carbon moderator only can be difficult due to the scale of the experimental facilities and the associated material masses. Legacy experiments of this nature used split-table equipment, for which "scram" system design and operation can present challenges.

For most areas of HTGR fuel cycle design, inadequate validation issues can possibly be mitigated with acceptable costs through more restrictive design or limited capacity. For example, storage vaults could employ use of small-volume storage containers for fuel compacts, with provision of fixed neutron absorber materials between storage positions. The containers could be of sufficiently limited geometry that validation of safety calculations for individual containers is not an issue, and nonbenchmark means (such as neutron transmission measurements) can be used to verify neutronic isolation of storage positions.

A potentially more feasible approach is to define some regulatory-specified additional margin of subcriticality, or "penalty" to be applied to a k_{USL} value, to account for the lack of adequate validation benchmarks.

This approach may be less feasible at reactor sites, where there may be a greater desire and need to store larger inventories of fuel (fresh or spent) with utilization of as little facility space as necessary. Until some preliminary designs for fuel storage at HTGR reactor sites are developed, this concern for validation needs for large-scale fuel storage remains speculative.

7.5 OBSERVATIONS REGARDING STATUS OF SENSITIVITY AND UNCERTAINTY METHODS FOR HTGR FUEL CYCLE APPLICATIONS

In Sections 4.7, 4.8, and 4.9 (development of process application models involving fuel compacts, prismatic fuel assemblies, and pebble fuel), it was noted that the "doublehet" cell data treatment for multigroup cross section calculations has not yet been implemented in the SCALE TSUNAMI sequence. To obtain sensitivity data files for process application models involving these fuel forms, cross section treatment options were employed that only partially account for needed problem-dependent cross section adjustments. Thus, the k_{eff} sensitivity profiles for models involving these materials may not be as accurate as desired.

In Section 6, the sensitivity profiles for the doubly heterogeneous application models were compared to currently available critical experiment benchmarks. Because the extent of dissimilarity of available

benchmarks and the application models was significant, the conclusion that poor benchmark coverage exists for doubly heterogeneous HTGR fuel cycle applications is not impacted by the current status of SCALE TSUNAMI methods.

However, to effectively apply results of future experiments involving doubly heterogeneous HTGR fuel materials for criticality safety validation, capability to apply sensitivity and uncertainty methods to doubly heterogeneous materials will be needed.

7.6 OBSERVATIONS REGARDING APPLICABILITY OF THIS REPORT TO THE LWR FUEL CYCLE

In recent years, developments in LWR fuel technology have resulted in gradual increase in the maximum enrichment levels employed in LWR fuel, resulting in contemporary use of enrichments approaching 5%. Further improvements in LWR fuel manufacture, combined with deployment of more advanced LWR designs, will drive demand for LWR fuel enrichments exceeding 5%.

Portions of this report that have potential relevance to criticality evaluations for LWR fuel cycles involving greater than 5% enrichment include

- Sections 3.1.1 through 3.1.4—criticality considerations for UF_6 enrichment processes, transport, storage, and chemical conversion;
- Sections 4.2 through 4.4—process application models for UF_6, homogeneous uranium solutions, and uncoated fuel particles;
- Sections 6.3.1 through 6.3.3—benchmark coverage analyses for models involving UF_6, uranium solutions, and uncoated fuel particles; and
- Sections 6.4.1 through 6.4.3—uncertainty analysis for computed k_{eff} values of models involving UF_6, homogeneous uranium solutions, and uncoated fuel particles.

Current LWR fuel manufacturing techniques do not involve fuel microspheres. However, due to the very small size of HTGR fuel particles, the process models and benchmark coverage conclusions of this report (for uncoated fuel particles) are likely applicable to certain LWR fuel cycle processes, such as blending of oxide powder and resin for pellet manufacture.

Appendix A identifies IHECSBE reports of potential utility for LWR fuel activities involving 5 to 10% enrichment materials.

8. CONCLUSIONS

The scope of NRC Project N6773 includes two tasks:

- Task 1 involves identification of non-reactor fuel cycle operations that may be challenged by an HTGR fuel cycle employing uranium within the 5% to 20% enrichment range.
- Task 2 involves assessment of the experimental benchmark data base for coverage of HTGR fuel cycle activities, identification of potential problem areas, and recommendation of approaches to address those issues.

Task 1 work determined that significant criticality safety challenges for deployment of a HTGR fuel cycle involve industrial-scale (bulk) storage and transport of UF_6 at enrichments greater than 5%, and fuel manufacturing operations that may involve large-scale blending operations of fuel particles, binder, and graphite. Fuel cycle economics provide incentive to maximize the capacity of equipment used for these two sets of activities.

Task 2 work determined that areas of poor benchmark data coverage included unmoderated UF_6, dual systems of UF_6 and reactant solution (i.e., water-intrusion scenarios for UF_6 cylinders), poorly (hydrogen) moderated oxides, and final HTGR fuel forms (carbon as the primary or only moderator).

Suggestions for mitigating these challenges include improvement of UF_6 cylinder or overpack designs to better resist water entry, performance of benchmark-quality subcritical measurements for UF_6 in the upper end of the HTGR enrichment range, performance of critical or subcritical measurements for poorly moderated particulate fuel forms, and use of increased margins of subcriticality (additional penalty for k_{USL} values) for large-inventory graphite-moderated final or near-final fuel forms.

Due to the paucity of currently available, appropriate critical and subcritical experiments, specific example biases or uncertainties are not provided. For coverage of operational conditions involving significant levels of hydrogen moderation, good to very good benchmark coverage exists. A licensee's ability to validate criticality safety computations in this area may be considered equivalent to current licensee abilities for LWR fuel fabrication facilities. For the areas of concern identified above, the current benchmark coverage is sufficiently limited that useful bias estimates are not presently attainable.

As noted above, there are significant overlaps in areas determined by Task 1 to potentially have small margins of subcriticality, and areas determined by Task 2 as lacking adequate benchmark coverage to support accurate determination of subcritical margins. This report provides a comprehensive view of criticality issues for the HTGR fuel cycle and fulfills deliverables for both Tasks 1 and 2 of NRC Project JCN N6773.

9. REFERENCES

1. *SCALE: A Modular Code System for Performing Standardized Computer Analyses for Licensing Evaluation,* ORNL/TM-2005/39, Version 6, Vols. I–III, Oak Ridge National Laboratory, Oak Ridge, Tennessee, January 2009. Available from Radiation Safety Information Computational Center at Oak Ridge National Laboratory as CCC-750.

2. T. Uckan, *Fissile Deposit Characterization at the Former Oak Ridge K-25 Gaseous Diffusion Plant by ^{252}Cf-Source-Driven Measurements*, ORNL/TM-13642, Oak Ridge National Laboratory, Lockheed Martin Energy Research Corporation, Oak Ridge, Tenn., May 1998.

3. "National Enrichment Facility—Safety Analysis Report," Revision 5, May 2005.

4. United States Code of Federal Regulations, Title 49—Transportation.

5. ANSI N14.1-2001, "American National Standard for Nuclear Materials—Uranium Hexafluoride Packaging for Transport," February 1, 2001. Includes Addendum 1 issued April 3, 2002.

6. Certificate of Compliance for Radioactive Material Packages, USA/6553/AF, U.S. Nuclear Regulatory Commission.

7. United States Code of Federal Regulations, Title 10—Energy.

8. Federal Register, **65**(137), July 17, 2000.

9. E. J. Barber et al., *Investigation of Breached Depleted UF_6 Cylinders*, ORNL/TM-11988 (POEF-2086), Oak Ridge National Laboratory and Uranium Enrichment, Martin Marietta Energy Systems, Inc., Oak Ridge, Tenn., September 1991.

10. S. L. Burnham, *Uranium Hexafluoride Bibliography*, K/HS-215, Martin Marietta Energy Systems, Inc., Oak Ridge, Tenn., April 1988.

11. *Regulatory Analysis of Major Revision of 10 CFR Part 71—Final Rule*, NUREG/CR-6713, U.S. Nuclear Regulatory Commission, July 2003.

12. C. E. Daugherty, G. E. Harris, and R. R. Wright, *Evaluation of Materials Used in Fire-Resistant Phenolic Foam*, K/TL-729, Oak Ridge Gaseous Diffusion Plant, Union Carbide Corporation, Oak Ridge, Tenn., March 1978.

13. A. J. Mallett and C. E. Newlon, *Protective Shipping Packages for 30-inch Diameter UF_6 Cylinders*, K-1686, Oak Ridge Gaseous Diffusion Plant, Oak Ridge, Tenn., April 1967.

14. R. W. Tayloe, Jr., et al, *Nuclear Criticality Safety Analysis for Increased Enrichment Limit in 10-Ton (48X) UF_6 Cylinders*, POEF-T-3563, Martin Marietta Energy Systems, Inc., Oak Ridge, Tenn., May 1991.

15. R. W. Tayloe, Jr., et al., *Nuclear Criticality Safety Study for Increased Enrichment Limit in 2 1/2-Ton (30B) UF_6 Cylinders*, POEF-T-3597, Martin Marietta Energy Systems, Inc., Oak Ridge, Tenn., October 1992.

16. B. G. Dekker, "Transport of UF_6 in Compliance with TS-R-1," World Nuclear Transport Institute, conference paper for PATRAM 2004 (Berlin), September 2004.

17. *IAEA Safety Standards Series—Regulations for the Safe Transport of Radioactive Material*, 1996 Edition (Revised), No. TS-R-1 (ST-1, Revised), International Atomic Energy Agency, 1996.

18. *IAEA Safety Standards Series for Protecting People and the Environment—Regulations for the Safe Transport of Radioactive Material*, 2005 Edition, No. TS-R-1, International Atomic Energy Agency, 2005.

19. Certificate of Compliance for Radioactive Material Packages, USA/9196/AF-96, U.S. Nuclear Regulatory Commission.

20. Certificate of Compliance for Radioactive Material Packages, USA/9234/B(U)F, U.S. Nuclear Regulatory Commission.

21. Certificate of Compliance for Radioactive Material Packages, USA/9284/B(U)F-85, U.S. Nuclear Regulatory Commission.

22. Federal Register **69**(16), January 26, 2004.

23. *Standard Review Plans for Transportation Packages for Radioactive Material*, NUREG-1609, U.S. Regulatory Commission, March 1999.

24. H. R. Dyer and C. V. Parks, *Recommendations for Preparing the Criticality Safety Evaluation of Transportation Packages*, NUREG/CR-5661 (ORNL/TM-11936), Oak Ridge National Laboratory, Oak Ridge, Tenn., April 1997.

25. U.S. NRC Regulatory Guide 7.9, Standard Format and Content of Part 71 Applications for Approval of Packages for Radioactive Material, U.S. Nuclear Regulatory Commission, March 2005.

26. N. L. Ranek and F. A. Monette, *Evaluation of UF_6-to-UO_2 Conversion Capability at Commercial Nuclear Fuel Fabrication Facilities*, ANL/EAD/TM-119, Environmental Assessment Division, Argonne National Laboratory, Argonne, Ill., May 2001.

27. DOE-HTGR-88165-0, "Critical Process Parameters for UCO Kernel Production," General Atomics, September 1988.

28. IAEA-TECDOC-978, "Fuel Performance and Fission Product Behaviour in Gas Cooled Reactors," International Atomic Energy Agency, November 1997.

29. IAEA-TECDOC-988, "High Temperature Gas Cooled Reactor Technology Development, *Proc. Technical Committee Meeting*, Johannesburg, South Africa, November 13–15, 1996.

30. C. M. Barnes, D. Husser, W. C. Richardson, and M. Ebner, "Fabrication Process and Product Quality Improvements in Advanced Gas Reactor UCO Kernels," HTR2008-58039, *Proc. 4th International Topical Meeting on High Temperature Reactor Technology*, Washington, D.C., October 2008.

31. C. M. Barnes, D. W. Marshall, J. Hunn, B. L. Tomlin, and J. T. Keeley, "Results of Test to Demonstrate a Six-Inch Diameter Coater for Production of TRISO-Coated Particles for Advanced

Reactor Experiments," HTR2008-58074, *Proc. 4th International Topical Meeting on High Temperature Reactor Technology*, Washington, D.C., October 2008.

32. Memo, "Final Environmental Assessment for the Renewal of U.S. Nuclear Regulatory Commission License No. SNM-1097 for Global Nuclear Fuel—Americas Fuel Fabrication Facility," from J. Moore (NRC Project Manager for Environmental Review) to A. Kock (NRC Chief for Environmental Review), May 14, 2009.

33. "Environmental Assessment for the Renewal of U.S. Nuclear Regulatory Commission License No. SNM-1227 for AREVA NP, Inc., Richland Fuel Fabrication Facility," Docket No. 70-1257, February 2009.

34. G. D. Del Cul, B. B. Spencer, C. W. Forsberg, E. D. Collins, and W. S. Rickman, *TRISO-Coated Fuel Processing to Support High-Temperature Gas-Cooled Reactors*, ORNL/TM-2002/156, OakRidge National Laboratory, Oak Ridge, Tenn., September 2002.

35. J. L. Collins, R. D. Hunt, G. D. Del Cul, and D. F. Williams, *Production of Depleted UO_2 Kernels for the Advanced Gas-Cooled Reactor Program for Use in TRISO Coating Development*, ORNL/TM-2004/123, Oak Ridge National Laboratory, Oak Ridge, Tenn., November 2004.

36. J. L. Collins, M. H. Lloyd, S. E. Shell, *Control of Uranium Crystallite Size by HTMA-Urea Reaction in the Internal Gelation Process for Preparing (U,Pu)O_2 Fuel Kernels*," ORNL/TM-2005/10, Oak Ridge National Laboratory, Oak Ridge, Tenn., April 2005.

37. J. L. Collins, *Experimental Methodology for Determining Optimum Process Parameters for Production of Hydrous Metal Oxides by Internal Gelation*, ORNL/TM-2005/102, Oak Ridge, Tenn., September 2005.

38. D. W. Marshall and C. M. Barnes, *AGR Fuel Development—Coater and Control System Upgrade*, INL/EXT-07-12458, Idaho National Laboratory, Idaho Falls, Id., March 2007.

39. J. D. Sease and A. L. Lotts, *Development of Processes and Equipment for the Refabrication of HTGR Fuels*, ORNL/TM-5334, Oak Ridge National Laboratory, Oak Ridge, Tenn. June 1976.

40. G. Kaiser, H. Barnet-Wiemer, N, Hoogen and J. Wolf, "Head-End Processing of HTR Fuel Elements," IAEA Meeting of the International Working Group on Gas Cooled Reactors (IWGGCR/8), Moscow USSR, 1983.

41. S. Kato, S. Yoshimuta, T. Hasumi, K. Sato, K. Sawa, S. Suzuki, H. Mogi, S. Shiozawa, and T. Tanaka, "Fabrication of HTTR First Loading Fuel, International Atomic Energy Agency," IAEA-TECDOC-1210, pp. 187–199, Vienna, Austria, April 2001.

42. Memo, S. W. Bodman to Senator P. Domenici transmitting the Nuclear Energy Research Advisory Committee report titled "A Review of the NGNP Project: February 22, 2006," memo dated April 6, 2006.

43. K. Sawa and S. Ueta, "Research and Development on HTGR Fuel in the HTTR Project," *Nuclear Engineering and Design* **233**, 163–172, October 2004.

44. F. Charollais, S. Fonquernie, C. Perrais, M. Perez, O. Dugne, F. Cellier, G. Harbonnier, and M. Vitali, "CEA and AREVA R&D on HTR Fuel Fabrication and Presentation of the CAPRI Experimental Manufacturing Line," *Nuclear Engineering and Design* **236**, 534–542, March 2006.

45. H. Zhao, T. Liang, J. Zhang, J. He, Y. Zou, and C. Tang, "Manufacture and Characteristics of Spherical Fuel Elements for the HTR-10," *Nuclear Engineering and Design* **236**, 643–647, March 2006.

46. Y. Lee, J. Park, Y. K. Kim, K. Jeong,W. Kim, B. Kim, Y. M. Kim, and M. Cho, "Development of HTGR-Coated Particle Fuel Technology in Korea," *Nuclear Engineering and Design* **238**, 2842-2853, November 2008.

47. F. Charollais, C. Perrais, D. Mouliniera, M. Perez, and M. Vitali, "Latest Achievements of CEA and AREVA NP on HTR Fuel Fabrication," *Nuclear Engineering and Design* **238**, 2854–2860, November 2008.

48. M. Makgae, "Radioactive Waste Management Plan for the PBMR (Pty) Ltd Fuel Plant," *Nuclear Engineering and Design* **239**, 2196–2200, October 2009.

49. D. Petti, J. Bongiorno, J. Maki and G. Miller, "Key Differences in the Fabrication of U.S. and German TRISO-Coated Particle Fuel, and their Implications on Fuel Performance," *Proc. Conference on High Temperature Reactors*, Petten, NL, April 22–24, 2002, p. 31–37, International Atomic Energy Agency, April 2002.

50. E. Brandau, "Microspheres of UO_2, ThO_2 and PuO_2 for the High Temperature Reactor," *Proc. Conference on High Temperature Reactors*, April 22–24, 2002, p. 38-42, Petten, NL, International Atomic Energy Agency, Brace GmbH, Germany, April 2002.

51. A. Muller, "Establishment of the Technology to Manufacture Uranium Dioxide Kernels for PBMR Fuel," *Proc. 3rd International Topical Meeting on High Temperature Reactor Technology*, Johannesburg, South Africa, October 1–4, 2006.

52. F. S. Patton, J. M. Googin, and W. L. Griffith, *Enriched Uranium Processing*, The Macmillan Company, New York, 1963.

53. M. Rosselet, R. Chawla, and T. Williams, "Investigation of the k_{eff}—Variation Upon Water Ingress in the Pebble-Bed LEU-HTR," *Annals of Nuclear Energy* **26**, 75–82, May 1998.

54. *Current Status and Future Development of Modular High Temperature Gas Cooled Reactor Technology*, IAEA-TECDOC-1198, International Atomic Energy Agency, February 2001.

55. S. Shiozawa, S. Fujikawa, T. Iyoku, K. Kunitomi, and Y. Tachibana, "Overview of HTTR Design Features," *Nuclear Engineering and Design* **233**, 11–21, October 2004.

56. N. Sakaba, T. Furusawa, T. Kawamoto, Y. Ishii, and Y. Oota, "Short Design Descriptions of Other Systems of the HTTR," *Nuclear Engineering and Design* **233**, 147–154, October 2004.

57. I. Minatsuki, M. Tanihira, Y. Mizokami, Y. Miyoshi, H. Hayakawa, F. Okamoto, I. Maekawa, K. Takeuchi, H. Kodama, M. Fukuie, N. Kan, S. Kato, K. Nishimura, and T. Konishi, "The Role of Japan's Industry in the HTTR Design and Its Construction," *Nuclear Engineering and Design* **233**, 377–390, October 2004.

58. P. Tsvetkov, *Utilization of Minor Actinides as a Fuel Component for Ultra-Long-Life VHTR Configurations: Designs, Advantages, and Limitations*, Nuclear Energy Research Initiative Annual Report, Project No. 05-094, July 7, 2006.

59. W. Fuls, C. Viljoen, C. Stoker, C. Koch, and E. Mathews, "The Interim Fuel Storage Facility of the PBMR," *Proc. Conference on High Temperature Reactors*, Beijing, China, September 22–24, 2004, International Atomic Energy Agency, September 2004.

60. *Critical Experiments and Reactor Physics Calculations for Low-Enriched High Temperature Gas Cooled Reactors*, IAEA-TECDOC-1249, International Atomic Energy Agency, 2001.

61. *Working Material—Gas-Cooled Reactor Technology—Safety and Siting*, IAEA-TC-389-26, International Atomic Energy Agency, February 2001

62. *Nuclear Energy Research Initiative—Project 01-124—Reactor Physics and Criticality Benchmark Evaluations for Advanced Nuclear Fuel—Final Technical Report*, TDR-3000849-000, September 10, 2008.

63. *Next Generation Nuclear Plant Methods Research and Development Technical Program Plan*, INL/EXT-06-11804 PLN-2498 Rev. 1, Idaho National Laboratory, Idaho Falls, Id., September 2008

64. J. D. Bess and N. Fujimoto, *Evaluation of the Start-Up Core Physics Tests at Japan's High Temperature Engineering Test Reactor (Fully-Loaded Core)*, HTTR-GCR-RESR-001 from NEA/NSC/DOC(2006) [International Reactor Physics Evaluation Project (IRPhEP)], 2006.

65. C. E. Newlon and A. J. Mallet, *Hydrogen Moderation—A Primary Nuclear Safety Control for Handling and Transporting Low-Enrichment UF_6*, K-1663, Oak Ridge Gaseous Diffusion Plant, Oak Ridge, Tenn., 1966.

66. Joseph J. Katz and Eugene Rabinowitch, *The Chemistry of Uranium, Part I, The Element, Its Binary and Related Compounds*, First Edition, McGraw-Hill Book Company, Inc., 1951.

67. Website maintained by the World Information Service on Energy, url http://www.wise-uranium.org (see "Calculators," "JOL's Friendly Enrichment Calculator" provided courtesy of J. O. Liljenzin).

68. A. de la Garza, G. A. Garrett, J. E. Murphy, *Some Value Functions of Mulicomponent Isotope Separation—Application to Unit Cost Scale for Uranium-235, 236, 238 Mixtures*, K-1445, Oak Ridge Gaseous Diffusion Plant, Oak Ridge, Tenn., 1960.

69. J. T. Thomas, *Critical Experiments with UF_6 Cylinder Model 8A Containers*, Y-DR-128, Union Carbide Corporation, Oak Ridge Y-12 Plant, Oak Ridge, Tenn., September 1974.

70. *Safety Evaluation Report for the American Centrifuge Plant in Piketon, Ohio*, NUREG-1851, USNRC Docket 70-7004, U.S. Nuclear Regulatory Commission, September 2006.

71. L. E. Paulson and J. F. Degolyer, "An Estimate of Minimum Critical Water Content for 10% Enriched UF_6 in 30-inch and 48-inch Diameter UF_6 Cylinders," *Trans. Am. Nucl. Soc.* **100 (**2008).

72. B. L. Broadhead, *Criticality Review of 2 $^1/_2$-, 10-, and 14-Ton UF_6 Cylinders*, ORNL/TM-11947, Oak Ridge National Laboratory, Oak Ridge, Tenn., October 1991.

73. *Release of UF_6 from a Ruptured Model 48Y Cylinder at Sequoyah Fuels Corporation Facility: Lessons-Learned Report*, NUREG-1198, U.S. Nuclear Regulatory Commission, June 1986.

74. "The Inside Story (of a Depleted Uranium Hexafluoride Cylinder)," video maintained by the Depleted UF_6 Management Information Network at internet url http://web.ead.anl.gov/uranium/guide/video/inside.cfm.

75. A. L. Mallett, *Water Immersion Tests of UF_6 Cylinders with Simulated Damage*, K-D-1987, Oak Ridge Gaseous Diffusion Plant, Oak Ridge, Tenn., November 1967.

76. W. C. Jordan and J. C. Turner, *Estimated Critical Conditions for UO_2F_2-H_2O Systems in Fully Water-Reflected Spherical Geometry*, ORNL/TM-12292, Oak Ridge National Laboratory, Oak Ridge, Tenn., December 1992.

77. C. H. Lee, Z. Zhong, T. A. Taiwo, W. S. Yang, M. A. Smith, and G. Palmiotti, *Status of Reactor Physics Activities on Cross Section Generation and Functionalization for the Prismatic Very High Temperature Reactor, and Development of Spatially-Heterogeneous Codes*, ANL-GenIV-075, Argonne National Laboratory, Argonne, Ill., August 2006.

78. *International Handbook of Evaluated Reactor Physics Benchmark Experiments* (IHERPHE), NEA/NSC/DOC(2006)1, Nuclear Energy Agency, Organisation for Economic Co-Operation and Development, March 2010 Edition.

79. D. Ilas and I. C. Gauld, "Source Term Uncertainties for High Burnup HTGR Fuel," Letter Report, prepared by Oak Ridge National Laboratory for the Office of Nuclear Regulatory Research, U.S. Regulatory Commission, under NRC Project JCN N6540, September 2010.

80. *International Handbook of Evaluated Criticality Safety Benchmark Experiments* (IHECSBE), NEA/NSC/DOC(95)03/III, Nuclear Energy Agency, Organisation for Economic Co-Operation and Development, September 2009 Edition.

81. "American National Standard for Validation of Computational Methods for Nuclear Criticality," ANSI N16.9-1975/ANS-8.11, American Nuclear Society, La Grange Park, Ill., 1975.

82. "American National Standard for Nuclear Criticality Safety in Operations with Fissionable Materials Outside Reactors," ANSI/ANS-8.1-1983, American Nuclear Society, La Grange Park, Ill., 1983.

83. *Justification for Minimum Margin of Subcriticality for Safety*, FCSS ISG-10, prepared by the Division of Fuel Cycle Safety and Safeguards, Nuclear Regulatory Commission, 2006.

84. "American National Standard Validation of Neutron Transport Methods for Nuclear Criticality Safety Calculations," ANSI/ANS-8.24-2007, American Nuclear Society, La Grange Park, Ill., 2007.

85. B. L. Koponen, T. P. Wilcox, and V. E. Hampel, *Nuclear Criticality Experiments from 1943 to 1978, An Annotated Bibliography: Volume 1, Main Listing*, UCRL-52768, Lawrence Livermore Laboratory, Livermore, Ca., 1979.

86. Email from Nigel Hancock to Davis Reed, "RE: Question re 30% Enrichment Experiments," with draft IHECSBE report IEU-COMP-THERM-002 "Bare and Water-Reflected Spheres and Hemispheres of Aqueous Uranyl Fluoride Solutions (30.45% ^{235}U)," April 12, 2010.

87. "American National Standard Safety in Conducting Subcritical Neutron-Multiplication Measurement In Situ," ANSI/ANS-8.6-1983 (R2001), American Nuclear Society, La Grange Park, Ill., 1983.

APPENDIX A

TABULATION OF IHECSBE EXPERIMENTS OF POTENTIAL UTILITY FOR VALIDATION OF HTGR FUEL CYCLE NCS COMPUTATIONS

Table A.1. IHECSBE experiments of potential utility for validation of HTGR fuel cycle NCS computations—intermediate and mixed enrichment uranium systems (10 to 60% enrichment)

% E[a]	Report	Cases[b]	Application area, basis, notes	LWR[c]
10	IEU-MET-FAST-007 Multiple Enrichments of U Metal Plates	1	Unmoderated UF_6 systems. Enrichment within HTGR range.	x
9	IEU-MET-FAST-010 U Metal	1	Unmoderated UF_6 systems. Enrichment within HTGR range.	x
16	IEU-MET-FAST-012 U Metal Plates Interleaved with Al and SS Plates	1	Unmoderated UF_6 systems. Enrichment within HTGR range.	
12	IEU-MET-FAST-013 U Metal Plates at 93% and 0.2%, Interleaved	1	Unmoderated UF_6 systems. Enrichment within HTGR range.	
16	IEU-MET-FAST-014 U Metal Plates Interleaved with W Plates	2	Unmoderated UF_6 systems. Enrichment within HTGR range.	
37.5	IEU-COMP-INTER-003 UF_4-CF_2 Mixtures	14	Unmoderated UF_6 systems. Enrichment above HTGR range.	
30	IEU-COMP-THERM-001 UF_4-CF_2 Blocks Intermixed With CH_2 Blocks	29	General application for water moderated conditions, may also be applicable to combined systems of UF_6 and solution. Enrichment above HTGR range.	

Table A.1. IHECSBE experiments of potential utility for validation of HTGR fuel cycle NCS computations—intermediate and mixed enrichment uranium systems (10 to 60% enrichment) (continued)

% E[a]	Report	Cases[b]	Application Area, Basis, Notes	LWR[c]
20	IEU-COMP-THERM-003 U-Zr-H Fuel Rods in Water, Radial Graphite Reflector	2	General application for water moderated conditions, also for systems with graphite reflection.	
21	IEU-COMP-THERM-008 UO_2-Graphite in Pebble- Fuel Form	5	Unmoderated pebble-fuel configurations. Enrichment slightly above HTGR range. (ASTRA Reactor)	
17	IEU-COMP-THERM-010 UO_2-Graphite in Pebble- Fuel Form	1	Unmoderated pebble-fuel configurations. Enrichment within HTGR range. Also included in IHERPBE March 2008 edition as HTR10-GCR-RESR-001.	
30, 25, 18.8, and 12.5	IEU-COMP-MIXED-002 U(37.5)F_4-CF_2 Blocks Intermixed with Depleted UF_4-CF_2 Blocks	9	Unmoderated UF_6 systems. Average enrichments above and within HTGR range.	
20.9	IEU-SOL-THERM-001 UO_2SO_4 Solutions	4	Chemical processing (solutions, material recovery). Enrichment slightly above HTGR range.	
14.7	IEU-SOL-THERM-004 UO_2SO_4 Solution	1	Chemical processing (solutions, material recovery). Enrichment within HTGR ranges.	

[a] ^{235}U enrichment.
[b] Number of experiments in the benchmark report.
[c] Of potential applicability to advanced LWR fuel cycles using 5 to 10% ^{235}U enrichment.

Table A.2. IHECSBE experiments of potential utility for validation of HTGR fuel cycle NCS computations—low enrichment uranium systems (<10 % enrichment)

% E	Report	Cases	Application area, basis, notes	LWR
4.738	LEU-COMP-THERM-007 UO_2 Rods in Water	10	General application for water moderated conditions. Enrichment near lower end of HTGR range. Variety of pitches in both square and triangular lattices.	x
4.31	LEU-COMP-THERM-009 UO_2 Rods in Water	27	General application for water moderated conditions. Enrichment near lower end of HTGR range. Various neutron isolators and structural materials.	x
7	LEU-COMP-THERM-018 UO_2 Rods in Water	1	General application for water moderated conditions. Enrichment within HTGR range.	x
5	LEU-COMP-THERM-019 UO_2 Rods in Water	3	General application for water moderated conditions. Enrichment near lower end of HTGR range. Small-diameter (0.438 cm) SS clad fuel rods.	x
5	LEU-COMP-THERM-020 UO_2 Rods in Water	7	General application for water moderated conditions. Enrichment near lower end of HTGR range. Small-diameter (0.46 cm) fuel rods.	x
10	LEU-COMP-THERM-022 UO_2 Rods in Water	7	General application for water moderated conditions. Enrichment within HTGR range. Small-diameter (0.416 cm) SS clad fuel rods. Wide variation in pitch, overmoderated to undermoderated.	x
10	LEU-COMP-THERM-023 UO_2 Rods in Water	6	General application for water moderated conditions. Enrichment within HTGR range. Small-diameter (0.416 cm) SS clad fuel rods.	x
10	LEU-COMP-THERM-024 UO_2 Rods in Water	2	General application for water moderated conditions. Enrichment within HTGR range. Small-diameter (0.416 cm) SS clad fuel rods, hard neutron spectra.	x

Table A.2. IHECSBE experiments of potential utility for validation of HTGR fuel cycle NCS computations—low enrichment uranium systems (<10 % enrichment) (continued)

% E	Report	Cases	Application Area, Basis, Notes	LWR
7.5	LEU-COMP-THERM-025 UO_2 Rods in Water	4	General application for water moderated conditions. Enrichment within HTGR range. Small-diameter (0.416 cm) SS clad fuel rods.	x
4.92	LEU-COMP-THERM-026 UO_2 Rods in Water	6	General application for water moderated conditions. Enrichment near lower end of HTGR range.	x
5	LEU-COMP-THERM-031 UO_2 Rods in Water	6	General application for water moderated conditions. Enrichment near lower end of HTGR range. Small-diameter (0.46 cm) clad fuel rods.	x
4.46	LEU-COMP-THERM-045 U_3O_8-H_2O Mixtures	21	General application for water moderated conditions. Chemical processing (solutions, material recovery) Enrichment near lower end of HTGR range.	x
5	LEU-COMP-THERM-049 UO_2-H_2O Mixtures	18	General application for water moderated conditions. Chemical processing (solutions, material recovery) Enrichment near lower end of HTGR range.	x
4.4	LEU-COMP-THERM-053 UO_2 Rods in Water	14	General application for water moderated conditions. Enrichment near lower end of HTGR range. Small-diameter (0.765 cm) fuel rods.	x
4.48	LEU-COMP-THERM-069 U_3O_8-H_2O Mixtures	5	General application for water moderated conditions. Chemical processing (solutions, material recovery) Enrichment near lower end of HTGR range.	x
6.5	LEU-COMP-THERM-070 UO_2 Rods in Water	12	General application for water moderated conditions. Enrichment within HTGR range. Small-diameter (0.76 cm) fuel rods, hard neutron spectra.	x

Table A.2. IHECSBE experiments of potential utility for validation of HTGR fuel cycle NCS computations—low enrichment uranium systems (<10 % enrichment) (continued)

% E	Report	Cases	Application Area, Basis, Notes	LWR
4.738	LEU-COMP-THERM-071 UO_2 Rods in Water	4	General application for water moderated conditions. Enrichment near lower end of HTGR range. Undermoderated lattices.	x
4.738	LEU-COMP-THERM-072 UO_2 Rods in Water	9	General application for water moderated conditions. Enrichment near lower end of HTGR range. Undermoderated lattices.	x
3.5 & 6.6	LEU-COMP-THERM-081 UO_2 Rods in Water	1	General application for water moderated conditions. Enrichment within HTGR range.	x
6.5	LEU-COMP-THERM-081 UO_2 Rods in Water	13	General application for water moderated conditions. Enrichment within HTGR range. Small-diameter (0.76 cm) fuel rods.	
4.4 & 6.5	LEU-COMP-THERM-094 UO_2 Rods in Water	11	General application for water moderated conditions. Enrichment within HTGR range. Small-diameter (0.76 cm) fuel rods, hard neutron spectra.	x
< 5.0	LEU-COMP-THERM-xxx	-	Many additional UO_2 rods-in-water benchmarks exist that may are potentially applicable to the HTGR fuel cycle or to advanced LWR fuel cycles.	x
5	LEU-SOL-THERM-001 UO_2F_2 Solutions	1	General application for water moderated conditions. Chemical processing (solutions, material recovery) Enrichment near lower end of HTGR range.	
4.9	LEU-SOL-THERM-002 UO_2F_2 Solutions	3	General application for water moderated conditions. Chemical processing (solutions, material recovery). Enrichment near lower end of HTGR range.	

Table A.2. IHECSBE experiments of potential utility for validation of HTGR fuel cycle NCS computations—low enrichment uranium systems (<10 % enrichment) (continued)

% E	Report	Cases	Application Area, Basis, Notes	LWR
10	LEU-SOL-THERM-003 $UO_2(NO_3)_2$ Solutions	9	General application for water moderated conditions. Chemical processing (solutions, material recovery). Enrichment within HTGR range.	x
10	LEU-SOL-THERM-004 $UO_2(NO_3)_2$ Solutions	7	General application for water moderated conditions. Chemical processing (solutions, material recovery). Enrichment within HTGR range.	x
5.64	LEU-SOL-THERM-005 $UO_2(NO_3)_2$ Solutions	3	General application for water moderated conditions. Chemical processing (solutions, material recovery). Enrichment within HTGR range.	x
10	LEU-SOL-THERM-006 $UO_2(NO_3)_2$ Solutions	5	General application for water moderated conditions. Chemical processing (solutions, material recovery). Enrichment within HTGR range.	x
10	LEU-SOL-THERM-007 LEU-SOL-THERM-008 LEU-SOL-THERM-009 LEU-SOL-THERM-010 $UO_2(NO_3)_2$ Solutions	5 4 3 4	General application for water moderated conditions. Chemical processing (solutions, material recovery). Enrichment within HTGR range.	x
6	LEU-SOL-THERM-011 $UO_2(NO_3)_2$ Solutions	7	General application for water moderated conditions. Chemical processing (solutions, material recovery). Enrichment within HTGR range.	x

Table A.2. IHECSBE experiments of potential utility for validation of HTGR fuel cycle NCS computations—low enrichment uranium systems (<10 % enrichment) (continued)

% E	Report	Cases	Application Area, Basis, Notes	LWR
10	LEU-SOL-THERM-016	7	General application for water moderated conditions.	x
	LEU-SOL-THERM-017	6	Chemical processing (solutions, material recovery).	
	LEU-SOL-THERM-018	6	Enrichment within HTGR range.	
	LEU-SOL-THERM-019	4		
	LEU-SOL-THERM-020	2		
	LEU-SOL-THERM-021	2		
	LEU-SOL-THERM-022	2		
	LEU-SOL-THERM-023	9		
	LEU-SOL-THERM-024	7		
	LEU-SOL-THERM-025	7		
	$UO_2(NO_3)_2$ Solutions			
5 & 6	LEU-MISC-THERM-001	5	General application for water moderated conditions.	x
	LEU-MISC-THERM-002	6	Chemical processing (solutions, material recovery).	
	LEU-MISC-THERM-003	15	Enrichment within HTGR range.	
	UO2 Rods in			
	$UO_2(NO_3)_2$ Solutions			

Table A.3. IHECSBE experiments of potential utility for validation of HTGR fuel cycle NCS computations—high enrichment uranium systems (>60% enrichment)

% E	Report	Cases	Application area, basis, notes	LWR
92	HEU-COMP-INTER-004 Uranium Oxide-Graphite Mixture, C:U=300	1	Unmoderated graphite mixtures with TRISO particles, unmoderated compacts. Enrichment well above the HTGR range.	
93	HEU-MET-INTER-006 Alternating Plates of U Metal and Graphite, C:U from 14 to 51	4	Unmoderated graphite mixtures with TRISO particles, unmoderated compacts. Enrichment well above the HTGR range.	
93	HEU-MET-THERM-035 2-Mil-Thick U Metal Foils Alternating with Graphite Plates, C:U=1200	2	Unmoderated graphite mixtures with TRISO particles, unmoderated pebbles. Enrichment well above the HTGR range. NOTE: This evaluation is listed in the IHECSBE but is not provided, nor is an advance copy available from the evaluators.	
93	HEU-COMP-THERM-002 Coated Particles of UC_2 Distributed in Graphite Rods, Submerged in Water	25	General application for mixtures of graphite, U and H_2O. Potential use for testing of "doublehet" treatment methods. Enrichment well above the HTGR range.	
90	HEU-COMP-THERM-016 Homogeneous Blocks of Graphite Containing Uranium	6	Unmoderated graphite mixtures with TRISO particles, unmoderated pebbles. Enrichment well above the HTGR range.	

Table A.3. IHECSBE experiments of potential utility for validation of HTGR fuel cycle NCS computations—high enrichment uranium systems (>60% enrichment) (continued)

% E	Report	Cases	Application Area, Basis, Notes	LWR
93	HEU-SOL-THERM-039 UF_6-HF Mixtures	6	Chemical processing (solutions, material recovery). Combined systems of UF_6 and solution. Enrichment well above the HTGR range.	
>60	HEU-SOL-THERM-xxx	-	Chemical processing (solutions, material recovery). Enrichment well above the HTGR range. NOTE: A large number of IHECSBE experiments address various concentrations and configurations of UO_2F_2 and $UO_2(NO_3)_2$ solutions. Additional specific entries are not provided here. Many of these experiments should be applicable to the upper range of HTGR enrichment.	

APPENDIX B

MATRIX TABLES OF TSUNAMI-IP SIMILARITY COEFFICIENTS (c_k) FOR HTGR APPLICATION AND COMPARISON MODELS

The following tables present the similarity coefficients for HTGR application models and comparison models. The comparison models are meant to simulate critical benchmarks. Application models are also compared to other application models.

Table B.1. c_k for HTGR application and comparison models

Unmoderated UF_6 configurations

#	% E	H:^{235}U	Case Description	1	2	3	4	5	6	7	8	9	10
1	5	0	UF_6, k	1.000									
2	7	0	UF_6, k	0.977	1.000								
3	9	0	UF_6, k	0.939	0.991	1.000							
4	10.3	0	UF_6, k	0.917	0.981	0.998	1.000						
5	12	0	UF_6 Sphere	0.885	0.963	0.990	0.997	1.000					
6	15	0	UF_6 Sphere	0.836	0.932	0.971	0.983	0.995	1.000				
7	20	0	UF_6 Sphere	0.773	0.887	0.939	0.957	0.977	0.994	1.000			
8	90	0	UF_6 Sphere	0.612	0.752	0.822	0.849	0.884	0.922	0.953	1.000		
9	15	0.59	UF_6, 30B Package Array	0.835	0.928	0.963	0.974	0.986	0.992	0.987	0.919	1.000	
10	20	0.44	UF_6, 30B Package Array	0.796	0.903	0.950	0.965	0.982	0.994	0.996	0.940	0.996	1.000

Table B.2. c_k for HTGR application and comparison models

Configurations with H_2O intrusion into 30B cylinders,
Select unmoderated UF6 systems and solution systems are included for comparison

#	% E	H:^{235}U	Case Description	6	7	8	9	10	11	12	13	14	23	24	27	28
6	15	0	UF_6 Sphere	1.000												
7	20	0	UF_6 Sphere	0.994	1.000											
8	90	0	UF_6 Sphere	0.922	0.953	1.000										
9	15	0.59	UF_6, 30B Package Array	0.992	0.987	0.919	1.000									
10	20	0.44	UF_6, 30B Package Array	0.994	0.996	0.940	0.996	1.000								
11	10	200	30B, Soln Hemisph	0.333	0.389	0.534	0.359	0.364	1.000							
12	10	700	30B, Soln Hemisph	0.321	0.368	0.500	0.339	0.342	0.976	1.000						
13	10	100	30B, Soln Slab	0.520	0.568	0.665	0.552	0.552	0.964	0.929	1.000					
14	20	500	30B, Soln Hemisph	0.732	0.778	0.868	0.745	0.757	0.874	0.853	0.930	1.000				
23	10	200	UO_2F_2 Soln Sph, Min Vol	0.047	0.089	0.226	0.048	0.058	0.850	0.884	0.749	0.618	1.000			
24	10	500	UO_2F_2 Soln Sph, Min Mass	0.023	0.056	0.185	0.018	0.025	0.800	0.868	0.687	0.574	0.986	1.000		
27	20	100	UO_2F_2 Soln Sph, Min Vol	0.088	0.131	0.273	0.086	0.099	0.844	0.875	0.744	0.641	0.995	0.979	1.000	
28	20	500	UO_2F_2 Soln Sph, Min Mass	0.018	0.049	0.183	0.009	0.018	0.767	0.842	0.646	0.555	0.974	0.995	0.975	1.000

Table B.3. c_k for HTGR application and comparison models

Solutions within HTGR enrichment range (5% to 20% ^{235}U), comparison models for solutions at higher enrichments included

#	% E	H:^{235}U	Case Description	21	22	23	24	25	26	27	28	29	30	31	32
21	5	200	UO_2F_2 Soln Sph, Min Vol	1.000											
22	5	500	UO_2F_2 Soln Sph, Min Mass	0.970	1.000										
23	10	200	UO_2F_2 Soln Sph, Min Vol	0.964	0.982	1.000									
24	10	500	UO_2F_2 Soln Sph, Min Mass	0.925	0.983	0.986	1.000								
25	15	200	UO_2F_2 Soln Sph, Min Vol	0.931	0.970	0.995	0.991	1.000							
26	15	500	UO_2F_2 Soln Sph, Min Mass	0.902	0.970	0.979	0.998	0.991	1.000						
27	20	100	UO_2F_2 Soln Sph, Min Vol	0.938	0.961	0.995	0.979	0.997	0.978	1.000					
28	20	500	UO_2F_2 Soln Sph, Min Mass	0.888	0.961	0.974	0.995	0.989	0.999	0.975	1.000				
29	50	100	UO_2F_2 Soln Sph, Min Vol	0.867	0.926	0.968	0.973	0.988	0.982	0.984	0.984	1.000			
30	50	500	UO_2F_2 Soln Sph, Min Mass	0.858	0.941	0.960	0.987	0.982	0.995	0.967	0.998	0.987	1.000		
31	93	50	UO_2F_2 Soln Sph, Min Vol	0.826	0.890	0.941	0.948	0.968	0.960	0.968	0.965	0.994	0.972	1.000	
32	93	500	UO_2F_2 Soln Sph, Min Mass	0.845	0.931	0.954	0.982	0.978	0.992	0.963	0.995	0.987	1.000	0.974	1.000

Table B.4. c_k for HTGR application and comparison models

Minimum-volume and -diameter solutions within HTGR enrichment range (5% to 20% ^{235}U), 93% uranyl nitrate cylinder comparison model included

#	% E	H:^{235}U	Case Description	21	23	25	27	33	34	35	36	37
21	5	200	UO_2F_2 Soln Sph, Min Vol	1.000								
23	10	200	UO_2F_2 Soln Sph, Min Vol	0.964	1.000							
25	15	200	UO_2F_2 Soln Sph, Min Vol	0.931	0.995	1.000						
27	20	100	UO_2F_2 Soln Sph, Min Vol	0.938	0.995	0.997	1.000					
33	5	300	$UO_2(NO_3)_2$ Soln Cyl, Min Dia	0.946	0.928	0.904	0.900	1.000				
34	10	200	$UO_2(NO_3)_2$ Soln Cyl, Min Dia	0.954	0.987	0.981	0.979	0.967	1.000			
35	15	200	$UO_2(NO_3)_2$ Soln Cyl, Min Dia	0.928	0.989	0.994	0.988	0.935	0.993	1.000		
36	20	100	$UO_2(NO_3)_2$ Soln Cyl, Min Dia	0.934	0.991	0.994	0.994	0.927	0.991	0.997	1.000	
37	93	50	$UO_2(NO_3)_2$ Soln Cyl, Min Dia	0.833	0.945	0.971	0.969	0.826	0.935	0.966	0.970	1.000

Table B.5. c_k for HTGR application and comparison models

HTGR solutions, water-moderated gels and kernels

#	%E	H:^{235}U	Case Description	21	22	23	24	27	28	31	32	38	39	40	41	42	43	44	45
21	5	200	UO_2F_2 Soln Sph, Min Vol	1.000															
22	5	500	UO_2F_2 Soln Sph, Min Mass	0.970	1.000														
23	10	200	UO_2F_2 Soln Sph, Min Vol	0.964	0.982	1.000													
24	10	500	UO_2F_2 Soln Sph, Min Mass	0.925	0.983	0.986	1.000												
27	20	100	UO_2F_2 Soln Sph, Min Vol	0.938	0.961	0.995	0.979	1.000											
28	20	500	UO_2F_2 Soln Sph, Min Mass	0.888	0.961	0.974	0.995	0.975	1.000										
31	93	50	UO_2F_2 Soln Sph, Min Vol	0.826	0.890	0.941	0.948	0.968	0.965	1.000									
32	93	500	UO_2F_2 Soln Sph, Min Mass	0.845	0.931	0.954	0.982	0.963	0.995	0.974	1.000								
38	5	50	Kernels w/ H_2O Intrusion	0.840	0.726	0.692	0.615	0.651	0.547	0.484	0.477	1.000							
39	5	300	Gels/kernels+H_2O, Min Mass	0.988	0.989	0.983	0.963	0.962	0.936	0.875	0.902	0.785	1.000						
40	10	20	Kernels w/ H_2O Intrusion	0.754	0.630	0.630	0.542	0.615	0.486	0.491	0.429	0.946	0.698	1.000					
41	10	300	Gels/kernels+H_2O, Min Mass	0.940	0.980	0.995	0.995	0.992	0.989	0.954	0.974	0.645	0.974	0.581	1.000				
42	15	10	Kernels w/ H_2O Intrusion	0.585	0.470	0.487	0.402	0.495	0.360	0.423	0.318	0.811	0.533	0.953	0.441	1.000			
43	15	300	Gels/kernels+H_2O, Min Mass	0.911	0.966	0.987	0.994	0.989	0.996	0.970	0.989	0.587	0.953	0.531	0.997	0.402	1.000		
44	20	10	Kernels w/ H_2O Intrusion	0.649	0.535	0.567	0.479	0.579	0.441	0.509	0.403	0.811	0.602	0.954	0.523	0.989	0.486	1.000	
45	20	300	Gels/kernels+H_2O, Min Mass	0.893	0.955	0.980	0.991	0.985	0.997	0.976	0.994	0.555	0.939	0.503	0.992	0.380	0.999	0.466	1.000

Table B.6. c_k for HTGR application and comparison models

HTGR solutions, water-moderated TRISO particles (CFPs)

#	% E	H:^{235}U	Case Description	23	24	25	26	27	28	31	32	46	47	48	49	50	51	52
23	10	200	UO_2F_2 Soln Sph, Min Vol	1.000														
24	10	500	UO_2F_2 Soln Sph, Min Mass	0.986	1.000													
25	15	200	UO_2F_2 Soln Sph, Min Vol	0.995	0.991	1.000												
26	15	500	UO_2F_2 Soln Sph, Min Mass	0.979	0.998	0.991	1.000											
27	20	100	UO_2F_2 Soln Sph, Min Vol	0.995	0.979	0.997	0.978	1.000										
28	20	500	UO_2F_2 Soln Sph, Min Mass	0.974	0.995	0.989	0.999	0.975	1.000									
31	93	50	UO_2F_2 Soln Sph, Min Vol	0.941	0.948	0.968	0.960	0.968	0.965	1.000								
32	93	500	UO_2F_2 Soln Sph, Min Mass	0.954	0.982	0.978	0.992	0.963	0.995	0.974	1.000							
46	5	300	CFP+H_2O, Min Mass	0.939	0.937	0.918	0.917	0.910	0.906	0.824	0.867	1.000						
47	10	20	CFP w/ H_2O Intrusion	0.612	0.574	0.566	0.539	0.590	0.521	0.503	0.461	0.748	1.000					
48	10	300	CFP+H_2O, Min Mass	0.984	0.991	0.985	0.987	0.976	0.983	0.936	0.965	0.964	0.625	1.000				
49	15	10	CFP w/ H_2O Intrusion	0.508	0.463	0.472	0.436	0.509	0.422	0.465	0.375	0.603	0.955	0.509	1.000			
50	15	300	CFP+H_2O, Min Mass	0.984	0.994	0.992	0.994	0.983	0.993	0.960	0.982	0.938	0.580	0.996	0.476	1.000		
51	20	5	CFP w/ H_2O Intrusion	0.379	0.334	0.353	0.315	0.398	0.305	0.394	0.272	0.438	0.853	0.372	0.969	0.351	1.000	
52	20	300	CFP+H_2O, Min Mass	0.978	0.993	0.992	0.997	0.981	0.997	0.969	0.992	0.918	0.543	0.990	0.446	0.998	0.327	1.000

Table B.7. c_k for HTGR application and comparison models

Pebble fuel–related models (C:U ~ 1235), HTGR solutions included for comparison

#	% E	H:^{235}U	Case Description	22	23	24	27	28	31	32	53	54	55	70	71	72	73	74	75
22	5	500	UO_2F_2 Soln Sph, Min Mass	1.000															
23	10	200	UO_2F_2 Soln Sph, Min Vol	0.982	1.000														
24	10	500	UO_2F_2 Soln Sph, Min Mass	0.983	0.986	1.000													
27	20	100	UO_2F_2 Soln Sph, Min Vol	0.961	0.995	0.979	1.000												
28	20	500	UO_2F_2 Soln Sph, Min Mass	0.961	0.974	0.995	0.975	1.000											
31	93	50	UO_2F_2 Soln Sph, Min Vol	0.890	0.941	0.948	0.968	0.965	1.000										
32	93	500	UO_2F_2 Soln Sph, Min Mass	0.931	0.954	0.982	0.963	0.995	0.974	1.000									
53	10	500	CFP+C+H_2O, C:U ~ 1235	0.966	0.947	0.973	0.932	0.963	0.895	0.945	1.000								
54	15	300	CFP+C+H_2O, C:U ~ 1235	0.960	0.961	0.979	0.956	0.976	0.931	0.964	0.994	1.000							
55	20	300	CFP+C+H_2O, C:U ~ 1235	0.956	0.965	0.984	0.964	0.986	0.949	0.978	0.987	0.998	1.000						
70	5	0	Pebbles, Dry	0.514	0.443	0.471	0.408	0.443	0.348	0.411	0.590	0.548	0.515	1.000					
71	10	0	Pebbles, Dry	0.589	0.528	0.557	0.498	0.534	0.444	0.505	0.695	0.661	0.627	0.950	1.000				
72	15	0	Pebbles, Dry	0.610	0.559	0.587	0.533	0.567	0.487	0.542	0.727	0.700	0.667	0.899	0.990	1.000			
73	20	0	Pebbles, Dry	0.636	0.590	0.617	0.566	0.600	0.523	0.576	0.756	0.732	0.700	0.863	0.976	0.996	1.000		
74	15		Pebbles + H_2O, Min Mass	0.705	0.643	0.683	0.613	0.662	0.562	0.636	0.814	0.779	0.748	0.895	0.973	0.978	0.978	1.000	
75	20		Pebbles + H_2O, Min Mass	0.699	0.649	0.685	0.624	0.668	0.582	0.646	0.817	0.790	0.761	0.863	0.967	0.984	0.990	0.994	1.000

Table B.8. c_k for HTGR application and comparison models

Compact fuel–related models (C:U ~ 95) compared to HTGR solutions

#	% E	H:^{235}U	Case Description	22	23	24	25	26	27	28	29	30	31	32
22	5	500	UO_2F_2 Soln Sph, Min Mass	1.000										
23	10	200	UO_2F_2 Soln Sph, Min Vol	0.982	1.000									
24	10	500	UO_2F_2 Soln Sph, Min Mass	0.983	0.986	1.000								
25	15	200	UO_2F_2 Soln Sph, Min Vol	0.970	0.995	0.991	1.000							
26	15	500	UO_2F_2 Soln Sph, Min Mass	0.970	0.979	0.998	0.991	1.000						
27	20	100	UO_2F_2 Soln Sph, Min Vol	0.961	0.995	0.979	0.997	0.978	1.000					
28	20	500	UO_2F_2 Soln Sph, Min Mass	0.961	0.974	0.995	0.989	0.999	0.975	1.000				
29	50	100	UO_2F_2 Soln Sph, Min Vol	0.926	0.968	0.973	0.988	0.982	0.984	0.984	1.000			
30	50	500	UO_2F_2 Soln Sph, Min Mass	0.941	0.960	0.987	0.982	0.995	0.967	0.998	0.987	1.000		
31	93	50	UO_2F_2 Soln Sph, Min Vol	0.890	0.941	0.948	0.968	0.960	0.968	0.965	0.994	0.972	1.000	
32	93	500	UO_2F_2 Soln Sph, Min Mass	0.931	0.954	0.982	0.978	0.992	0.963	0.995	0.987	1.000	0.974	1.000
56	10	500	CFP+C+H_2O, C:U ~ 95	0.758	0.687	0.732	0.677	0.718	0.653	0.709	0.631	0.689	0.597	0.679
57	15	300	CFP+C+H_2O, C:U ~ 95	0.771	0.722	0.760	0.718	0.750	0.698	0.744	0.684	0.729	0.655	0.721
58	20	300	CFP+C+H_2O, C:U ~ 95	0.797	0.758	0.795	0.759	0.789	0.739	0.784	0.731	0.771	0.704	0.765
59	5		Compacts+H_2O, Min Mass	0.929	0.866	0.900	0.852	0.883	0.831	0.873	0.801	0.849	0.762	0.838
60	5		Compacts w/ H_2O Intrusion	0.885	0.826	0.834	0.801	0.810	0.789	0.796	0.741	0.765	0.700	0.750
61	10		Compacts+H_2O, Min Mass	0.962	0.937	0.970	0.940	0.965	0.921	0.961	0.914	0.950	0.885	0.944
62	10	0	Compacts w/ H_2O Intrusion	0.914	0.890	0.891	0.876	0.876	0.870	0.867	0.836	0.845	0.807	0.833
63	10		Compacts, Dry	0.455	0.381	0.360	0.338	0.324	0.350	0.305	0.280	0.263	0.269	0.241
64	15		Compacts+H_2O, Min Mass	0.961	0.947	0.981	0.956	0.980	0.937	0.979	0.939	0.972	0.914	0.967
65	15		Compacts w/ H_2O Intrusion	0.913	0.903	0.901	0.894	0.890	0.893	0.883	0.865	0.865	0.844	0.856
66	15	0	Compacts, Dry	0.455	0.403	0.375	0.365	0.345	0.389	0.328	0.325	0.292	0.335	0.273
67	20		Compacts+H_2O, Min Mass	0.958	0.954	0.986	0.966	0.988	0.949	0.987	0.956	0.983	0.933	0.980
68	20		Compacts w/ H_2O Intrusion	0.907	0.906	0.903	0.900	0.894	0.902	0.888	0.878	0.873	0.863	0.864
69	20	0	Compacts, Dry	0.439	0.408	0.376	0.377	0.352	0.409	0.338	0.354	0.308	0.381	0.293

Table B.9. c_k for HTGR application and comparison models

All compact fuel–related models (C:U ~ 95) plus prism fuel assembly models

#	% E	H:^{235}U	Case Description	56	57	58	60	62	63	65	66	68	69	76	77	78	79
56	10	500	CFP+C+H_2O, C:U ~ 95	1.000													
57	15	300	CFP+C+H_2O, C:U ~ 95	0.987	1.000												
58	20	300	CFP+C+H_2O, C:U ~ 95	0.973	0.996	1.000											
60	5		Compacts w/ H_2O Intrusion	0.912	0.917	0.916	1.000										
62	10	0	Compacts w/ H_2O Intrusion	0.894	0.925	0.938	0.977	1.000									
63	10		Compacts, Dry	0.554	0.533	0.500	0.691	0.616	1.000								
65	15		Compacts w/ H_2O Intrusion	0.872	0.912	0.932	0.952	0.995	0.586	1.000							
66	15	0	Compacts, Dry	0.539	0.530	0.506	0.668	0.624	0.973	0.611	1.000						
68	20		Compacts w/ H_2O Intrusion	0.853	0.899	0.922	0.933	0.987	0.572	0.998	0.610	1.000					
69	20	0	Compacts, Dry	0.505	0.507	0.491	0.624	0.607	0.911	0.610	0.981	0.620	1.000				
76	5	0	Prism Assemblies, k	0.832	0.774	0.731	0.835	0.730	0.797	0.678	0.727	0.645	0.639	1.000			
77	10	0	Prism Assemblies, k	0.831	0.782	0.744	0.838	0.750	0.820	0.706	0.767	0.678	0.690	0.988	1.000		
78	15	0	Prism Assemblies, k	0.819	0.774	0.739	0.829	0.753	0.831	0.715	0.795	0.693	0.732	0.969	0.995	1.000	
79	20	0	Prism Assemblies, k	0.801	0.761	0.729	0.814	0.748	0.839	0.716	0.820	0.699	0.770	0.945	0.982	0.996	1.000

Table B.10. c_k for HTGR application and comparison models

Unmoderated (H:^{235}U = 0) fuel item models

#	% E	H:^{235}U	Case Description	63	66	69	70	71	72	73	76	77	78	79
63	10		Compacts, Dry	1.000										
66	15	0	Compacts, Dry	0.973	1.000									
69	20	0	Compacts, Dry	0.911	0.981	1.000								
70	5	0	Pebbles, Dry	0.528	0.493	0.444	1.000							
71	10	0	Pebbles, Dry	0.574	0.551	0.509	0.950	1.000						
72	15	0	Pebbles, Dry	0.571	0.558	0.524	0.899	0.990	1.000					
73	20	0	Pebbles, Dry	0.571	0.564	0.534	0.863	0.976	0.996	1.000				
76	5	0	Prism Assemblies, k	0.797	0.727	0.639	0.819	0.837	0.811	0.801	1.000			
77	10	0	Prism Assemblies, k	0.820	0.767	0.690	0.784	0.822	0.805	0.803	0.988	1.000		
78	15	0	Prism Assemblies, k	0.831	0.795	0.732	0.754	0.801	0.789	0.791	0.969	0.995	1.000	
79	20	0	Prism Assemblies, k	0.839	0.820	0.770	0.727	0.780	0.772	0.776	0.945	0.982	0.996	1.000